INVESTIGATIONS OF BACTERIVORY AND MICROPLASTICS IN THE SOUTHERN OCEAN

A Dissertation
Submitted to
the Temple University Graduate Board

In Partial Fulfillment
of the Requirements for the Degree
DOCTOR OF PHILOSOPHY

---

by
Christopher Bruce Carnivale
May 2025

Examining Committee Members:

Robert Sanders, Advisory Chair, Biology
Erik Cordes, Biology
Amy Freestone, Biology
Jonathan Cohen, External Reader, University of Delaware

ABSTRACT

Anthropogenic-driven change is widely considered the largest threat to global ecosystem health and function, with consequences that are of particular significance to aquatic ecosystems. Specifically, the global increase in microplastic production, accumulation, and deposition are now recognized as a serious pollution hazard, much of which makes its way into aquatic systems. Microplastics, traditionally defined as plastic within the range of 5 mm to 0.1 µm, have been shown to interact with local organisms, both large and small, with differing results. Some of the latest findings revealed protists colonize, ingest, and egest microplastics in both *in situ* and laboratory conditions. In this dissertation, the consequences of both direct and indirect microplastic exposure with mixotrophic protists, those that are both photosynthetic and phagotrophic are assessed. Current literature indicates microplastic distribution in the oceans to be ubiquitous, reaching from coastal communities to the deepest depths of the Mariana Trench. However, their distribution is not homogenous, with current studies showing elevated levels of microplastics near coastal regions compared to offshore stations. Relatively few studies have investigated microplastics in the Southern Ocean, but surveys indicate the presence of plastic pollution in several oceanic areas surrounding the continent. This dissertation expands on those investigations by enumerating the total microplastic pollution during two seasons at a single oceanic station off the Western Antarctic Peninsula, plus for the first time, identifying the types of plastic polymers within three size fractions (0.22 – 20 µm, 20 – 100 µm, and > 100 µm) across several depths.

Another anthropogenically driven change is the global rise of temperature. Within the Southern Ocean, the effects of elevated temperatures are associated with reduced ice formation, longer growing seasons, and potentially a novel thermocline not characteristic of the Antarctic maritime, indicative of altered light regimes and nutrient availability. Current projections suggest a regional response shifting in the microbial community from larger protists (i.e., diatoms) to smaller pico- and nanoplankton (i.e., cryptophytes and/or mixed flagellates), a trend that's starting to occur in the Western Antarctic Peninsula (WAP) region. Many of these smaller flagellates are mixotrophic, which is the ability to utilize both photosynthesis and phagocytosis. Lastly, I reveal the impact of mixotrophic nanoplankton throughout the WAP region by assessing their distribution, activity (utilizing a novel approach to estimate their role as a bacterivore and their ever-elusive role as a primary producer), and the percent of the mixotrophic carbon demand input from either bacterivory or primary production *in situ*. The results of this study will aid in the understanding of the balance between phagotrophy and phototrophy in Antarctic mixotrophs, how microplastics may impact the mixotrophic community, and help to parameterize predictive models of microbial communities' response to increasing microplastic pollution.

ACKNOWLEDGEMENTS

I would like to express the deepest gratitude to my advisor, Bob Sanders. I am truly incapable of expressing the amount of trust, support, and patience Bob has shown me over the years. He took me on as an undergraduate student and has continued to provide valuable insights and guidance on my journey towards becoming a scientist.

I would like to extend the unending gratefulness towards Jean-David Grattepanche who provided many rounds of extensive and honest feedback. Reading and providing advice above and beyond anything I could have asked for. He provided guidance on my academic and personal success, and I will be forever grateful for our day-to-day conversations as desk mates.

I would also like to thank my fellow, now former lab mates, Dr. Andrew Van Kuren and Dr. Eli Chang. They provided the fun and support that helped me get through some of the toughest of times during this process.

To my committee members Erik Cordes, Amy Freestone, and Jonathan Cohen. I would like to express my deepest appreciation for your time, wisdom, and patience. I am thankful and have great respect for all of you and couldn't have asked for a better committee. Amy and Erik have continued to guide me from undergraduate until this moment and for that I am eternally grateful.

I would like to thank all the staff and faculty in the Department of Biology at Temple University. Thank you to Dr. Richard Waring, Sandy Verma, and Dr. Tonia Hsieh for helping me navigate all the administrative matters. Additionally, I would like to thank Rob Jennings for all the guidance into becoming a better teacher. It was truly a pleasure teaching for you.

I would finally like to thank the many members of my graduate cohort, who have provided a great deal of support and comradery over the years. I truly enjoyed our social gatherings, and comradery formed through our now former weekly gatherings. Special thanks to Andrew, JJ, and Mark who I can call on as great friends for life. Especially to my lab brother Andrew, who has provided me with never-ending support, laughs, and general fun through our off-the-cuff stimulating discussions and fun gatherings at the corner table.

To my friends and family, I would like to thank you all for your unending support. I would like to thank my parents Bruce and Carolyn, for all their emotional, moral, and financial support. I would also like to thank my sister, Nicole, and brother-in-law, Matt, who have provided the gift of levity during tough times.

To my significant other, Kat, I truly would not have finished this feat without your strong words of affirmation and encouragement throughout the final years of my dissertation.

TABLE OF CONTENTS

LIST OF TABLES

Table Page

LIST OF FIGURES

CHAPTER 1

INTRODUCTION

1.1 Microplastics in the World's Oceans

Plastics, which were introduced into the world's mainstream economy in response to the scarcity and expense of natural resources, had their production vastly expanded over the last century. Over that period, they became essential to nearly all industries within the consumer marketplace (Verma, 2008). Consequentially, plastics have become a significant global pollutant, with their presence in the world's oceans documented since the 1970s, marking the onset of a new 'Plastic Age ' or 'Plasticene' era (Carpenter & Smith Jr, 1972; Lewis et al., 2016). Current models have conservatively projected that over 5 trillion pieces or 250,000 tons have been deposited (Eriksen et al., 2014), mostly floating in the Earth's oceans, with an estimated 300 million tons more being released globally every year (PlasticsEurope, 2015). A separate study found an estimated 4.8-12.7 million tons were released into the oceans in 2010 (Jambeck et al., 2015). Irrespective of the study, there is a large amount of annual dumping not accounted for in current model estimates of global plastic pollution (Thompson et al., 2004). This incongruency may be a reflection of overly conservative estimates of global plastic pollution *in situ*, the lack of data on the vertical distribution of microplastics, or a focus on plastics larger than 5 mm, neglecting microplastics (5mm – 0.1 μm in size) (Galloway et al., 2017). Van Sebille et al. (2015) suggested a modest estimate of 15-51 trillion microplastic particles, or 93–236 thousand tons, are in our oceans.

Plastics are chemically inert, persistent, and ubiquitous pollutants that pose substantial risks to the environment (Galloway et al., 2017; Rowlands et al., 2023). Their physical and chemical resilience increases accumulation capacity resulting in their current dominance of marine debris, estimated at 60-80% of all marine debris and over 90% of all floating marine debris (Gordon, 2006). Marine debris is now recognized as negatively impacting both individual fitness (reproduction, growth, and/or death) and community biodiversity, which primarily consists of plastic both large and small, but particularly in the microplastic size range (Ogonowski et al., 2016; Thevenon & Carroll, 2015).

Microplastics are often defined as any plastic piece that is smaller than 5 mm but larger than 0.1 µm (Andrady, 2017). In aquatic ecosystems, plastic particle size inversely relates to both the number of species capable of consuming the particle and the total number of microplastic particles available to consume (Auta et al., 2017; Thompson, 2017). The physical and photooxidative degradation of larger plastic particles exponentially increases the number of plastic particles (secondary microplastics) and their derived compounds in the ecosystem (Amaral-Zettler et al., 2015; Gulizia et al., 2023; Marturano et al., 2019). In addition, some microplastics are produced within the defined size range ($0.1\ \mu m < x < 5\ mm$), deemed primary microplastics, and enter the environment directly via spills or wastewater treatment plants (Andrady, 2022). It has been well established that microplastics are ingested by filter, suspension, and detritus feeders (Andrady, 2022; Sfriso et al., 2020), and are consequently found in the guts of invertebrates and their vertebrate predators (Galloway et al., 2017; Setälä et al., 2014, 2016).

1.2 Microplastics and Biota

The initial documentation of microplastics consumed within marine life that captured widespread attention was in 2004, where ocean sediment and beach sampling uncovered microplastics within the trapped sediment marine worms (Thompson et al., 2004). Since then, the continued research into microplastics and their interactions with organisms has uncovered their pervasiveness within the biotic community. All facets of the food web, large and small, have shown some measure of contamination with microplastics with differing levels of impact (Cozar et al., 2014; Nerland et al., 2014). Larger vertebrates such as fish, seals, whales, and seabirds have all had microplastics identified within their guts or other tissues (Azzarello & Van Vleet, 1987; Boerger et al., 2010; Choy & Drazen, 2013; De Stephanis et al., 2013; Sletten, 2023). Additionally, they have been found in invertebrates such as bivalves, worms, and arthropods (including smaller microscopic copepods), across a variety of feeding strategies and mechanisms (Cole et al., 2013; Paul-Pont et al., 2016; Santana et al., 2016; Thompson et al., 2004; Ward & Kach, 2009).

Beyond the macrofaunal food web, microplastics can enter the microbial food web through a variety of paths due to their small size and chemical properties. For example, microplastics can be ingested by zooplankton and smaller heterotrophic plankton (Cole et al., 2013; Geng et al., 2021). Their bioavailability of microplastics to potential predation can be altered via interactions with bacteria (i.e. colonization) and other compounds (i.e. sorption) to form what is known as the 'Plastiphere' (Amaral-Zettler et al., 2020; Galloway et al., 2017). Microplastics have been reported to negatively impact a vast range of taxa, including phytoplankton and zooplankton (Chae et al., 2019; Cole et al., 2013; Fulfer & Menden-Deuer, 2021; Geng et al., 2021; Ogonowski et al., 2016; Rist et al., 2017). However, microplastic impacts on phagotrophic phytoflagellates (mixotrophs that use their own photosynthesis machinery and can consume bacteria; constitutive mixotrophs) continue to be vastly overlooked, even relative to other eukaryotic microbes. But few studies have examined how specific mixotrophs respond to microplastic pollution (Fulfer & Menden-Deuer, 2021; Kong et al., 2021; M'Rabet et al., 2018; Pennati et al., 2022).

1.3 The Microbial Food Web and Mixotrophy

The microbial food web, composed primarily of protists (eukaryotic microorganisms) and prokaryotes (bacteria and archaea), is a critical part of aquatic ecosystems because of the multiple roles it plays in photosynthesis, remineralization and in transferring energy, carbon, and nutrients to higher trophic levels (Azam et al., 1983; Stoecker, 1998). Protists are the major planktonic predators of bacteria and exhibit the top-down pressure to maintain the balance between phytoplankton and bacteria (Hulot et al., 2001; Sanders et al., 1989;Sherr & Sherr, 2002).These bacterivorous protists include species that are strictly heterotrophic and those that are mixotrophic. Mixotrophic protists combine photosynthesis with phagotrophy gaining benefit from two trophic modes in a variety of mechanisms to gain energy and carbon to create biomass (Sanders & Porter, 1988; Stoecker et al., 2017).

Mixotrophic protists have been shown to significantly affect aquatic ecosystems across a variety of habitats (Hartmann et al., 2012; Havskum & Hansen, 1997; Sanders & Porter, 1988; Stoecker, 1998). Modeling studies examining the potential contribution of mixotrophy to the carbon cycle have proposed that mixotrophs could increase the amount of primary production and the transfer of carbon to higher trophic levels, while also being higher quality food sources for their predators (Mitra et al., 2014; Traboni, Calbet, & Saiz, 2021; Ward & Follows, 2016). *In situ*, mixotrophic protists were shown to contribute in up to 86% of the bacterivory within Danish coastal waters, 35-65 % of the flagellate bacterivory in the Mediterranean Sea, and 60-77 % of the bacterivory in oligotrophic regions of the Atlantic Ocean (Hartmann et al., 2012; Havskum & Riemann, 1996; Unrein et al., 2007). Yet, the impact of phagotrophic phytoplankton regarding *in situ* primary production (phototrophy) remains largely unknown due to methodological constraints. Despite our inability to quantify their role as primary producers in the field or *in situ*, it is clear by their wide distribution and thriving in a myriad of environments that mixotrophy is a successful strategy, and the Southern Ocean is no exception (Gast et al., 2018; Grattepanche et al., 2022). To date, very few studies in the Southern Ocean have considered mixotrophy when assessing plankton dynamics and assessing roles plankton play in the community carbon flux. None of the studies took place within the WAP region, leaving gaps in a potentially large, unique, and important portion of the microbial community.

1.4 The Oceanic Environment Off the Western Antarctic Peninsula (WAP)

Overall, the Southern Ocean has been estimated to account for approximately one third of the global carbon flux (Schlitzer, 2002); it is characterized by a short, highly productive growing season during the austral spring and summer, peaking in January and February (Arrigo et al., 2017; Z. Li et al., 2016; Nardelli et al., 2023; Schofield et al., 2018a). The Western Antarctic Peninsula (WAP) region is at the convergence of permanently open ocean, a seasonal ice zone and the continental shelf, resulting in environmental gradients in both coastal-to-open ocean and latitudinal directions (Henley et al., 2019; Treguer & Jacques, 1992). As a consequence, the southern portion of the Antarctic circumpolar current flows close to the shelf edge (Orsi et al., 1995), and mid-depth circumpolar deep water impinges more directly onto the shelf bringing macronutrient replete conditions during the phytoplankton growing season (Arrigo et al., 2017; Hofmann et al., 1996; Klinck, 1998). By providing a uniquely rich water column for significant phytoplankton growth, the WAP is important to Antarctic krill stocks, their predators and an ideal location as breeding grounds for marine megafauna for both seasonal and year-round species (Atkinson et al., 2004; Costa & Crocker, 1996; Ducklow et al., 2007; Friedlaender et al., 2006; Quetin et al., 1996).

Over recent decades the Southern Ocean has undergone some of the most rapid climate changes compared to more temperate or tropical oceanic regions (King et al., 2003; Metzl, 2019; Vaughan et al., 2003). Increases in temperature led to overall reductions in seasonal sea ice extent, plus subsequent warming and freshening of the water column combined with deepening of the mixed layer depth (Brown et al., 2019; Meredith & King, 2005; Stammerjohn et al., 2012; Stammerjohn et al., 2008). Changes to the depth of the mixed layer influences several key abiotic and biotic environmental factors throughout the water column including light attenuation, nutrient availability and vertical distribution of plankton (Dong et al., 2008; Kara et al., 2003; Korb & Whitehouse, 2004; Paul Bissett et al., 1994; Pinkerton et al., 2021; Prend et al., 2022; Sallée et al., 2021). In addition the physical oceanographic shifts in the Southern Ocean led to latitudinal changes in surface chlorophyll a that track differences in sea ice (Montes-Hugo et al. 2009).

Given the differences of biota and diversity across depths in the Southern Ocean for planktonic species (Flegontova et al., 2023; Grattepanche et al., 2022), combined with the disproportionate lack of research into the impacts microplastics have on biota (especially mixotrophs), the knowledge of microplastic bioavailability in both the overall distribution and their types of polymers as well as their interactions within the region deserves greater attention. In this dissertation, I examine how a phagotrophic phytoflagellate species, *Ochromonas* sp. (strain BG-IV), interacts with increasing microplastic pollution and their physiological responses over a weeklong exposure period. Then, I investigate the distribution of total microplastics and individual polymers along a bathymetrical gradient, using two samplings at the same oceanographic station during different seasons and years. Finally, the distribution of, the carbon flow, and *in situ* consumption of microplastic particles by phagotrophic phytoflagellates throughout the WAP region of the Southern Ocean is explored.

CHAPTER 2

PHYSIOLOGICAL RESPONSE OF A MIXOTROPH (*OCHROMONAS SP.*) TO MICROPLASTICS OVER A WEEK

2.1 Abstract

Microplastics are now recognized as a significant concern to individual fitness and thereby overall biodiversity. Microplastics can interact with microorganisms directly in several ways, from ingestion to external colonization by organisms. Recent investigations into the interaction and impact that microplastics have on microbial organisms showed the potential to negatively influence their physiology, including growth, bacterivory, and primary production. However, the current literature ignored mixotrophic organisms. To date, no study simultaneously investigated all three physiological responses in a single study. To address this gap, I investigated the impacts on the growth, bacterivory, and primary production of a mixotroph (*Ochromonas sp.*) to increasing microplastic concentrations using polystyrene microspheres over a weeklong period. Results from the microplastic exposure experiment saw the reduction in growth and bacterivory rates, while primary production rates increased at the end of seven days. Indirect exposure experiment yielded a decrease of bacterivory rates in the direct and indirect microplastic conditions. These results demonstrate the capability of microplastic pollution, either through direct or indirect exposure, to influence a mixotrophic organism's behavior via reduction in bacterivory. While the reduction in bacterivory did not lead to significant organismal loss over the course of the week, it may alter their role in the microbial food web. By influencing their behavior, a mixotrophic organism's role in the system may change and potentially lead to cascading changes to carbon flux within the microbial community.

2.2 Introduction

One major factor recognized as impacting organismal physiology and contributing to biodiversity loss is marine debris, which consists of both large plastic components, such as bottles, to microplastics (Thevenon & Carroll, 2015). In aquatic ecosystems, plastic particle size inversely relates to both; the number of species capable of consuming the particle and the total number of particles available to consume (Auta et al., 2017b; Bergmann et al., 2022). The physical and photooxidative degradation of larger plastic particles exponentially increases the number of plastic particles (secondary microplastics) and their derived compounds in the ecosystem (Amaral-Zettler et al., 2015; Gulizia et al., 2023; Marturano et al., 2019). In addition, microplastics are produced within the defined size range and inputted directly into the environment via spills or wastewater treatment plants; whereby they can be ingested by filter, suspension, and detritus feeders (Andrady, 2022; Woodward et al., 2021). As such, microplastics are found in the guts of invertebrates, vertebrates (including humans), and many planktonic microbial species (Cole et al., 2013; Galloway et al., 2017; Setälä et al., 2016). For several decades, a common method to estimate of bacterivory by both heterotrophic and mixotrophic plankton has used plastic microspheres at tracer amounts in short-term experiments and their ingestion was observed for a broad range of taxa (Gast et al., 2014; Sanders et al., 1989, 1992; Sanders & Gast, 2012). However, few studies have investigated the physiological impacts they incur on organismal health, especially over longer periods of time.

While many physiological studies examining the impacts of plastics focused on megafauna, there is a growing body of literature surrounding the impact of microplastic on the microscopic fraction of the community and inversely, the impact of microorganisms on microplastics (Nava & Leoni, 2021). Several studies involving phytoplankton found that microplastics can form species-specific hetero-aggregates dependent on the physiological state of the phytoplankton, altering microplastic sinking rates and bioavailability with no adverse impacts on the phytoplankton growth (Long et al., 2015, 2017). Additionally, a recent study on a freshwater alga (*Chlorella pyrenoidosa*) showed negative impacts of microplastics on the photosynthetic efficiency using microplastics composed of two different polymers, polyvinyl chloride (PVC) and polypropylene (PP) (Wu et al., 2019). Heterotrophic plankton elicit species-specific responses to increasing microplastic concentrations. For example, the rotifer *Brachionus koreanus* had reduced growth rate, fecundity, and lifespan with increasing microplastic concentrations (Jeong et al., 2016). Guilhermino et al. (2021) saw negative effects of microplastics on survival, somatic growth, and population growth to *Daphnia magna* that were interactive with temperature. In other studies, *Daphnia magna* and multiple species of copepods saw reductions in grazing rates but saw no effect on fecundity dependent on the size of the microspheres to which they were exposed (Cole et al., 2013, 2015; Rist et al., 2017). Despite recent literature indicating the wide taxonomic and geographic breadth of phagotrophic phytoplankton (mixotrophic plankton), they are frequently ignored during ecological surveys, and this problem extends into the realm of microplastic research. To my knowledge, there are only four recorded microplastic studies have included mixotrophic plankton (Fulfer & Menden-Deuer, 2021; Kong et al., 2021; M'Rabet et al., 2018; Pennati et al., 2022).

Species-specific responses of three different mixotrophic dinoflagellates were recorded in the Fulfer and Menden-Deuer (2021) study. They found two of the dinoflagellates consumed microplastic microspheres with varying degrees of selectivity and impact. The two species that consumed microplastics saw significant reductions to growth and bacterivory; the third species had no observed ingestions of plastic microspheres and no negative impact, likely due to either fast ingestion/egestion or a selectivity against microplastic consumption (Fulfer & Menden-Deuer, 2021). A separate study looking at a different species of dinoflagellates saw plastic-derived chemicals, without the microplastic, alter the primary production rates of the *Alexandrium pacificum* Litaker sp. nov (Group IV) (ABZ1), a mixotrophic strain. Specifically, Bisphenol A and Di(2-ethylhexyl) phthalate (DEHP), a chemical that makes plastics more flexible, reduced the efficiency of photosystem II, resulting in decreased growth rates (M'Rabet et al., 2018), which suggests chemicals leached from microplastics can impact the ecosystem in the absence of the particle. Kong et al. (2021) showed plastic microspheres of two size classes (0.07 µm and 3 µm diameter) reduced the grazing pressure of *Ochromonas gleopara* on *Microcystis aeruginosa*, however, only the larger size class significantly reduced growth and abundance of *Ochromonas gleopara*. Finally, although Pennati et al. (2022) did not test for microplastic effects on a mixotrophic cryptomonad, they did show the microplastic spheres it ingested bioaccumulates in their predators.

The genus *Ochromonas* is a chrysophyte genus containing many strains of mixotrophs and is found in a variety of aquatic ecosystems, ranging from freshwater to marine and even hypersaline and acidic environments (Elloumi et al., 2009; Porter, 1988; Schmidtke et al., 2006; Segal et al., 2006; Wollmann et al., 2000). Despite utilizing multiple forms of nutritional strategies, *Ochromonas* sp. (including the BG-1 strain used here), have been shown to attain most of their nutrition from bacterivory over primary production and be an impactful consumer in planktonic communities (Koid et al., 2014; Sanders et al., 1990, 2001; Schmidtke et al., 2006). Several studies also show *Ochromonas* species can utilize photosynthesis and osmotrophy, and at least one was able to grow on phenol as the only carbon source (a breakdown product of plasticizer bisphenol-A) to compensate for insufficient bacterivory when prey abundances are low (Andersson et al., 1989; Boenigk et al., 2005; Cimmino et al., 2020; Posch et al., 1999; Sanders et al., 2001). Their unique nutritional plasticity, ubiquitous distribution, and ecological relevance make them an ideal group to study the impacts of microplastics on mixotrophy.

Comprehending the impact of primary microplastics on mixotrophic plankton is crucial to the understanding and prediction of how increasing microplastic pollution and their leaching compounds would impact the microbial food web, the trophic transfer of carbon and energy through the classical food web, and the potential implications on fishery production. To my knowledge, there has been no study investigating microplastic and their leaching compounds on mixotrophs which simultaneously measured responses for growth, primary production, and bacterivory. This study investigates how these three components of energy and carbon flux in *Ochromonas* sp. are affected by varying concentrations of microplastic over the course of one week. I hypothesized that direct exposure to microspheres would negatively impact the feeding, growth, and primary production by the mixotroph. Additionally, I hypothesized that indirect exposure would not have any impact on the physiology of *Ochromonas* sp., as the amount of leaching would not be enough to have effects within a seven-day span.

2.3 Materials and Methods

The physiological response of mixotrophic organisms to exposure of microplastics was assessed using a unifactorial experimental design. *Ochromonas* sp. was exposed to a range of microplastic concentrations from 2 x 10^1 to 2 x 10^5 mL^{-1} over a one-week period to account for a wide range of *in situ* microplastic pollution. Plastic blue fluorescing polystyrene microspheres (Flouresbrite 0.5 µm blue, Polysciences) were used to simulate primary microplastic contamination. The growth, primary production, and bacterial consumption of the mixotroph were measured periodically throughout the duration of the experiment. Multiple physiological responses were quantified throughout the experiment as measures for mixotrophic response: growth (specific growth rate), primary production rate (pg carbon $cell^{-1}$ h^{-1}), bacteria size particle ingestion rates (BSP; ingestions $cell^{-1}$ h^{-1}, pg carbon $cell^{-1}$ h^{-1}).

2.3.1 Culture Condition and Maintenance

For microplastic exposure experiments, cultures of *Ochromonas* sp. (BG-1 strain), originally isolated from a freshwater pond in Malaysia by enriching water samples in the dark, were maintained in glass culture flasks of DY-IV medium at room temperature with natural light conditions on the benchtop. For the indirect experiments (leaching), a separate batch of *Ochromonas sp.* were maintained in culture flasks of DY-IV medium at in an incubator at 20 °C in a 12-hour/12-hour day/night cycle (Sanders et al., 2001).

2.3.2 *Microplastic Exposure Design*

Quadruplicate glass bottles of 100 mL *Ochromonas* sp. (BG-1) in DY-IV medium were inoculated with blue fluorescing polystyrene microspheres (proxy for primary microplastic) at varying concentrations (Flouresbrite 0.5 µm blue, Polysciences). Therefore, along with a control, I employed a range of microplastic contamination concentrations (0.5 µm diameter) along a logarithmic scale of exposure: low (2×10^1 microspheres mL^{-1}), medium (2×10^3 microspheres mL^{-1}), and high ($2\ 10^5$ microspheres mL^{-1}). This range accounts for the current low concentrations in more remote regions but would also encompass spills of primary microplastics within busy port/shipping regions or future scenarios with microplastic accumulating in the environment (Eriksen et al., 2014; Sonke et al., 2022). Culture flasks were maintained on benchtop for the duration of the experiment with abundances monitored daily. Primary production was measured on every other day and bacterial ingestion was measured at the start (day 0), mid-week (day 3), and at the end of the experiment (day 7).

2.3.3 *Indirect Microplastic Exposure Design*

To test the potential for impacts of compounds leaching from the microspheres an additional experiment was conducted over a weeklong period. However, as the purpose was to assess leaching, I used only the high treatment (2×10^5) concentration of microplastics. Quadruplicate glass bottle with 60 mL of *Ochromonas* sp. (BG-1) were inoculated with blue fluorescing polystyrene microplastics (Flouresbrite 0.5 µm blue, Polysciences) at the high condition used in the direct assessment experiment. To decipher the impact of the microplastic particle from the leaching compounds, dialysis bags containing only 60 mL of *Ochromonas* sp. in DY-IV medium were added to the glass bottle containing *Ochromonas* sp. plus microplastic spheres. Dialysis bags with a molecular weight cutoff of 12,000 to 14,000 Daltons (Caroline Biological Supply Company reference 684226) were used to prevent migration of microspheres between treatments. Controls were quadruplicate glass bottles with a total of 120 mL of *Ochromonas* sp. (BG-1) in DY-IV medium inside (60 mL) the dialysis bag and outside (60 mL) the dialysis bag in the absence of microplastic microspheres. Abundance, primary production, and bacterivory were determined at the start (day 0) and the end of the weeklong period (day 7).

2.3.4 Abundance and Growth

Ochromonas sp. abundance was quantified via examination of 1 mL subsamples filtered onto a 25 mm, 0.8 μm pore sized polycarbonate membranes (GE Osmonics, Minnetonka MN, USA). Filters were then mounted on glass slides using Vectashield DAPI (Vector Laboratories) and enumerated under 1000x magnification using Olympus BX 41 epifluorescence microscope. Initial concentrations of *Ochromonas* sp. were all between 0.8 and 1.2 x 10^4 cells mL^{-1}. No additional media was added throughout the duration of either experiment. Results are reported as the specific growth rate (μ day^{-1}), which was calculated as the slope of log transformed data during the exponential growth phase between days 2 and 4.

For quantification of bacterial abundance and microsphere estimation, 0.5 mL subsamples were filtered onto a 25 mm, 0.2 μm pore sized polycarbonate membranes (GE Osmonics, Minnetonka MN, USA). Filters were then mounted on glass slides using immersion oil, stained using acridine orange (final concentration 0.001 M), and enumerated under 1000x magnification using Olympus BX 41 epifluorescence microscope. At least 20 grids were counted to ensure accurate estimation of bacterial abundance and microsphere estimation. Acridine orange was used so the blue microspheres and stained bacteria had different fluorescing wavelengths for more precise enumeration.

2.3.5 Primary Production

Carbon fixation rates by *Ochromonas* sp. grown in different plastic pollution conditions were measured under the same irradiances exposed for the entire culture flasks using the method of MacIntyre et al. (MacIntyre et al., 1996), which has been modified by the addition of centrifugation techniques in Smith and Azam (Smith & Azam, 1992). Primary production was quantified by incubating 2 mL of *Ochromonas* sp. with the addition of [^{14}C] sodium bicarbonate, having a final specific activity per sample of 0.5 μCi (18.5 kBq). Samples were incubated at photosynthetically active radiation levels at either 3 µE m^{-2} s^{-1} (microplastic exposure experiment) or 50 µE m^{-2} s^{-1} (indirect experiment). Post incubation, samples were centrifuged at 16000g for 30 minutes, followed by aspiration of the supernatant. Algal pellets were resuspended in 125 µL of double deionized water and fumed overnight with 150 µL of 6 N HCl to remove any residual ^{14}C not incorporated by the cells. The solution was neutralized using 150 µL of 6 N NaOH, followed by the addition of 200 µL of scintillation fluid (Econo-Safe, Research Products International). Radioactivity of the samples were measured using a scintillation counter (Beckman LS 6500). and converted to disintegrations per minute using a quench correction curve. Rates of carbon fixation were determined using the equation:

$$\frac{C_{Fixed}}{hour} = \frac{DIC_{sample} \times DPM_{^{14}C\ \mathrm{sample}}}{DPM_{^{14}C\ \mathrm{total}}} \times incubation\ time$$

Where, C_{Fixed} = the amount of carbon fixed by photosynthesis, DIC_{sample} = total dissolved carbon available for fixation in the sample, $DPM_{^{14}C\ \mathrm{sample}}$ = disintegrations per minute for the algal pellet, $DPM_{^{14}C\ \mathrm{total}}$ = disintegrations per minute of total ^{14}C available for incorporation. DIC per sample was calculated using the "seacarb" package in R. The resulting gross primary productivity was normalized to a per cell basis utilizing the enumeration of algal abundance estimated from epifluorescent microscopy.

2.3.6 Bacterivory Assessment

For bacterivory assessment, yellow-green fluorescing microspheres (0.5 µm diameter (Flouresbrite, Polysciences) were added at ~ 10% background bacterial concentration (1.0 x 10^5 to 3.7 x 10^5 microspheres mL^{-1}) and incubated for thirty minutes (Sanders et al., 1989, 2001). The 'pristine' yellow-green microspheres (bacteria proxy) fluoresce at a different wavelength from those added to simulate primary microplastic pollution (blue fluorescing) and at a much brighter intensity than the bacteria stained with acridine orange. Prior to the study, a time course experiment determined that there was linear uptake of microspheres without saturation and egestion for 30 minutes by *Ochromonas* sp. At the end of the incubation period, samples were fixed with 90 µL of Lugol's solution (3% final concentration), cleared with 90 µL of sodium thiosulfate, and preserved with 300 µL of formalin to prevent egestion and improve plastid preservation (Sherr & Sherr, 2018). Subsamples of 1 mL were then filtered onto a 25 mm diameter, 0.8 µm pore sized polycarbonate membranes (GE Osmonics, Minnetonka MN, USA) with 200 µL of acridine orange to a final concentration of 0.001 M (Hobbie et al., 1977). Filters were mounted on glass slides using immersion oil and kept at 4 ºC to reduce loss of chlorophyll fluorescence until enumeration under 1000x magnification using Olympus

BX 41 epifluorescence microscope. At least 100 cells were counted for each replicate with positive feeding events being a plastidic cell with a nucleus and containing a microsphere. To remove random association events, a sample (T0) was taken and fixed immediately after microsphere addition following the same procedure. The value for T0 was then subtracted from the estimated ingestions; the background was very low throughout the experiment. The amount of microsphere proxy addition was confirmed via enumeration as described for bacterial abundance, with a minimum of 20 grids assessed. Bacterivory was calculated by assuming the number of ingestions were related to the ratio of microspheres and bacteria in the following equation (Sherr & Sherr, 2018):

$$\frac{Ingestions}{cell \times hour} = \left(\%\, mixotrophy \times \frac{bacteria}{microsphere} + \%\, mixotrophy\right) \times \text{incubation time}$$

Where, % mixotrophy = the percentage of beads ingested per 100 cells of protists, bacteria = the concentration of bacterial cells mL^{-1}, microsphere = the concentration of microsphere particles mL^{-1}. The estimated ingestion rate was extrapolated to a per hour ingestion rate for comparison with primary production. Using the bacterial conversion factor of 22 femtograms carbon per bacteria, ingestion rates were converted into biomass (pg carbon) consumed (Lee & Fuhrman, 1987). Both bacterivory, as bacterial sized particle ingestions, and carbon consumption rates are reported as calculated on a per cell basis.

There may be concern for using microspheres as a proxy for bacterial ingestion due to potential for selectivity, but there frequently is little selectivity between live prey and microspheres of this size during short-term experiments (Sanders et al., 2001). The shortest time period indicating negative impacts of plastics on estimated feeding rates is on the order of several hours (Fulfer & Menden-Deuer, 2021).

2.3.7 Statistical Analysis

After logarithmic transformation, *Ochromonas* sp. abundances in the microplastic exposure and indirect experiment were compared using repeated measures one-way ANOVA with microplastic concentration as the independent variable. Specific growth rate was compared using one-way ANOVA. Post-hoc pairwise comparisons were analyzed using a Tukey HSD test. All calculations and data analysis were calculated using the R base stats package (R Core Team, 2020).

2.4 Results

2.4.1 Impacts on Abundance and Growth

Ochromonas sp. was able to consume both the blue and yellow-green microspheres, including the ingestion of both microspheres (blue and yellow-green) by the same cell (Figure 2.1), although ingestion of blue microspheres was rarely observed. Due to the order of magnitude difference in blue and yellow-green microspheres added in the lesser plastic pollution treatments, no blue microsphere ingestions were observed in the lowest plastic treatment.

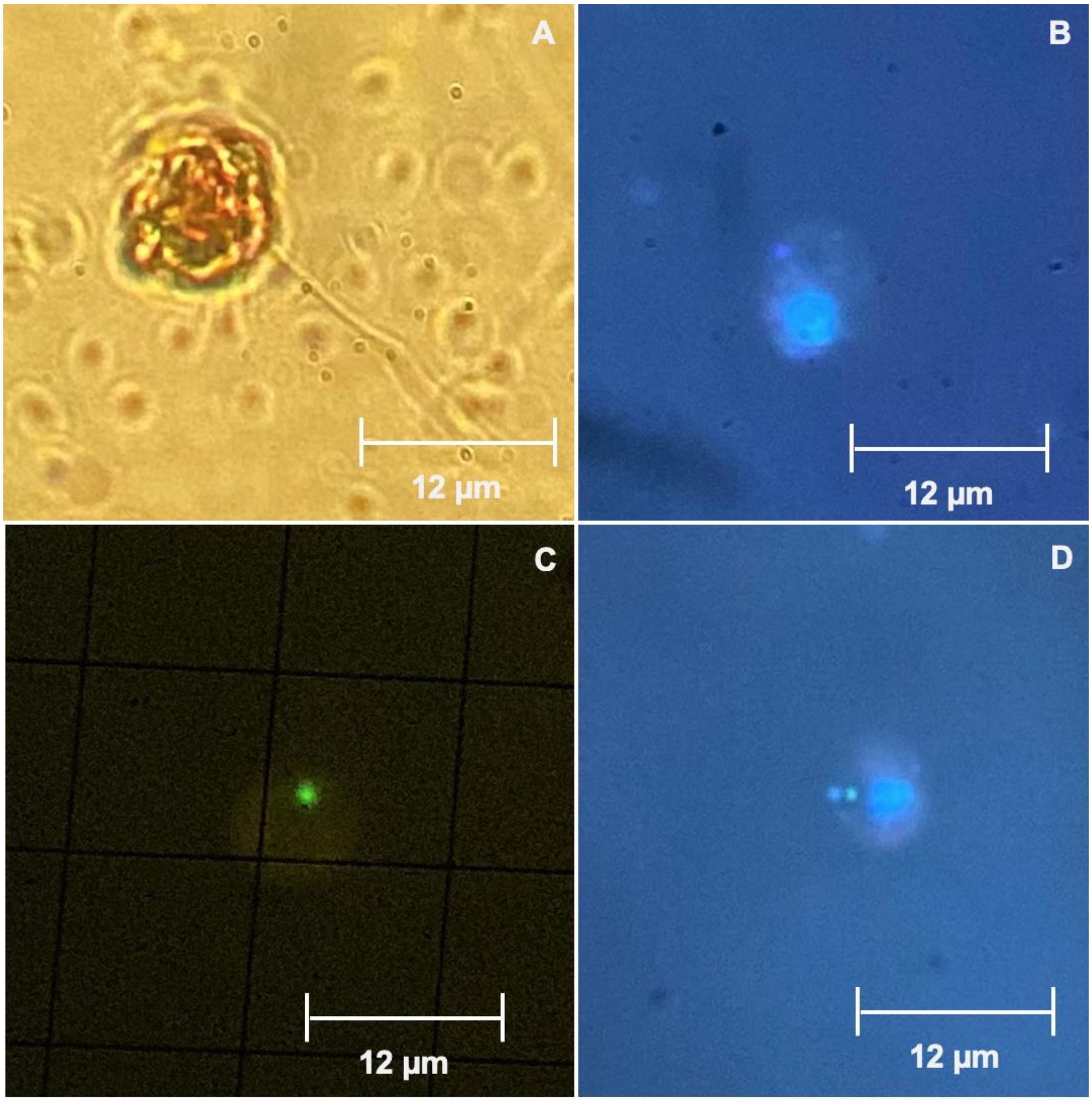

Figure 2.1 Pictures from light and fluorescent microscopy. Showed are the (A) *Ochromonas* sp., the ingestion of (B) blue (plastic treatment) microsphere under the DAPI filter, yellow-green microspheres under FITC filter (C) and the simultaneous ingestion of (D) both a blue and yellow-green microsphere under a DAPI filter.

The microplastic exposure and indirect experiments began at approximately the same concentration of *Ochromonas* cells ~1 x 10^7 cells L^{-1}. Over the course of the week in the microplastic exposure experiment, *Ochromonas* sp. populations persisted regardless of plastic pollution concentrations, ranging in abundance from 3.3 x 10^6 to 8.5 x 10^7 cells L^{-1} (Figure 2.2A, Appendix A). Repeated measures ANOVA analysis of the log transformed abundance data revealed significant differences over the course of the week ($p < 0.05$). On day seven, the relative differences between the microplastic treatments and the control were -1.3 ± 0.4 x 10^7, -1.2 ± 0.1 x 10^7, and -0.8 ± 0.4 x 10^7 cells L^{-1}, from high to low treatment respectively (Figure 2.2A). The corresponding absolute abundances were 1.4 ± 0.4 x 10^7, 1.4 ± 0.1 x 10^7, and 1.8 ± 0.4 x 10^7 cells L^{-1}, from high to low treatment respectively (Appendix A).

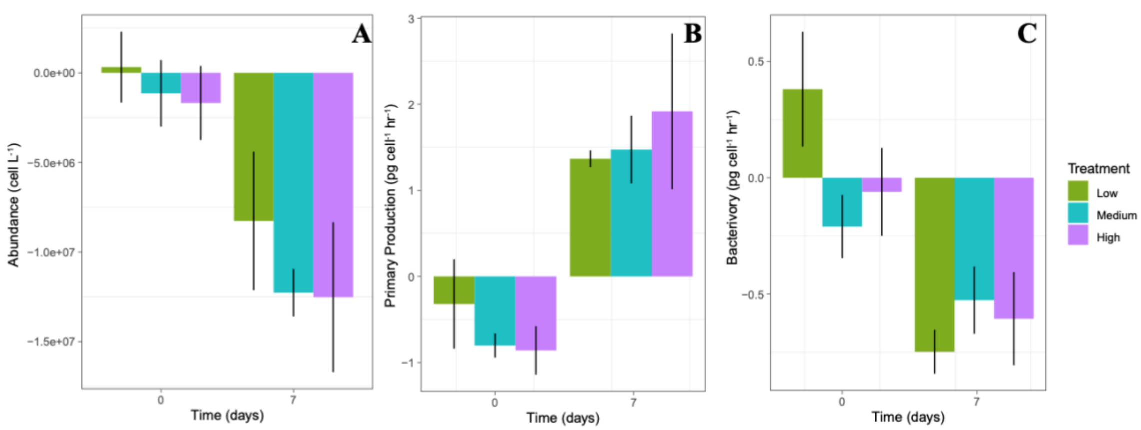

Figure 2.2 <u>(A) Abundance, (B) primary production, and (C) bacterivory per cell assessed during microplastic exposure experiment scaled by the control mean.</u> By day seven, both abundance (A) and bacterivory (C) showed significant reductions relative to control. Inversely, primary production (B) increased relative to control by the end of the week.

At the end of the indirect experiments, no significant differences in abundance were observed on day seven, regardless of microplastic treatment in the direct or indirect condition (Figure 2.3A).

In the microplastic exposure experiment, the exponential growth phase was between days two and day four for all microplastic treatments, which was used to calculate the maximal growth rate (μ) for *Ochromonas* sp. in each treatment (Table 2.1). Estimated specific growth rates were the largest for the control treatment and medium microplastic treatments, with an average μ of 0.42 and 0.44 d^{-1}, respectively. The low and high microplastic treatments had much lower μ of 0.31 and 0.29 d^{-1}, respectively (Table 2.1). The differences across the groups were not statistically significant ($p > 0.05$).

2.4.2 Impacts on Primary Production

Over the course of the week in the direct experiment, *Ochromonas sp.* had a nonlinear response of primary production (Appendix A). The primary production ranged from 1.0 to 4.3 pg C $cell^{-1}h^{-1}$ in the microplastic treatments (Appendix A). Contrary to the abundance analysis, the differences from the control were positive on day seven. Primary production in all microplastic treatments were higher than the control with the lowest estimated relative difference of 1.4 ± 0.1 pg C $cell^{-1}$ h^{-1} in the low condition, followed by 1.5 ± 0.4 pg C $cell^{-1}$ h^{-1} in the medium condition, and 1.9 ± 0.9 pg C $cell^{-1}$ h^{-1} in the high treatment (Figure 2.2B) These correspond to absolute primary production values of 2.0 ± 0.01, 2.1 ± 0.4, 2.5 ± 0.9 pg C $cell^{-1}$ h^{-1}, respectively. The control had a value of 0.6 ± 0.5 pg C $cell^{-1}h^{-1}$ (Appendix A).

During the indirect experiment, the primary production ranged from 0.15 to 0.61 pg C $cell^{-1}h^{-1}$ and did not show statistically significant differences between treatment and control, in direct or indirect (within dialysis bag) microplastic exposure (Figure 2.3B).

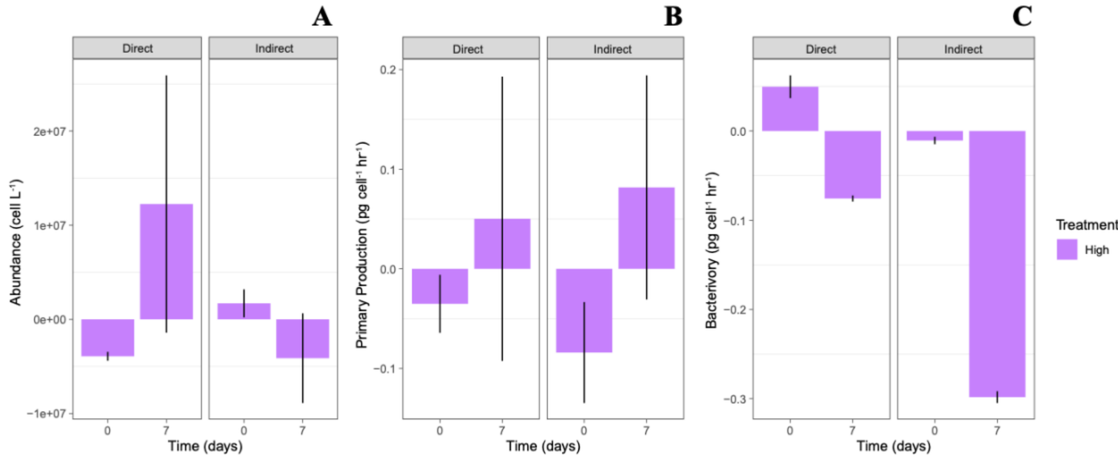

Figure 2.3 <u>(A) Abundance, (B) primary production, and (C) bacterivory per cell assessed during indirect exposure experiment scaled by the control mean.</u> There was no significant difference in the abundance (A) and primary production (B) between control and the high microplastic treatment. For ingestions (C), inversely, there was a significant reduction in estimated feeding rates between the plastic and control treatments at day seven, in both direct and indirect exposure of microplastics.

2.4.3 Impacts on Bacterivory

Like primary production results in the microplastic exposure experiment, *Ochromonas sp.* had a nonlinear response for bacterivory (Appendix A). Bacterivory ranged from 0.3 to 1.4 pg C cell^{-1}h^{-1} throughout the microplastic exposure experiment. At the start, there were no statistically significant differences between the microplastic treatments and control. However, microplastic treatments showed significant differences from control on day seven ($p < 0.05$; Figure 2.2C, Appendix A). Contrary to the primary production, the observed relative differences from control were negative on day seven, with values of -0.7 ± 0.01, -0.5 ± 0.1, -0.6 ± 0.2 pg C cell^{-1} h^{-1}, from low to high microplastic treatment respectively (Figure 2.2C). The observed differences correspond to absolute bacterivory rates of 0.3 ± 0.1, 0.5 ± 0.1, 0.5 ± 0.2 pg C $cell^{-1}$ h^{-1}, respectively. The control had a value of 1.1 ± 0.2 pg C $cell^{-1}h^{-1}$ (Appendix A).

The bacterivory results at the end of the indirect experiment showed significant differences between microplastic treatments and control, for both direct and indirect exposure ($p < 0.05$; Figure 2.3C). The differences were much larger in the dialysis bag (indirect) compared to outside (direct) of the dialysis bag (Figure 2.3C). After seven days, indirect exposure showed a decrease of -0.07 ± 0.003 pg C $cell^{-1}$ h^{-1}, while outside the dialysis bag showed a decrease of -0.3 ± 0.007 pg C $cell^{-1}$ h^{-1} (Figure 2.3C).

Table 2.1 Maximal growth rates of *Ochomonas* sp. during the microplastic exposure experiment.

Treatment	Growth Rate (μ)	Ingested Carbon	PP Carbon
Control	0.42	12.3	14.5
Low	0.31	3.9	47.3
Medium	0.44	6.5	49.9
High	0.29	5.6	60.5

Acquired carbon reported as daily pg of Carbon per cell; Ingested Carbon received a 50% penalty due to respiration

Note. Estimated carbon acquisition rates of bacterivory and primary production in pg C $cell^{-1}d^{-1}$. Only the control treatment gained nearly half of their carbon through bacterivory, while the microplastic treatments acquired most of their carbon through photosynthesis.

2.5 Discussion

This study is the first work investigating the physiological responses of a mixotrophic organism to microplastics including abundance, growth, primary production, and bacterivory. Despite the use of microspheres as bacteria proxies in the estimation of bacterial ingestion rates in a plethora of different studies (Caron et al., 1993; McKie-Krisberg & Sanders, 2014; Princiotta et al., 2016; Princiotta & Sanders, 2017; Sanders & Gast, 2012), there are little to no studies of the impacts microplastics have on phagotrophic phytoplankton. In my study, *Ochromonas sp.* was directly exposed to plastic microspheres outside of the bag, but also to leaching compounds from microplastic using dialysis bags. The upper range of microplastic exposure levels (2×10^5 microspheres L^{-1}) exceeds the typical environmental concentrations, these concentrations could be relevant of brief (primary plastic) or could reach these concentrations in the future (Free et al., 2014; Magalhães et al., 2022; Tommy, 2007; van Sebille et al., 2015; Woodward et al., 2021). The purpose of this study is to estimate the physiological tolerance limits of a mixotrophic plankton to an ever-rising plastic polluted environment. The impacts were examined via growth, primary production, bacterial ingestion rates periodically measured throughout the course of the week.

2.5.1 Impacts on Abundance and Growth

Regardless of microplastic contamination level, *Ochromonas* sp. were able to persist through the weeklong exposure to microplastics for both experiments. In agreement with my hypothesis, the microplastic exposure observed significant negative differences relative to control (Figure 2.2A). Contrary to what I hypothesized, there were only marginal, non-significant differences in abundance at the end of the indirect experiment (Figure 2.3A). On average, the control treatment saw the highest peak *Ochromonas* sp. concentrations, which occurred on days four and five of the week (Appendix A). Despite this, they only had the second highest on average estimated growth rate and doubling time. This difference is likely due to the overall higher concentrations at the start (day two) of the exponential growth phase of control compared to the medium microplastic treatment. While the estimated growth rates were similar over the course of days two to four, the abundance in the medium microplastic treatment were consistently lower than the control treatment during this exponential growth period.

On average, the plastic treatments presented a reduction in the maximal abundance during the exponential growth phase and the estimated growth rates support it. The medium microplastic treatment did not reflect this, as previously mentioned. Despite the lower concentration on the second day of the microplastic exposure experiment, the medium microplastic treatment rebounded to peak concentration values like those of the other plastic treatments (low and high). By day seven, all treatments were in their stationary phase and the control group remained the most abundant, however, the microplastic treatments saw their post exponential phase decline a day earlier.

Similar results have been shown in *Daphnia* sp., where there was no reduction in fecundity, brood size, or date of first neonate over a longer twenty-one-day period. This remained consistent regardless of microplastic concentration or size, with 0.2 µm polystyrene (PS) as their smallest size (Rist et al., 2017). However, Guilhermino et al. (2021) found the effects of microplastic pollution to *Daphnia magna* increases with temperature. Temperature influences could explain the incongruency between the indirect and microplastic exposure experiments but is outside the scope of this study. In 2021, Kong et al.investigated the physiological response of a closely related *Ochromonas gleopara*, and found a difference in their growth and grazing rates based on size of the microplastic particle exposed. Only the larger size particles (3µm), which are similar size to their preferred prey, showed negative impacts on abundance and growth of *Ochromonas gleopara* over a two-week period (Kong et al., 2021). Similarly, Fulfer and Menden-Deuer (2021) examined growth on 3 different dinoflagellate species (*Oxyrrhis marina, Gyrodinium sp., and Protoperidinium sp.*) and found a 25 – 35% reduction in growth rates but using a larger sized microplastic particle ranging from 2.5 – 4.5 µm to be similar with the algal prey (Fulfer & Menden-Deuer, 2021). The current study utilizes particle sizes (0.5 µm) that emulated the preferred prey size for *Ochromonas* sp. (BG-1) and found similar results to Kong et al. (2021), especially in the microplastic exposure experiment.

2.5.2 Impacts of Primary Production

A unique feature of mixotrophic protists is the ability to behave as both a primary producer and prey consumer. Their role as a primary producer presented inconsistent results at the end of the seven days when estimated on a per cell basis. The incongruence between experiments was likely caused by the smaller difference in estimated population abundance between plastic treatments and control at the end of seven days for experiment two (Indirect, Figure 2.3). No significant differences between the plastic treatments for primary production of the sample at the end of the seven-day incubation were observed for both the microplastic direct exposure and indirect exposure experiments. The different results between the experiments suggests negligible impacts of microplastics and their leaching compounds on *Ochromonas* sp. through differing temperatures could be influencing the microplastics effect (Guilhermino et al., 2021).

There is much less literature of mixotrophy and how they act as a primary producer compared to how they are assessed as primary and secondary prey consumers

(Stoecker et al., 2017). The same is evident with the impacts of microplastics and their primary production to microplastic exposure. Only one study has attempted to quantify the impacts of microplastics on mixotrophy photosynthetic activity, and they only exposed them to varying levels of plastic derived chemicals: Bisphenol A and di-2-ethylhexyl phthalate (BPA and DEHP, respectively). These plastic derived chemicals showed negative impact on the photosynthetic rates and their growth rates, specifically impacting the efficiency of photosystem II (M'Rabet et al., 2018). While these chemicals are not known to be leaching from polystyrene microspheres, they are commonly found together in the environment as many different forms of polystyrenes have them added as a common plasticiser (Gulizia et al., 2023). Together with phthalate acid ester make up over 80% of all plasticizers (Geyer et al., 2017; Marturano et al., 2019). Even though our microspheres are currently unknown to release BPA and DEHP, recent studies have found that BPA and DEHP added in conjunction with microsphere exposure has synergistic effects in both mice and humans, suggesting a potential impact in the environment when exposed together (Cheng et al., 2023; Wu et al., 2023). Our results likely differ due to the lack of direct addition of BPA and DEHP to *Ochromonas* sp. There is also potential for species-specific responses, where *Ochromonas* sp. may be more tolerable to the stress caused by leaching compounds from the plastic microspheres regarding primary production.

2.5.3 Impacts on Bacterivory

The strongest measured impact of microplastics on *Ochromonas* sp. was on their bacterivory. Despite the blue fluorescing microspheres use to simulate primary microplastic contamination, *Ochromonas* sp showed the ability to consume all forms of microspheres used in the experiments. Both experiments, across all microplastic treatment concentrations, presented significant reduction in estimated bacterivory at the end of the seven-day incubation. During the experiment with varying microplastic concentrations, all plastic concentrations showed a similar decrease in ingestions per cell contrary to what was expected. For the indirect experiment, *Ochromonas sp.* exhibited a significant reduction in bacterivory both inside and outside of the bag. This suggests that both the plastic microspheres themselves, and the potential leaching of toxic compounds from the plastic microspheres can impact *Ochromonas* sp. feeding. Although no intentional weathering of the microspheres was conducted, the blue microspheres used in the week-long incubation were 35 years old, which may have resulted in greater degradation and leaching, contributing to the negative impacts observed in the indirect experiment.

A recent study on a closely related species, *Ochromonas gleopara*, found similar effects, with the feeding clearance rates on *Microcystis aeruginosa* reduced with increasing microplastic concentrations (Kong et al., 2021). The effects of microplastic were much strong at the larger size (3 µm diameter, same size as cyanobacteria *Microcystis aeruginosa*) with greater reductions to clearance rates and additional reduction to algal growth. The current study was similar to the results of Kong et al. (2021), in that microsphere's (0.5 µm) that inhibited bacterivory emulated the prey's size. Additionally, there are species specific responses to microplastic pollution as suggested by Fulfer and Menden-Deuer (2021) to be considered. Two different species of dinoflagellates showed as high as 50% reduction in miximal ingestions rates estimated from *Oxyrrhis marina* and *Gyrodinium sp* (Fulfer & Menden-Deuer, 2021). However, the third species of dinoflagellates, *Protoperidinium bipes*, saw no ingestion of plastic microspheres (Fulfer & Menden-Deuer, 2021; Goldstein et al., 2012).The differences between *Ochromonas sp.* (BG-1) and *Ochromonas gleopara* studied by Kong et al. (2021) could be due to differences in the size of plastic microspheres used, which has been identified as a key contributor to plastic influence on organisms, or there may be species specific responses to microplastic stress as noted for other protists (Fulfer & Menden-Deuer, 2021; Lehtiniemi et al., 2018).

Mixotrophic protists are an essential portion of the microbial community that plays an important role both as prey for higher trophic levels of the food web (i.e., mesoplankton) and as predators of bacteria, which links bacterial production to the classical food web (Mitra et al., 2016; Stoecker, 1998; B. A. Ward & Follows, 2016). Specifically, it is the ability of phagotrophic phytoplankton to consume bacterial prey and photosynthesize which may boost their gross growth efficiency (GEE) (Menden-Deuer & Lessard, 2000; Schoener & McManus, 2012; Stoecker et al., 2009). By consuming prey, their C:N and C:P ratios decrease, which make them a higher quality food source for consumers (Sanders & Wickham, 1993). A significant reduction in phagotrophic phytoplankton's ability to act as a consumer would potentially reduce their GEE and reduce the food quality for their predators. Consequentially, disruption of mixotrophic secondary production could alter the rate of carbon flux, including the amount of bacterial production reaching the eukaryotic portion of the microbial and the classic food web (Fulfer & Menden-Deuer, 2021). This could potentially result in cascading effects, reducing population sizes and/or overall biomass of organisms higher up the food chain, especially important for fisheries and their management.

2.5.4 Conclusion

Overall, contrary to the hypothesis, microplastic at the end of a weeklong incubation period have minimal to negligible impacts on the growth and primary production of *Ochromonas sp.* (BG-1). However, in congruence with the hypothesis, there are significant decreases of the bacterivorous activity of *Ochromonas sp.*, which may result in an overall weakening in the link between bacteria production, microbial food web, and the greater classical food web. This weakening could potentially cascade into a reduction in the overall planktonic food quality and decrease the efficiency in the carbon pump that could lead to negative impacts to fishery production. Additional work is needed to determine the leaching compounds causing the negative impact. Future testing is needed to establish whether the results of this study using only polystyrene is consistent across the different types of plastic, some have already been shown to negatively impact phytoplankton to varying degrees (PVC compared to PP) in other freshwater algae (Wu et al., 2019).

CHAPTER 3

MICROPLASTIC DISTRIBUTION WITHIN THE SOUTHERN OCEAN WATER COLUMN ALONG BATHYMETRICAL AND TEMPORAL GRADIENTS

3.1 Abstract

The global rise of plastic deposition and accumulation is of growing concern. Plastics, including microplastics, are pervasive throughout the world's water bodies, reaching from local freshwater systems to the Southern Ocean. The isolating circumpolar current enhances the potential for accumulation of plastics, including microplastics. Initial research in the Southern Ocean suggests low amounts of microplastic pollution comparable to the offshore maritime regions. However, only the surface and shallow subsurface samplings were considered, ignoring polymer type identification, bathymetrical, and temporal gradients. Here, I assess overall abundance, polymer type, and polymer density group (positively or negatively buoyant microplastics) compositional changes in the Western Antarctic Peninsula. Microplastic distributions are based most strongly on size fraction with depth and time as potential secondary influencers. While the mechanisms by which seasonality influences microplastic distribution is undiscernible, these results provide context for the amount and types of microplastics that the local fauna and microorganisms of the Southern Ocean are exposed to. This research will inform future investigations simulating microplastic distribution and the interactions between microplastics and the local community of the Southern Ocean.

3.2 Introduction

Accumulation has resulted in plastics becoming the most common form of marine debris, with an estimated 60%-80% of all marine debris and over 90% of all floating debris (Gordon, 2006). In addition, signs of the accumulation can start to be seen in the geological record, known as the plasticene (Haram et al., 2020; Ilechukwu et al., 2023; Lewis et al., 2016; Rangel-Buitrago et al., 2022; C. Reed, 2015). The Plasticene stands to prevail well beyond the cessation of plastic production because of their environmental persistence. Plastic persistence is a result of larger-sized plastics continuously degrading into smaller and smaller fragments via biodegradation, mechanical action, and photooxidation (secondary microplastics) (Andrady, 2011; Gewert et al., 2015). While the timescale and scope remain largely unknown, one study estimated it could take 300 years for a 1 mm polyethylene particle to be reduced to 100 nm particle in marine sediments and waters (Harshvardhan & Jha, 2013). Alternatively, another source of (primary) microplastics is their direct production by factories for use in industries such as cosmetics, sand-blast media, and use in research (Andrady, 2017; Fendall & Sewell, 2009; Millette et al., 2023; Sanders et al., 1989; Sanders & Porter, 1988; Setälä et al., 2014).

Although microplastic distribution is considered ubiquitous, it is not homogenous with pattern related to marine current and bathymetry. High concentrations have been reported at the surface in central areas of the North Atlantic and Pacific oceans (Eriksen et al., 2013; Goldstein et al., 2012; Law et al., 2010). Current ocean circulation models suggest five possible accumulation areas in all five subtropical gyres, but they do not consider the Southern Ocean (Lebreton et al., 2012; Maximenko et al., 2012). In addition to regional differences by current, there is a growing body of research, suggesting heterogeneous distribution of microplastics along a bathymetrical gradient (Choy et al., 2019; Enders et al., 2015; Reisser et al., 2015; Rowlands et al., 2023). For example, Peng et al. (2018) documented low concentrations of microplastics at the deepest depths of the Mariana Trench. Recent models project the greatest frequency of microplastics at the surface with the most substantial dip in microplastic concentration occurring over the first few meters (Enders et al., 2015; Reisser et al., 2015). Choy et al. (2019), found a different trend with significant amount of microplastics concentrated within the upper 200 m of the water column. Rowlands et al. (2023), showed varying degrees of microplastic flux throughout the depth profile of the water column. This included variation across sizes, with the largest flux within the smallest size fraction (Rowlands et al., 2023).

The amount of research within the Southern Ocean is reduced compared to other ocean bodies (Waller et al., 2017). However, there are several studies which have investigated microplastics and their distribution within the Southern Ocean. Isobe et al. (2017) estimated >100,000 pieces of microplastic pollution per km^{-2} in the open waters of Antarctica, similar to those of the subtropical and temperate waters estimated by Eriksen et al (2014). Waller et al. (2017) estimated an average microplastic density of 22 particles L^{-1} and max of 117 particles L^{-1} around the Western Antarctic Peninsula (WAP) region. Along a circumpolar navigation study, Suaria et al. (2020) found low microplastic densities averaging 187.6 particle km^{-1} throughout the polar open ocean compared to coastal, temperate regions. Due to the logistical constraints of *in situ* microplastic sampling and labor intensive microplastic polymer identification, these studies only provide a snapshot of either total microplastic pollution by weight or by number of particles at the ocean's surface and didn't aim to identify and assess the distribution of plastic polymer composition on either bathymetrical or temporal gradients.

Plastics differ in origin, composition, and size, all of which dictate their fate in aquatic ecosystems. Differing polymer types between microplastics relate to a wide range of densities associated with each polymer, which has implications for their occurrence throughout the water column. Polymer densities range from 0.85 g cm^{-3} (polystyrene) to 2.3 g cm^{-3} (polytetrafluoroethylene, PFTE) corresponding to positive and negatively buoyant microplastics, respectively (Enders et al., 2015). Wave action and ocean turbulence of the upper-ocean can also lead to vertical mixing (Price et al., 1987), especially of buoyant particles. Most recently, Rowlands et al. (2023) found decreasing flux of microplastic particles with depth, dropping from 306 particles m^2 d^{-1} at 50 meters to 96 m^2 d^{-1} at 150 meters. Whereas Galloway et al (2017) suggested mechanisms by which sediment bioturbation from benthic fauna could potentially re-release settled microplastic particles back into solution, but has yet to be seen *in situ* (Näkki et al., 2019). Additionally, seasonal ice formation and ice melt provide a mechanism for microplastic entrapment and release, and the degree of annual ice melt can change (Bergmann et al., 2022; Galloway et al., 2017; Henley et al., 2019; Kelly et al., 2020; Obbard et al., 2014). Microplastics have been recorded in the benthic sediments (2×10^2 particles L^{-1}) and the floating sea ice (11.71 particles L^{-1}) within the Southern Ocean (Kelly et al., 2020; Reed et al., 2018). Yet, much of our knowledge is based on temperate and tropical waters with disproportionately few studies investigating polar waters. Of these studies, only one investigated the water column at depth, increasing the difficulty to infer the impact microplastics have in the Antarctic, particularly at deeper depths and changing seasons.

This work aims to aid in the understanding of the microplastic vertical distribution across temporal and bathymetrical gradients. Seawater was sampled from the same location within the Western Antarctic Peninsula (WAP) during two different years and seasons (late spring 2019 and winter 2022) throughout the water column. Microplastics were collect through serial filtration to evaluate different size ranges of microplastic contamination including small-microplastics (0.22 – 20 µm; S-MP), medium-microplastic (20 µm – 100 µm; M-MP), and large-microplastics (>100 µm; L-MP). Determining the seasonal and environmental influence on the distribution of microplastics is critical in determining the bioavailability to local biota and pervasiveness of microplastic pollution within the Southern Ocean (Andrady, 2022; Galloway et al., 2017). This work can provide an empirical dataset to better inform prediction models of oceanic microplastic distribution within polar waters, which can help inform more effective microplastic pollution policy and conservation strategies.

3.3 Methods

Samples were collected aboard the Nathaniel B. Palmer during two expeditions along the Western Antarctic Peninsula (-64.54º; -62.37º to -68.05º; -68.30º) occurred from November 6th – December 9th, 2019 (NBP 1910) and the second cruise occurred from May 31st – July 25th (NBP 2205). During these cruises, we collected samples from the same station in Paradise Bay (station R in late spring and station PS15 in early winter, Figure 4.1) over a range of depths starting from the subsurface (~1m depth) to the CTD depth limit (~10m above the seafloor: 281m) using 12 L Niskin bottles mounted on a

CTD rosette. This sampling included the Deep Chlorophyll Maxima (DCM, ~23m) depth during the Late Spring season station (station R). In Early Winter (station PS15), there was no clear DCM and changes to the physical oceanography of the water column (i.e., temperature, salinity, and pressure) indicating distinct water features were used to determine sampling depths. Logistical limitations and differential physical oceanography of the water column created a difference in the number of depths represented between the two sampling periods and size fractions. Late Spring had six total depths (n = 6) and Early Winter had eight total depths (n = 8). During both seasons the smallest size fraction was not assessed for all depths. The Late Spring only had three depths (Surface, 23 m, and Deep) analyzed and the Early Winter had four depths (Surface, 15m, 120m, Deep) analyzed for the small-microplastic size fraction. Conductivity, water temperature, depth, salinity, oxygen, oxygen saturation, fluorescence, percent beam transmission, irradiance (PAR), time, latitude, and longitude were estimated *in situ* with a CTD Sea-Bird SBE 9-11plus V5.1g, with WET Labs ECO-AFL/FL and C-Star probes.

3.3.1 Sample Collection

Seawater samples were fractionated to assess microplastic pollution in biologically relevant size classes, which nanoplankton could theoretically consume (0.22 µm – 20 µm, small-microplastic), adhere to (20 µm – 100 µm, medium-microplastic), and/or colonize (>100 µm, large-microplastic). Whole seawater samples were placed through a filtration series of 100 µm and 20 µm nylon mesh (Wildlife Supply, Yulee, FL, USA). The amount filtered varied due to logistical limitations of sampling with the volume of seawater for the medium- and large-microplastic size fraction ranging from 12 to 24 L. The resulting filtrate (2 to 4 L of < 20 µm filtered seawater) was then filtered on to 0.22 µm mixed cellulosic ester filters (Whatman, Cytivia). After filtration, the 100 and 20 µm nylon mesh were placed into 50 mL tubes with 45 mL of 0.22 µm filtered seawater from the same sample and shaken for 15 minutes to resuspend the microplastics, which were then also filtered onto 0.22 µm mixed cellulosic ester filters. Filters were then wrapped in aluminum foil and placed into -80 ºC incubator until processing. Samples were not subjected to acid digestion due to evidence suggesting remaining residues from the digestion process could lead to an increase in false positive identification of microplastic particles (Primpke et al., 2024).

3.3.2 Contamination Control

To control for contamination of aerosol microplastics, a dry filter 0.22 µm, 47mm filter was placed on the bench at the start of sampling. Nitrile gloves were worn when handling seawater samples and only glass containers were used during the filtration process. All glassware was sterilized via acid washing and triple rinsed with MilliQ water. At the end of each cruise, a Niskin blank was prepared: a Niskin bottle, washed between each station, was filled with filtered 0.22 µm seawater, then the seawater was filtered as previously described for field seawater samples. Only 2 plastic particles were identified via the Niskin blanks, and no contamination could be identified via air controls.

3.3.3 Spectral Acquisition

Micro-Raman imaging was conducted using a Renishaw InVia confocal microscope (Renishaw, UK) controlled by WiRE software (version 4.4.0.6908). Prior to spectral acquisition, filtered samples were visually inspected for potential microplastic particles via confocal microscopy. The large-microplastic size fraction was analyzed from half of a filter at 50x magnification, the medium-microplastic size fraction from one twentieth of a filter at 200x magnification, and the small-microplastic size fraction from one full diameter cross section at 500x magnification for spectral analysis. Raman spectra for each particle of interest was then acquired using a 15 mW with a 2 µm diameter beam 532 nm wavelength laser (Renishaw RL532C50), at 1 – 5% laser intensity with ten separated, 1 second exposures. All collected spectra were centered at 1250 cm^{-1}, with a range of 370 to 2100 cm^{-1}.

3.3.4 Spectral Preprocessing and Identification

Collected Raman spectra for potential microplastic identification were subjected to preprocessing and smoothing of spectra for increased microplastic identification accuracy. Filter background, background noise, and elevated intensity baselines were removed via 6th order polynomial baselines and the subtraction of scattering caused by the filter, using the hyperspec package in R (Beleites & Sergo, n.d.). Spectral analyses were then smoothed using 1st degree derivative transformation. All spectra were then standardized using standard normal variate and min-max standardization, within 0 – 1, in accordance with spectroscopy microplastic identification methods outlined in Cowger et al. (2020). Processed spectra were then compared to reference polymer spectra within the OpenSpecy library with product moment correlation coefficients to create a hit-index matrix (Cowger et al., 2021; Ng et al., 2009). Highest matches above 0.5 hit index were used to positively identify plastic polymers. Abundance of positively identified polymers were estimated using a correction factor like those carried out for microscopic enumeration of protistan abundance. Post identification, particles were then classified as either more or less dense by comparing the polymer density noted in the OpenSpecy library to the density of the water column from which the particle was identified. Of the identified polymers, 40% were positively buoyant (PE and PP), and 60% were negatively buoyant (PET, ABS, and PA).

Detection limit equation:

$$\text{Limit of Detection} = \left(\frac{1}{fraction\ of\ filter\ analyzed}\right) \times \text{ volume filtered}$$

Detection limits for the small-, medium-, and large-microplastic size classes were 140.25, 2.25, and 0.1 particles L^{-1}, respectively. For clarity in the results and discussion, below detection limit (BDL) refers to these values for each size class, respectively.

3.3.5 Data Analysis

To assess the collinearity between environmental variables, a correlation matrix calculating the Pearson's r coefficient of all environmental variables. Principal Component Analysis (PCA) using z-scores of environmental variables was used to identify the seasonal differences between stations. Fisher's exact test was used to calculate differences in the frequency of microplastic detection between stations and size fractions. To assess relationships between microplastic and environmental parameters a correlation matrix was used to calculate Pearson's r coefficients. All calculations and data analysis were performed using the R base stats, hyperspec, and propectr packages (Beleites & Sergo, n.d.; R Core Team, 2020; Stevens & Ramirez-Lopez, 2022).

3.4 Results

3.4.1 Environmental Conditions

The same location was sampled on two different cruises (NBP 1910 and NBP 2205) in Paradise Bay within the Southern Ocean. For clarity in the results and discussion, Stations R and PS15 with be identified as Late Spring and station Early

Winter, respectively. Changes to physical properties of the water column (i.e. beam transmission and temperature) were used to determine sampling depths. While the sampled stations were in the same location, there were strong differences between the water column properties. Temperature, conductivity, fluorescence, PAR, and surface PAR were consistently higher in Late Spring with an average of 0.20 ± 0.38 ˚C, 28.6 ± 0.2 mS cm^{-1}, 1.43 ± 1.38 mg m^{-3}, 90.07 ± 172 µmol m^{-2} s^{-1}, and 1132.97 ± 32 µmol m^{-2} s^{-1}, respectively. In comparison, Early Winter presented lower averages of -0.45 ± 0.29 ˚C, 28.1 ± 0.04 mS cm^{-1}, 0.01 ± 0.02 mg m^{-3}, 0.08 ± 0.19 µmol m^{-2} s^{-1}, and 23.91 ± 0.84 µmol m^{-2} s^{-1}, respectively. The inverse was observed with percent transmission and density where Late Spring presented an average of 92.85 ± 5.84 % transmission and 1027.4 ± 0.3 kg m^{-3}. Early Winter saw increased averages of percent transmission (97.03 ± 0.51) and density (1028.1 ± 0.6 kg m^{-3}) (Figure 3.1). Salinity, dissolved oxygen, and dissolve oxygen saturation did not present significant differences between seasons with values of 34.15 ± 0.29 and 34.15 ± 0.15 PSU, 6.49 ± 0.96 and 6.45 ± 0.41 mL L^{-1}, and 8.02 ± 0.07 and 8.15 ± 0.07 mL L^{-1}, respectively.

To further understand the differences between Late Spring and Early Winter samplings, a principal components analysis was performed using z-scores of depth (m), temperature (˚C), surface PAR, PAR, salinity, fluorescence, percent transmission, Dissolved Oxygen, and Dissolve Oxygen saturation. The first two principal components explain 81% of the variability in this dataset. There was a clear distinction between the two seasons, which decreased with the bathymetrical gradient. The largest distance between samples in the principal component analysis occured at the surface (Figure 3.1). Late Spring was associated with a shallower mixed layer (ZML; 17.83 m), with a deeper depth of photic zone (Ze, 28.71 m) and deep chlorophyll maxima (ZCM, 10.89 m) (Figure 3.1) The inverse was true for Early winter, which presented a deeper mixed layer (ZML; 56.44 m), combined with a shallower depth of photic zone (Ze; 14.85 m) and deep chlorophyll maxima (ZCM; 3.96 m).

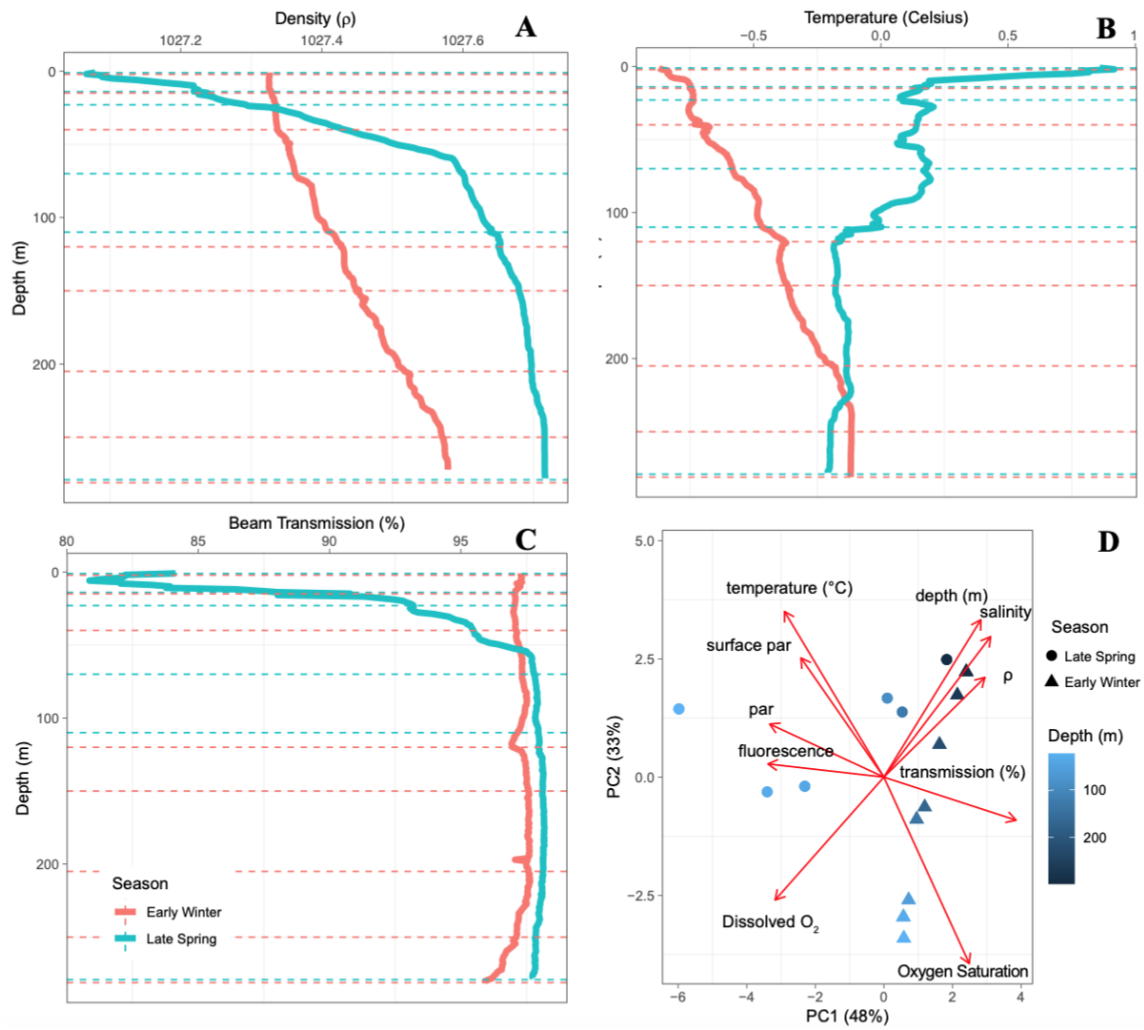

Figure 3.1 Analysis of physical oceanographic properties of the water column between seasons. (A) The depth profile of water column density (ρ) shows a reduced change in density below 60 m in the Late Spring, that was not observed in Early Winter. (B) The depth profile of water column temperature (°C) shows a strong thermocline at 15m with a smaller deeper thermocline at approximately 120m in the Late Spring, while the Early

Winter increases in temperature throughout the water column until a plateau starting at 220m. (C) The percent beam transmission (%) was relatively constant below 50 m in the Late Spring, while in Early Winter the beam transmission was consistent throughout the water column, except for small peaks at depths of 120m and 205m. (D) Principal Components Analysis (PCA) of selected environmental factors showed significant differences between Late Spring and Early Winter, but the depth differences, indicated by symbol color, occur along a similar path. The distance between Late Spring and Early Winter was reduced as the depth increases. The largest environmental differences occur at the surface waters and most driven by PAR, fluorescence, temperature, and % transmission. Dotted lines indicate depth of sampling for each season, indicated by the line color.

3.4.2 Microplastic Distribution by Abundance

While Late Spring samples contained some level of microplastic pollution at all depths sampled (100%; n = 6), microplastics were detected in only 63% (n = 8) of Early Winter samples (5 of 8 total) (Figure 3.2). All the samples examined for the small-microplastic were positive (n = 7), while only subsets contained medium- and large-microplastics (64% or 9 of 14 and 36% or 5 of 14, respectively Figure 3.2). During the Late Spring expedition, large-microplastics were detected in all depths (n = 6), except the Deep sample, for which the detection was below the limit. During Early Winter, no large-microplastics were detected at any depth and the number of undetectable samples differed significantly (Fisher's exact test; $p < 0.05$) (Figure 3.2). The range of the amount of analyzed particles positively identified as microplastics varied across size and season. The S-MP saw the largest percentage of particles identified as microplastic with an upper range of 62% (Table 3.1). Overall, a larger percentage of particles were identified as microplastics in the Late Spring compared to the Early Winter (Table 3.1).

Table 3.1 Ranges of microplastic identification as a percentage of the total number of particles analyzed per sample.

Season	Size Fraction: S-MP	M-MP	L-MP
Late Spring	3 - 62%	16 - 24%	0 - 47%
Early Winter	8 - 26%	0 - 20%	0%

Note. Ranges are categorized by size fraction and season. In general, a larger percentage of particles were identified as microplastics in the Late Spring compared to the Early Winter. Overall, the percentage of positively identified particles had an inverse relationship with size. The S-MP (0.22µm – 20µm) showed the highest percentage identified and decreasing percentages with each increase in size class (M-MP and L-MP).

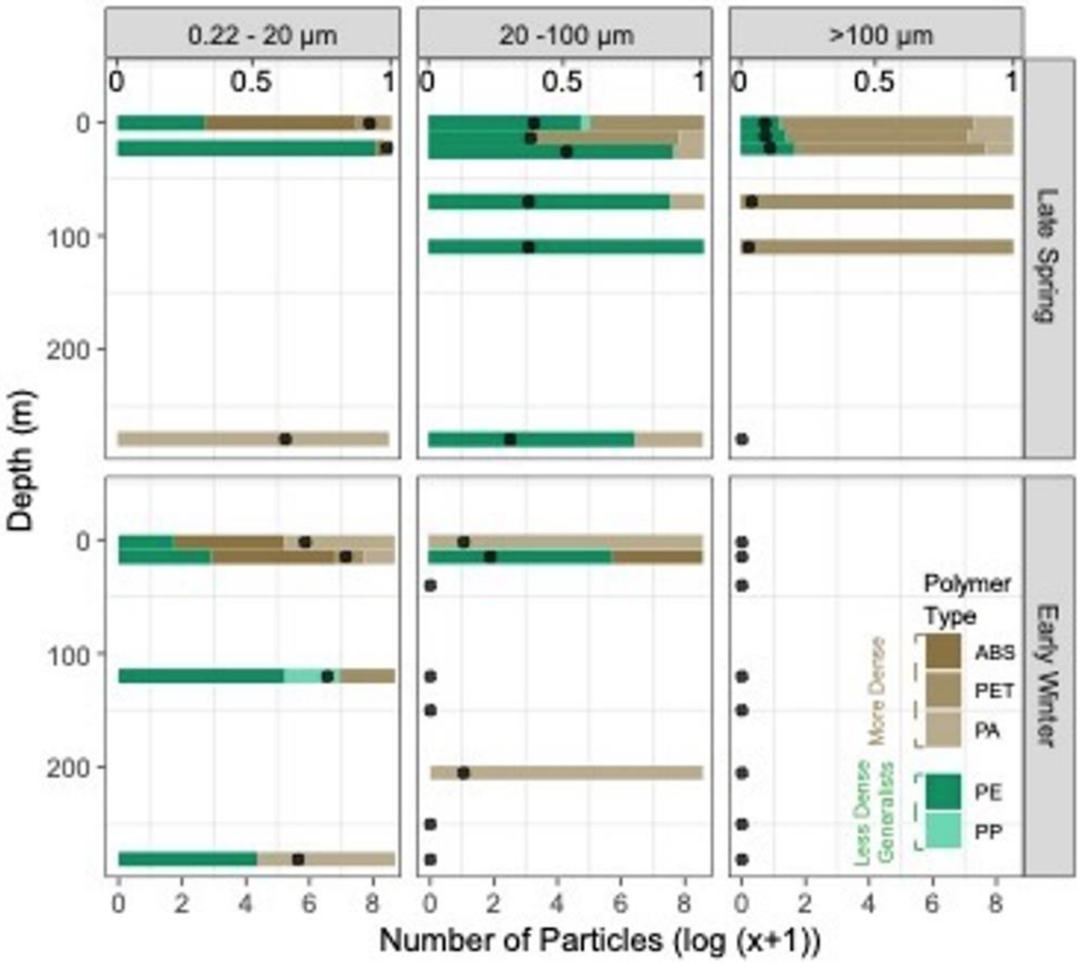

Figure 3.2 Estimates of microplastic concentrations reported as number of particles L^{-1} (log (x +1)) for both seasons, by size fractions, and with the proportion of each polymer types detected for this study. Black dots represent the number of particles L^{-1} (log[x+1]); samples below detection limit (BDL) were indicated by a dot at zero and without a proportional bar. Depths without dots were not evaluated within this study, i.e., small-microplastics were evaluated at fewer depths than medium-, and large-microplastic size classes. Early Winter showed a greater amount of BDL samples compared to the Late Spring. Denser particles dominated the largest size fraction, while the less dense particles increased in the two smaller fractions. Detection limits of 140.25, 2.25, and 0.1 particles

L^{-1}, were calculated for small-, medium-, and large-microplastic size classes, respectively. The relative densities of microplastics were compared to the water column density.

The microplastic pollution estimates in the smallest size fraction (0.22 µm – 20 µm) consistently showed at least an order of magnitude greater concentration than either of the other size fractions (Figure 3.2). Throughout the entire study, small-microplastic estimations ranged from 187 to 4628 particles L^{-1} (Figure 3.2). Where detectable, Late Spring showed both the lowest and highest estimations of microplastic, which occurred at the Deep and 23 m depths, respectively. The Early Winter showed a narrower range from 280 to 1262 small-microplastic particles L^{-1}. Both sampling periods showed the highest estimates in the middle pycnocline depths of 23m and 15m, during the Late Spring and Early Winter, respectively (Figure 3.2). The surface waters differed markedly across the season with estimates of 2665 and 351 particles L^{-1}, in the Late Spring and Early Winter, respectively. The Deep samples showed reduced differences with estimates of 187 in the Late Spring and 280 particles L^{-1} in the Early Winter (Figure 3.2).

The second largest size fraction by abundance was the medium-microplastic (20 – 100 µm), consistently estimated an order of magnitude higher than the large-microplastic size class, but an order of magnitude lower than small-microplastics (Figure 3.2). Across the seasons, the medium-microplastic size fraction estimated a distinctly lower concentration of particles, ranging from 1.9 to 72.1 particles L^{-1}, in samples with detectable amounts of microplastics (Figure 3.2). Akin to the small-microplastic size class, the medium-microplastics showed an elevated range of 11.2 to 72.1 particles L^{-1} in the Late Spring, and an order of magnitude lower range (1.87 to 5.61 particles L^{-1}) in the

Early Winter (Figure 3.2). The maximal estimates of medium-microplastics during either season occurred at the same depths of the small-microplastic size class (Figure 3.2).

The large-microplastic fraction (> 100 µm) showed the lowest abundance, with an order of magnitude lower than the medium-microplastic size fraction. The large-microplastic estimates ranged from 0.24 to 1.42 particles L^{-1}, among samples with detectable levels of microplastics (Figure 3.2). As previously mentioned, no large-microplastics were detected during the Early Winter with the detectable limits of the method used. During the Late Spring, the highest estimate of large-microplastic of 1.42 particles L^{-1} occurred at 23 m depth in the Late Spring, while the lowest value of 0.24 particles L^{-1} within the Late Spring was at the Deep, i.e at similar depths as the two other size fractions (Figure 3.2).

Results of the correlation matrix found no significant correlation results when including all size fractions with estimated abundance. However, this is not the case when we evaluate each size class separately. From smallest to largest size class, all size classes showed significant positive correlations with fluorescence coefficients of 0.97, 0.72, 0.94 ($p < 0.05$). The largest size fraction also showed significant negative correlations with percent beam transmission ($r = -0.77$, $p < 0.05$) and water column density ($r = -0.58$, $p < 0.05$; Appendix C).

3.4.3 Microplastic Composition by Polymer and Density Class

Overall, there were a total of five different plastic polymers, which were predominantly fragments or fibers, found throughout the study: Acrylonitrile Butadiene Styrene (ABS), Polyethylene Terephthalate (PET), Polyamide (PA, nylon), Polyethylene (PE), and Polypropylene (PP) (Figure 3.2). Whenever detected, the polymers ABS, PET, and PA were identified as negatively buoyant, while PE and PP were identified as positively buoyant. All five polymers were found in both seasons, but not in all size fractions. In both the small- and medium-sized microplastics, all the polymers classified in the study were detected at some depth, while only PA, PET, and PE were identified in the large-microplastic fraction (Figure 3.2). PE was the most frequently detected polymer and was found in 46% (n = 35 total samples), while PA, PET, ABS, and finally PP with detection frequencies of 37%, 26%, 14%, and 6% of the samples, respectively. However, like overall abundance, there are marked differences in polymer composition and density class by size and season.

Within the small-microplastic size, PE was the most detected and abundant microplastic polymer, found in all but one sample (Late Spring, Deep) (Figure 3.2). Maximal PE contribution to the microplastic community occurred in the Late Spring (0.94 proportion, 23 m) and the range reduced in the Early Winter, with a maximal proportion of 0.6 at 120 m (Figure 3.2). The second most common polymer, PA, ranged from undetectable to a proportion of 1 (100%) in the water column and like PE, PA saw a reduction in the range during the Early Winter (Figure 3.2). When detectable in a sample, ABS consisted of up to a proportion of 0.55 of the observed particles in the Late Spring, with a maximal proportion of 0.44 in the Early Winter (Figure 3.2). PET and PP were never greater than 0.13 and 0.2 proportion of total detected particles and PP was detected in only one sample (Early Winter, 120m). As a result, positively and negatively buoyant particles constitute similar proportions of the microplastic community.

Microplastic polymer distributions showed unique relationships with environmental variables within the small-microplastic size fraction (Figure 3.2). ABS distribution is limited to the upper water column (at 23 m and above) and exhibited a significant negative correlation with depth, salinity, and positive correlation with dissolved O_2 ($r = -0.8$, $p < 0.05$; $r = -0.81$, $p < 0.05$; $r = 0.82$), $p < 0.05$; respectively, Figure 3.2). PA distribution was the inverse, with a significant positive correlation with depth, salinity, and negative correlation with dissolved O_2 ($r = 0.77$, $p < 0.05$; $r = 0.83$, $p < 0.05$; $r = -0.78$), $p < 0.05$; respectively, Figure 3.2, Appendix D). Similarly, the proportion of PE in samples had a significant positive relationship with the water column density ($r = 0.81$, $p < 0.05$, Figure 3.2). Interestingly, these depth distributions do not correspond with the polymers' relative density to water, with the densest polymer (ABS) frequently the most abundant at the surface and the less dens PE detected commonly at the surface, but also in the deepest samples (Figure 3.2).

PE was the most common polymer detected in the medium-microplastic size class and ranged from 0 to 1 (100%) proportion of the community (Figure 3.2). There was a notable difference between seasons, with a simultaneous in both the range (BDL to 0.67 proportion) and frequency of detection (from 100% to 12.5%) during the Early Winter ($n = 6$ and 8, respectively). PA was the second most detected polymer and ranged from undetectable to 1 proportion of the community (Figure 3.2). Unlike the small-microplastic size class, the distribution range of PA decreased in the Late Spring, with a maximal proportion of 0.25, compared to 1 (100%) in the Early Winter. In contrast, PET exhibited a distribution range from BDL to 0.55 proportion but was only detected in the two upper depths in the Late Spring (Figure 3.2). ABS ranged from BDL to 0.33 but was only detectable in a single depth (Late Winter pycnocline, 15 m). Additionally, PP was identified in just one sample and was never more than 0.03 proportion of the detected polymers (Figure 3.2). Consequentially, the positively buoyant particles dominated the community in the Late Spring, while the negatively buoyant particles constituted a greater proportion of the Early Winter (Figure 3.2).

Distinct associations with environmental variables were observed for some polymers within the medium-microplastic size range. PET and PP saw strong significant negative correlations with percent transmission ($r = -0.86, -0.83$; $p < 0.5$) (Appendix C). But a significant positive relationship with PAR, temperature, and fluorescence ($r = 0.68, 0.99, 0.7$; $p < 0.5$) (Appendix C). PE saw significant correlation with density ($r = -0.61$, $p < 0.05$) and ZML ($r = -0.85$, $p < 0.05$, Appendix C).

In contrast to small- and medium-microplastic size ranges, PET was the most common polymer in the large-microplastic size class, both in terms of abundance and frequency of detection (Figure 3.2). The most frequently detected polymers were PET (detected in 5 of 14), followed by PE (3 of 14) and PA (3 of 14, Figure 3.2). In Late Spring, PET clearly dominated, ranging from BDL to 1 (100%) proportion of the microplastic community in Late Spring (Figure 3.2). PE and PA both shared the second most frequently detected polymers, with proportions ranging from BDL to 0.2 and BDL to 0.17, respectively. In Early Winter, no microplastic pollution was detected in any samples, and PP and ABS polymers remained undetectable in both seasons (Figure 3.2).

For large-microplastics, several potentially influential environmental variables, such as density, depth, and percent transmission, and fluorescence, were found to have significant correlations. However, only two variables that were significantly correlated with all polymer types identified in this size class were density and fluorescence (Appendix C). Both PE and PA exhibited a significant negative relationship with density

($r = -0.95, 0.96, p < 0.05$), while PET showed a positive correlation ($r = 0.9, p < 0.05$) (Appendix C). Regarding fluorescence, the correlations were inverse for the polymers: PE and PA shared a significant positive relationship ($r = 0.93, 0.89, p < 0.05$), whereas PET had a negative relationship ($r = -0.88, p < 0.05$, Appendix C). However, due to the limitations discussed earlier, only Late Spring data were available for these environmental correlations within the largest size class.

3.5 Discussion

There is a growing body of literature that examines the distribution and abundance of microplastic throughout the world's water bodies (Cozar et al., 2014; Eriksen et al., 2014; Miller et al., 2017; Sonke et al., 2022). However, very few studies that involve polymer enumeration along bathymetric gradient and different seasons, especially in the Southern Ocean. Most studies within the Southern Ocean were restricted to only the neuston layer, subsurface layers (up to at most 1m of depth), deep-sea sediments, and ice layer. These investigations assessed the total amount of plastic pollution by weight, without the consideration of either size class or polymer composition at a single moment in time (Kelly et al., 2020; Kuklinski et al., 2019; S. Reed et al., 2018; Rowlands et al., 2023; Shannon, 2020; Waller et al., 2017). This study is among the earliest to examine microplastic pollution with size fractionation and polymer identification at depth in the Southern Ocean, and the first within the Western Antarctic Peninsula region. I investigated the microplastic distribution of three different size classes (> 100 µm, 100 µm - 20 µm, and 20 µm - 0.22 µm) and estimated microplastic abundance (number of particles) by polymer type throughout the water column.

Moreover, this study is the first to include microplastic polymer enumeration in different seasons within the Southern Ocean.

3.5.1 Water Column Differences Between Seasons

The structure of the water column in Paradise Bay showed strong differences between the late Spring, and the early Winter. Values reported here are well within the ranges reported over the last few decades (Arrigo et al., 2017; Grattepanche et al., 2022; Ishikawa et al., 2002; Martinson et al., 2008; Nardelli et al., 2023; Schofield et al., 2018). The mixed layer, calculated based on salinity and temperature profiles, were significantly deeper in the early winter of 2022 versus the late spring of 2019 and is consistent with previous recordings within the region (Grattepanche et al., 2022; Martinson et al., 2008; Schofield et al., 2018b). The mixed layer was also deeper than the deep chlorophyll maxima in Late Spring and Early Winter, which may explain some of the similarities in the upper sampled depths in abundance and polymer composition. Although there is a peak fluorescence depth (ZCM) in Early Winter, the values of fluorescence are extremely low, and the season can be considered to lack a true ZCM layer. Additionally, average PAR, Surface PAR, and depth of the euphotic zone (Ze) are all significantly lower in Early Winter than Late Spring. The discrepancy between fluorescence paired with differences in irradiance between the stations could explain the significant differences in the observed percent beam transmission, which was significantly higher in Early Winter (Arrigo et al., 2017; Coble et al., 1991). In contrast, the overall temperature is lower in Early Winter, which is reflected in the increase in average water density between early winter and late spring with little to no change in the average salinity.

3.5.2 Seasonal Impacts on Microplastic Abundance and Composition

There were differences in estimated abundance, polymer composition, and detectable depths between late Spring and early Winter seasons, however, differences were not consistent across microplastic size. The macro- and medium-microplastic size classes exhibited greater differences between seasons in both abundance and proportional composition than the small-microplastic size. The large-microplastic size fraction observed a dominance of negatively buoyant (mostly PET) microplastic particles in the late Spring, while there is no presence of microplastics in the early Winter. The medium-microplastic size class presented with higher total abundance and higher proportional composition of positively buoyant particles, mainly PE. Inversely, the early Winter presented with lower abundances and higher proportions of negatively buoyant particles, which is driven by PA. The small-microplastic size fraction presented with the lowest difference between seasons, with similar ranges and proportional compositions of microplastic polymers.

There are several mechanisms which could theoretically cause seasonal variation in microplastics, including physical oceanographic and biotic changes to the water column. For example, a change in temperature as the water cools during the Winter months and subsequential increased mixed layer depth, ice formation, water density could all impact microplastic distribution by altering the amount of mixing, ice entrapment, and flux towards the seafloor (Cozar et al., 2014; Kelly et al., 2020; Obbard et al., 2014; Rowlands et al., 2023; Shannon, 2020). In addition to physical oceanographic indicators, seasonal changes to biological indicators such as increased fluorescence, which is strongly correlated with phytoplankton abundance, and the consequential reduction percent beam transmission may impact the amount of microplastics in the upper portion of the water column. Recently, several studies revealed microplastic interaction with the biotic portion of the water column via ingestion, colonization, and/or extracellular matrix entrapment potentially. This interaction could prevent the sinking of plastics during the growing season by being caught in the biomass during Spring and Summer, or increased microplastic seafloor deposition as marine snow in the Winter (Alimi et al., 2018; Amaral-Zettler et al., 2020; Galloway et al., 2017; Hitchcock, 2022).

While there are no seasonal studies along a bathymetrical gradient within the Southern Ocean to compare, there was a 9 year study by Shannon (2008 – 2017) conducted from New Zealand to the Ross Sea investigating microplastics along the surface waters (Shannon, 2020). Contrary to the current study, Shannon (2020) found no consistent positive or negative relationships between microplastics and year but found highly variable and significant differences across the years. However, no samplings occurred over the winter months and the study was performed in a different region of the Southern Ocean. The potential for interannual variation could be caused by large scale current flow differences between years such as a La Niña or El Niño events, or differences in ice flow dynamics caused by global warming throughout the region (Henley et al., 2019; Nardelli et al., 2023; Shannon, 2020). Further research is needed to determine whether the differences observed are caused by interannual variability or seasonal effects.

3.5.3 Size Fraction Differences in Abundance

As expected, the amount of microplastics estimated increased as the size of the microplastics decreased (Alimi et al., 2018; Andrady, 2017). Microplastic abundance differed by several orders of magnitude across the difference size ranges. On average, the small-microplastic fraction consisted of 99% of the total amount of plastic estimated within the samples. Followed by medium-microplastic size fraction, which contributes 0.99% of the total abundance. The rest was contributed by the largest size fraction (>100 µm), which contributed 0.01% of the total microplastic estimated.

The amount of microplastic in this study was higher than most other investigations within the Southern Ocean (Kelly et al., 2020; Le Guen et al., 2020; Rowlands et al., 2023; Suaria et al., 2020; Waller et al., 2017). However, this study investigates a considerably smaller size fraction than all other studies conducted within the region, with the smallest size fraction of 0.22 µm – 20 µm fraction. A recent polar study from the Arctic Ocean used a comparable lower size limit of 2.2 µm and uncovered microplastic contamination at similar quantities (10^2 - 10^3 particles L^{-1}) and percentage composition (>90% of total microplastic particles) within the smallest size fraction as indicated in the present study (Bergmann et al., 2023). Of all the microplastic distribution analyses within the Southern Ocean, the Rowlands et al. study used the next smallest fraction with a minimum size of 45 µm and their results are comparable to the medium-microplastic fraction used here. Although they were measuring the daily flux of microplastic movement, their results were on the scale of 10^2 microplastic pieces m^{-2} d^{-1} (Rowlands et al., 2023).

However, majority of research within the Southern Ocean focused on the larger portion of the microplastic size fraction (1 - 5 mm) at the surface of the water column (Suaria et al., 2020; Waller et al., 2017). Due to the continued lack of standardized reporting (weight vs particles) and identification (spectral analysis versus light or epifluorescent microscopy), comparison to previous works can be difficult (Shannon, 2020; Waller et al., 2017). Only a subset of the research considered microplastic by number of particles with the use of spectral analysis for particle identification. The amount of microplastic from the largest size fraction reported in this study is well within the range of those established throughout the Southern Ocean, ranging from the Ross to the Weddell Seas and up through the King George Island (Gurumoorthi & Luis, 2023; Kuklinski et al., 2019; Leistenschneider et al., 2024; Lozoya et al., 2022; Suaria et al., 2020; Waller et al., 2017). In addition, the frequency of non-detectable samples observed in this study significantly increased as the size of the microplastic increased, which are similar to the frequencies found in the larger sized fractionated studies such as Kuklinski et al. (2019) and Shannon (2020).

3.5.4 Microplastic Community Polymer Composition and the Potential Influence of Environmental Variables

Only five unique polymers emerged throughout the analysis of the water column within Paradise Bay, which is lower than most studies including polymer identification throughout the world’s oceans (Bergmann et al., 2022; Choy et al., 2019; Erni-Cassola et al., 2019; Rowlands et al., 2023). Of the identified polymers, 40% were positively buoyant (PE and PP), and 60% were negatively buoyant (PET, ABS, and PA). Generally, there was no clear dominance of a particular polymer or density class of polymers, yet there are several instances where a particular polymer (and thereby density class) dominated (i.e., the large-microplastic size class of Late Spring).

Positively buoyant particles were the most abundant polymers, primarily due to the prominence of PE in the small-microplastic size range. Several studies, including a microplastic meta-analysis of polymer enumeration studies, found PE to be one of the most abundant polymers in the world, especially among studies including the smallest microplastic particle sizes (Bergmann et al., 2022; Erni-Cassola et al., 2019; Everaert et al., 2018; Ghosal et al., 2018). Even though both, PE and PP are both widely used polymers with a myriad of end-use industries, PP was the least commonly found polymer throughout this study by both abundance and proportional metrics, especially compared to PE. This report in conjunction with others reinforces the importance of research into the impacts of PE to elucidate potential impacts of microplastic pollution on the ecosystem, especially those smaller than 100 µm.

Overall, negatively buoyant particles were generally minor contributors to total abundance but not necessarily to proportional composition. Denser microplastic polymers were sizable contributors within the medium- and large-microplastic size classes. Unlike the positively buoyant portion of the community, their occurrence depended on multiple polymers, which varied by size fraction and season. ABS was the most abundant dense polymer throughout the study due to its presence in the small-microplastic size fraction. Despite this, ABS never dominated in abundance due to the prevalence of the positively buoyant PE in the smallest size class. Both ABS and PA, were most abundant in the smallest size fraction and displayed a negative relationship with increased fractionation size. Inversely, PET revealed a positive relationship with size and was most abundant in the largest size fraction, dominating the microplastic community by consistent making up greater than half of the community in all detectable samples.

There remain several potential mechanisms which may theoretically result in the observed differences between polymer density groups. The innate chemical property of each polymer, specifically density, has been purported to influence plastic deposition and distribution (Erni-Cassola et al., 2019; Galloway et al., 2017). This allows for the possibility of the denser polymers to settle out of the pelagic into the benthic sediments as marine snow, while the less dense polymers may be entrapped in the uppermost layer of the ice (Galloway et al., 2017; Leistenschneider et al., 2024; Obbard et al., 2014). However, as particles get smaller inertial forces give way for viscous forces to dominate, suggesting that currents, mixing, and water column stability could significantly impact microplastic vertical distribution in the water column. (Ijaz et al., 2024; Shamskhany et al., 2021)

Potential environmental indicators for microplastic pollution and distribution varied by microplastic size and polymer type. Overall, PA, PET, and ABS displayed negative relationships with either percent transmission or depth. However, examination of the size fractions reveals differing and some concealed potential relationships between microplastics and environmental indicators, especially for the positively buoyant polymers. In the small-microplastic size class, PE and PA showed significant correlations with water column density and depth, respectively. Within the medium-microplastic fraction, PET was significantly correlated with fluorescence and percent transmission, while PA was only correlated with percent transmission. Meanwhile PA, PET, and PE were all correlated with density, fluorescence, and depth in the large-microplastic size class. Shamskhany et al. (2021) found congruent results suggesting the physical hydrodynamic and environmental factors that influence microplastic distribution vary by size and polymer type (i.e. density and depth). The influence of fluorescence of and percent transmission indicate a potential influence by the biotic portion of the community. For example, Bergmann et al. (2023) estimated significantly higher levels of microplastic contamination entrained within *Melosira arctica* extracellular matrices than those in the water column. These results indicate the use of biotic and abiotic variables in the prediction of microplastic distribution must be approached with caution and analyzed separately by microplastic size and polymer.

3.5.5 Potential Impacts on the Biotic Community by Polymers Identified

Among the polymers identified within this study, PE,PP, ABS, and PET have all been recently shown to impact an organism's physiology (Chae et al., 2019; Manríquez-Guzmán & Ramírez-García, 2023; Mateos-Cárdenas et al., 2019; Piccardo et al., 2020; Y. Wu et al., 2019). Recent studies into the impacts of PE microspheres indicated they can be toxic to microorganisms, albeit, in much larger concentrations than reported here (Chae et al., 2019). They have been found to interact with much larger species and accumulate via trophic transfer, but had negligible impacts on the larger organism's physiology (Mateos-Cárdenas et al., 2019). Both ABS and PET have been shown to negatively impact protists, bacteria, and larger macro organisms (Manríquez-Guzmán & Ramírez-García, 2023; Piccardo et al., 2020). While not ABS or PET, related dense chlorinated plastic (PVC) polymers have been shown to have differential effects on the photosynthetic efficiency of algae compared to a less dense (PP) polymer (Wu et al., 2019). All of these impacts could have profound repercussions felt throughout the Southern Ocean's food web (Galloway et al., 2017; Rowlands et al., 2021).

3.5.6 Conclusions

This study within the Paradise Bay region of the Southern Ocean observed microplastic pollution regardless of season and depths. The number of unique polymers that crossed into the traditionally considered "isolated" waters of the Southern Ocean are smaller compared to more coastal regions but the amount of microplastic particles were significantly abundant. The smallest size fraction composed nearly all (99%) of the total number of particles identified within the water column. While there was a low number of unique polymers found, the most common type of plastic identified was PE (positively buoyant), which was consistent among the small- and medium-microplastic groups. Contrary, PET (negatively buoyant) was the most common microplastic within the largest size fraction. Greatest differences in microplastics were seen between size class and season, but there are several environmental variables identified to potentially influence microplastic distribution. Forces such as density, depth, fluorescence, and beam transmission all differed in their relationship with microplastics across size fraction and polymer, either in their directionality and/or significance. Additionally, there is evidence that the environmental parameters influence on microplastic distribution is dependent upon both the size of the plastic particle and the chemical composition (polymer), suggesting microplastic pollution should be assessed accordingly. The partitioning of microplastics into size fractions and polymer is crucial to investigate potential environmental indicators used to predict their distributions. This study provides an important empirical dataset to aid in the accurate estimation, modeling, and prediction of microplastic pollution in future *in situ* and *in silico* studies.

CHAPTER 4

BACTERIVORY AND PRODUCTION OF NANOFLAGELLATES OFF THE WESTERN ANTARCTIC PENINSULA WITH A FOCUS ON MIXOTROPHY

4.1 Abstract

Throughout a cruise along the Western Antarctic Peninsula (WAP) during the Antarctic early summer (October - November) of 2019, we quantified the occurrence and assessed activity of the three major trophic strategies (heterotrophy, mixotrophy, and photoautotrophy) within the nano- (20 - 5 μm) and picoplanktonic communities (5 - 0.2 μm) at multiple depths. With regards to abundance, we observed no marked difference between the sub-surface and deep chlorophyll maxima (DCM) depths. However, strong latitudinal differences were detected, particularly within the southernmost samples taken from Marguerite Bay, which was attributed to changes in the amount of HNANs/ANANs in the samples. We did note, however, a low chlorophyll concentration throughout the season, with a max PNAN abundance of ~6000 cells mL^{-1}. Using microspheres, heterotrophic/mixotrophic bacterivorous activity were quantified with max mixotrophic and heterotrophic activity being 79% and 68% of system bacterivory, respectively. Like trophic abundance, there was no observed difference with depth but there was a latitudinal effect characterized by a change in heterotrophic activity between the northern and southern (Marguerite Bay) stations. Throughout the study, mixotrophic abundance and activity were relatively consistent across stations and strongly, negatively correlated with ammonium concentration and PAR, suggesting low light, low nutrient conditions allow for mixotrophy to thrive in the WAP region. While the systems were primarily dominated by phototrophs (max ~90% of system abundance), both phototrophs were and

heterotrophs showed strong signals of latitudinal effect described by environmental variables such as PAR, ice coverage, mixed layer depth. This results in environmental changes shifting trophic activity and thereby mixotrophic influence within the microbial community.

4.2 Introduction

The Southern Ocean has undergone some of the most rapid changes compared to more temperate or tropical oceanic regions (King et al., 2003; Metzl, 2019; Vaughan et al., 2003). Over the last few decades, it experienced drastic increases in temperature leading to overall reductions in sea ice extent, plus subsequent warming and freshening of the water column combined with deepening of the mixed layer depth (Brown et al., 2019; Meredith & King, 2005; S. Stammerjohn et al., 2012; S. E. Stammerjohn et al., 2008). Changes to the depth of the mixed layer influences several key abiotic and biotic environmental factors throughout the water column such as light availability/penetration depth, nutrient availability, planktonic vertical distribution (Dong et al., 2008; Kara et al., 2003; Korb & Whitehouse, 2004; Paul Bissett et al., 1994; Pinkerton et al., 2021; Prend et al., 2022; Sallée et al., 2021). Shifts in the physical oceanographic landscape of the Southern Ocean resulted in changes to selective pressure which favors smaller (pico- and nanoflagellate) plankton (Li et al., 2009; Montes-Hugo et al., 2009). Freshening of the water column through glacial and sea ice melt favor smaller cryptophytes over larger diatoms, although the mechanisms by which they outcompete remain poorly understood. The region is characterized by a short but highly productive growing season during the austral spring and summer, peaking in January – February (Arrigo et al., 2017; Li et al., 2016; Nardelli et al., 2023; Schofield et al., 2018a). As a result, the Southern Ocean accounts for approximately one third of the global carbon flux and considered to be a bottom-up controlled system (Schlitzer, 2002).

The world's oceans are critical to the control of the atmospheric CO_2 and the Earth's climate. In the oceans the base of the food web consists of the interactions between bacteria and single celled protists (phototrophic, heterotrophic, or mixotrophic nanoflagellates; PNAN, HNAN, MNAN, respectively), together, they make up the microbial loop (Caron, 2016; Mitra et al., 2016; Stoecker et al., 2017). Primary producing plankton, including PNANs and MNANs, are large drivers of atmospheric CO^2 control and play a significant role in the Southern Ocean food web and its carbon cycle (Saba et al., 2014). In addition to the importance of phytoplankton in the Southern Ocean, heterotrophic plankton, including HNANs and MNANs, also play an important role and showed the ability to remove most of daily bacterial production from the water column from a variety of environments and in some cases >100% of bacterial production and also contribute significantly to the carbon flux (Anderson & Rivkin, 2001; Becquevort et al., 2000; Duarte et al., 2005a; Vaque et al., 2004; Vaqué et al., 2008). Moreover, interannual plankton dynamics are intertwined with krill recruitment and the main food source supporting most of the megafauna (i.e. penguins) within the Southern Ocean (Garzio et al., 2013; Saba et al., 2014). Studying how functional coastal planktonic communities are impacted by physiochemical drivers is essential to better understand how the functioning of the ecosystem, and plankton structure will change with deviations from current climatic norms (i.e. warming).

Unique to the Western Antarctic Peninsula region, the southern portion of the Antarctic circumpolar current (ACC) flows closely to the shelf edge (Orsi et al., 1995), resulting in mid-depth circumpolar deep water to integrate more freely with less modifications onto the shelf. The increase in connectivity of surface ocean and intermediate water masses cannot occur elsewhere in the Southern Ocean, greatly influencing the regions physical oceanography and biogeochemistry, such as nutrient replete conditions for macronutrients during growing season (Arrigo et al., 2017; Hofmann et al., 1996; Klinck, 1998). As such, the productive WAP ecosystem is incredibly important to Antarctic krill stocks across the shelf and further downstream in the greater Southern Ocean circulation system, which makes the WAP an ideal location as breeding grounds for marine megafauna for both seasonal and year-round species (Atkinson et al., 2004; Costa & Crocker, 1996; Ducklow et al., 2007; Friedlaender et al., 2006; Quetin et al., 1996). The WAP region also hosts a variety of microbial planktonic clades that can act as important prey for krill, including diatoms, cryptophytes, prasinophytes, haptophytes, ciliates, and mixed flagellates. Many of these clades contain taxa that exhibit the capability of mixotrophic growth in laboratory culture settings (Booth & Horner, 1997; Grattepanche et al., 2022; Lovejoy et al., 2002; McKie-Krisberg et al., 2015; Princiotta & Sanders, 2017; Sellers et al., 2014). Potential changes to the functional community will not only impact the nutrient availability and greater cycling of ecologically significant elements (C, N, P, Si, and Fe), but also more broadly the greater food web dynamics that support the higher trophic levels, such as krill, penguins, and seals.

Mixotrophic plankton, including phagotrophic phytoplankton, play a critical role in a variety of aquatic food webs, especially in the carbon flux transferring organic matter and energy to higher trophic levels (Stoecker, 1998). As important bacterivores, mixotrophic plankton may also provide a link between bacterial production and the eukaryotic portion of the food web (Stoecker et al., 2017). For example, in the polar regions, analysis of the Beaufort Sea and the Canada Basin found mixotrophic nanoflagellates (MNANs) comprised 1-22% of heterotrophic abundance and 2-32% of phototrophic abundance. On average the bacterivorous impact of mixotrophic plankton in the region was typically low at <5% of bacterial production but impacts peaked at 25% of bacterial production at a singular station (Sanders & Gast, 2012). In the Southern Ocean, most studies have been confined to the Ross Sea during the austral summer/spring and phagotrophic phytoflagellates contributed largely to the carbon flux of the region. For example, in the Ross Sea during the 2005 austral spring, MNANs comprised 4-24% of phototrophic nanoflagellates and 8-42% of heterotrophic nanoflagellates, while also removing 11-100% of bacterial standing stock (Moorthi et al., 2009). In 2011, MNANs contributed 4-33% of phototrophic nanoflagellates and 9-75% of heterotrophic nanoflagellates, while consuming a much lower 2-14% of bacterial standing stock (Gast et al., 2014b). Even though the impact of mixotrophs at the local scale can be variable, their influence can be significant, especially within the Southern Ocean.

The impact of phagotrophic phytoplankton regarding *in situ* primary production remains largely unknown. Much of what is known is postulated through theoretical modelling of mixotrophic activity based on laboratory experimentation (Edwards, 2019; Mitra et al., 2016). Current measures of mixotrophic primary production are limited to laboratory settings. Laboratory experiments of mixotrophic plankton cultures have yielded valuable insights to the primary production rates of specific species or groups and the light/nutrient conditions to which they are triggered (Anderson et al., 2018; Princiotta et al., 2016; Sanders et al., 1990). However, lab experiments can get us only so far in estimating mixotrophic impacts as a primary producer because we cannot perfectly replicate *in situ* conditions. Current methods estimate primary production for the entire phototrophic community, and we are incapable of attributing the *in situ* primary production to various functional groups. However, several studies have considered the amount of carbon demand comes from bacterivory *in situ* and thereby indirectly attribute how much of the carbon demand is attributed to primary production by assuming the residual carbon needed for growth is attribute to primary production (Crespo et al., 2011; Havskum & Hansen, 1997). Despite our inability to quantify their role as primary producers, it is clear by their wide distribution and thriving in a myriad of environments that mixotrophy is a successful strategy, and the Southern Ocean is no exception (Gast et al., 2018; Grattepanche et al., 2022). To date, very few studies in the Southern Ocean have considered mixotrophy when assessing plankton dynamics and assessing roles plankton play in the community carbon flux. None of the studies took place within the WAP region, leaving gaps in a potentially large, unique, and important portion of the microbial community.

In this study, the occurrence of phototrophic, heterotrophic, and mixotrophic nanoflagellates and their respective influence (or impact) throughout the WAP region were examined. The abundances and activity (bacterivory and/or primary production) of each functional group were quantified at multiple depths along the latitudinal gradient of the WAP region during the austral spring (October – December 2019). Epifluorescence microscopy was used for abundance enumeration and bacterivorous feeding estimation. We used a novel approach for estimating mixotrophic plankton primary production based on the percentage of RNA reads per functional group to partition the primary production estimates and applied it to the bacterivorous dataset. During the austral spring in the WAP region, we hypothesized that 1) the mixotrophic portion of the community would be the dominant grazer, while acting as an auxiliary source of primary production relative to strict phototrophs; 2) MNANs abundance and activity would increase along the latitudinal gradient and with the depth; 3) MNANs would attain/obtain more of their carbon budget from bacterivory than primary production.

4.3 Methods

The study occurred aboard the Nathaniel B. Palmer to the Western Antarctic Peninsula (-64.54º; -62.37º to -68.05º; -68.30º) occurred from November 6^{th} – December 9^{th}, 2019 (NBP 1910). During this cruise we collected samples from 9 stations at both the surface (~1m depth) and the Deep Chlorophyll Maxima (DCM, ranging from 9m to 45m) depths using 12 L Niskin bottles mounted on a CTD rosette.

4.3.1 Environmental Parameters

Measurements of conductivity, water temperature, depth, salinity, oxygen, oxygen saturation, fluorescence, percent beam transmission, irradiance (PAR), time, latitude, and longitude were collected *in situ* with a CTD Sea-Bird SBE 9-11plus V5.1g, with WET Labs ECO-AFL/FL and C-Star probes. Quantification of chlorophyll a were performed in triplicate with samples of 100 mL- 200 mL filtered onto a 25 mm GF/F filter (Whatman, UK) and frozen at -80°C until extraction. Filters were extracted in 90% acetone overnight at -20°C and fluorescence was determined with a Model TD-700 fluorometer (Turner Designs, Sunnyvale, CA, USA). Local ice coverage was estimated by the crew aboard the

N.B.P. based on direct observations at the time of CTD sampling. The northern stations had mostly free-floating ice floes, while the southern stations had mostly pack ice.

Filtrates from GF/F filters using colorimetric methods with an Autoanalyzer were used to quantify the amount of dissolve inorganic nutrients. For each dissolved inorganic nutrient, a standard curve was created to calculate the concentration of nutrients in each sample. Dissolved inorganic phosphate (DIP) was analyzed as in Parsons et al. (1984)using a composite reagent, containing molybdic acid, ascorbic acid, and trivalent antimony, turning blue in the presence of DIP. For quantification of total dissolved inorganic nitrogen (DIN), which is the sum of ammonia, nitrates, and nitrites (NH_4^+, NO^{3-}, NO^{2-}, respectively), each nitrogenous form was determined individually. For NH_4^+ quantification, we used a compound that fluoresces in the presence of ammonium, orthophthaldialdehyde (OPA), a method outlined by Holmes et al. (1999). Nitrate and nitrite concentrations were determined via the results of a Griess-Ilosvay reaction causing the purplish solution color when acidic vanadium-(III)-solution is utilized (Schnetger & Lehners, 2014).

4.3.2 Bacterial Production and Abundance

Bacterial abundance was quantified via examination of samples filtered onto a 25 mm, 0.2 μm pore sized polycarbonate membranes (GE Osmonics, Minnetonka MN, USA). Filters are then mounted on glass slides using Vectashield DAPI (Vector Laboratories) and enumerated under 1000x magnification using Olympus BX 41epifluorescence microscope. Bacterial production was determined using ^{3}H-leucine incorporation into protein as described in by Smith and Azam (1992). Production was then calculated using a conversion factor of 1.55 kg C mol^{-1} of leucine incorporated

(Simon & Azam, 1989). For additional information about the procedure, see Grattepanche et al. 2022.

4.3.3 Primary Production

Total community phytoplankton primary production (PP) was determined in 24-h incubations conducted at *in situ* temperature in deck incubators on the ship under 50% neutral density screens (Matrai et al., 1995).The procedure to quantify the amount of primary production was accomplished via the method outlined in Grattepanche et al (2022). Briefly, primary production was determined in 24-h incubations conducted at *in situ* temperature in deck incubators. Triplicate polyethylene bags (WhirlPak) containing 16 mL seawater samples were placed under 50% neutral density screens and inoculated with ^{14}C-bicarbonate (Moravec inc., Brea, Ca) to a final concentration of 2.0 µCi mL^{-1} (Matrai et al., 1995). An additional three were placed into opaque bags for the 24-h incubation period. To determine the primary production for the nanoflagellate portion of the community (< 20 µm), seawater samples were prescreened through 20 µm acid-washed nylon mesh filters and then quantified using the same method.

4.3.4 Direct Grazing Assessment of Mixotrophs and Heterotrophs

For ingestion experiments, triplicate 300 mL samples of seawater, prescreened with a 100 um and 20 um acid-washed nylon mesh to remove larger phyto- and zooplankton, were prepared in 500 mL Whirlpack bags. Bacteria-sized polycarbonate microspheres (0.6 µm, Polysciences, Inc., Warrington, PA, USA) were then added at trace concentrations (<20%) of in situ levels of bacterial abundance. The number of microspheres added to each replicate were verified following the same procedure as bacterial abundance assessment (see 2.3). At the start of each incubation period, a T0 sample was taken to correct for background microsphere associations (false positives). After the 30-minute incubation period (T30), samples were then fixed with Lugol's iodine solution (3% final concentration) to prevent egestion and preserved with 50% formalin and sodium thiosulfate, which neutralizes the Lugol's solution (Sherr & Sherr, 1993). Depending on the nanoflagellate concentration at the station either 50 mL or 100 mL of sample were then filtered onto a 25 mm diameter, 0.8 μm pore sized polycarbonate membranes (GE Osmonics, Minnetonka MN, USA). Filters were then mounted on glass slides using Vectashield DAPI (Vector Laboratories) and frozen at -20 ^{o} C to prevent reduce loss of chlorophyll fluorescence until enumeration under 1000x magnification using Olympus BX 41 epifluorescence microscope. Optimal duration of the incubation was assessed at the start of the cruise, where 30 minutes was estimated to have a linear uptake of microspheres without observing food saturation. Positive feeding events were counted as microspheres within plastidic (mixotrophic) or non-plastidic (heterotrophic) cells. Feeding rates for both heterotrophic and mixotrophic nanoflagellates were calculated by multiplying the rates of microsphere uptake and the ratio of the in-situ bacteria abundance to microsphere concentrations in the sample after removal of the background associations (T0) (Sherr & Sherr, 1993).The grazing impact (bacteria d^{-1} mL^{-1}) for each nanoflagellate functional group was estimated by multiplying the specific feeding rates by their abundance and assumed to be constant throughout a 24-hour period. This value was then used to determine the percent of bacterial standing stock consumed daily due to HNAN or MNAN grazing. Percentage of standing stock removed was then converted to biomass ingested using an average bacterial diameter of 0.2 μm, assuming a spherical shape, and a conversion factor of 2.2×10^{-13} g C μm^{-3} (Lee & Fuhrman, 1987) for comparison of carbon uptake from primary production and reported as μg C L^{-1} d^{-1}.

4.3.5 Enumeration of Nanoflagellate Groups

Abundances of phototrophic (PNAN), heterotrophic (HNAN), and mixotrophic (MNAN) were estimated from the same slides used for nanoflagellate feeding estimation described previously (see 2.4). Nanoplankton (3 – 20 μm) were counted in 20 – 40 fields of view, or a minimum of 100 cells. PNANs were identified as all cells with a presence of a DAPI stained nucleus and the presence of a chloroplast regardless of microsphere ingestion status. ANANs were identified by the presence of a DAPI stained nucleus and chloroplast without microsphere association. MNANs were counted as cells with a chloroplast and at least 1 microsphere ingestion. HNANs were classified by the presence of a nucleus and the absence of a chloroplast. All abundances of protists were calculated as per milliliter.

4.3.6 Indirect Assessment of Nanoflagellate Bacterivory and Primary Production

Bacterivory and primary production produced from nanoflagellates were also indirectly estimated using activity assessed as the percent of community ribosomal RNA reads for each functional group, as identified and reported by Grattepanche et al (Grattepanche et al., 2022). While there are limitations to the rRNA approach to the estimation of the "active" members of the protistan community (i.e. lineage-specific differences in copy number, growth, or activity related to RNA translation; (Blazewicz et al., 2013)) this approach has been widely applied throughout the literature in a variety of environments and considered an acceptable proxy for active, living members of the community (Freudenthal et al., 2022; Geisen et al., 2015; Inkinen et al., 2019).

For indirect estimates of activity, percentage of rRNA reads from the pico- and nano-sized fractions from Grattepanche (2022) study were used to partition the amount of activity that should be attributed to each functional group. There is molecular information for all the stations and depths sampled in the direct measurements, except for station A. For indirect estimation of bacterivory, total bacterivory was calculated from both the MNAN and HNAN direct estimates to provide a total heterotrophic nanoflagellate bacterivory (> 20 µm bacterivory). The total nanoflagellate bacterivory was then partitioned to either HNAN or MNAN activity by multiplying the total bacterivory by the percent of HNAN or MNAN ribosomal RNA reads of the total heterotrophic ribosomal RNA reads (HNAN + MNAN RNA reads). Primary production was calculated in a similar fashion, where the amount of primary production from the nanoflagellate community (< 20 µm primary production) was partitioned to either MNANs or PNANs.

Equation for indirect bacterivory:

$$MNAN\ indirect\ bacterivory = \frac{MNAN\ RNA\ reads}{MNAN + HNAN\ RNA\ reads} \times\ Total\ direct\ bacterivory$$

$$HNAN\ indirect\ bacterivory = \frac{HNAN\ RNA\ reads}{MNAN + HNAN\ RNA\ reads} \times\ Total\ direct\ bacterivory$$

Equation for indirect Primary Production:

$$MNAN\ indirect\ PP = \frac{MNAN\ RNA\ reads}{MNAN + PNAN\ RNA\ reads} \times < 20\mu m\ Primary\ Production$$

$$PNAN\ indirect\ PP = \frac{PNAN\ RNA\ reads}{MNAN + PNAN\ RNA\ reads} \times < 20\mu m\ Primary\ Production$$

4.3.7 Indirect Method Caveats

This indirect approach allows for estimation of the MNANs contribution to the primary production in the *in situ* system. However, as with any new method, there are a few assumptions/caveats that need to be considered. This method assumes carbon used for respiration comes from the primary production that was subtracted out during the 24-hour incubation experiment for Net PP produced from the community. All nanoflagellate respiration that would occur during a 24-hour period is accounted for in the dark incubation condition measurements. In this method, we are assuming there is a 1 to 1 relationship between rRNA copy number and activity, ignoring possible intra- and inter-specific differences in activity for each functional group (including species-specific differences). We acknowledge there are a wide range of protist lineages whose amount of primary production per cell/chlorophyll a can vary widely between large clades or even within the same genus for both mixotrophic and strictly phototropic nanoflagellates (Koppelle et al., 2024; Sanders et al., 2001). The same is also true for the heterotrophic portion of the community, made even more complex by the wide range of physiological rates along the spectrum of mixotrophy. Even though this method may be a crude estimate, a 1 to 1 assumption for all functional groups across the entire community composition is the most efficient approach and allows for the estimation of the upper limit for mixotrophic activity. Conversely, this would make PNAN and HNAN activity estimates from this approach the lower limit as a larger portion of the activity is attributed to MNANs. To accommodate the potential difference in "phototrophically originated" carbon acquisition of MNANs compared to a strict phototroph we employed a 80% and a 67% penalties due to reports of reduced phototrophy by mixotrophs when exposed to bacterial prey (Holen, 2001; Wilken et al., 2014). Grattepanche et al. identified a wide range of organisms identified as possibly mixotrophic were merged with mixotrophic species to help identify the full potential influence of MNANs in the WAP and all interpretations of this dataset should consider this to be a range of MNAN contribution to carbon acquisition (Grattepanche et al., 2022). Given these caveats, we believe we can elucidate general trends within and between MNAN and PNAN activity, provide a range for MNAN impact, and contribute empirical data for the potential mixotrophic contribution toward community primary production to aid in the parameterization of future modelling approaches and guide subsequent research.

4.3.8 Data Analysis

To assess the collinearity between environmental variables, a correlation matrix calculating the Pearson's r coefficient of all environmental variables. Additionally, a variation inflation factor (VIF) was calculated to help detect collinearity between all environmental and response variables. PCA analysis and k-means clustering with environmental variables were used to identify the latitudinal station groups. All calculations and data analysis were calculated using the R base stats package (R Core Team, 2020).

4.4 Results

The stations sampled encompassed a large area from just above Palmer station to Marguerite Bay. Tested stations were consistently sampled at just below surface (between 1- 2 m depth on average), while the DCM depth varied from 15 m to 45 m. On average, DCM depth was deeper at the southern stations with an average depth of 36 m, while the northern stations averaged 31 m (Table 4.1). The mixed layer depth (ZML) followed a similar trend. ZML depth ranged from 12 m to 43 m, with the southern stations averaging

35.62 ± 5.75 m and the northern stations averaging 17.08 ± 5.26m. Ice floe coverage also shared a negative relationship with latitude, with ice floe covering a much larger percent area in the north than the southern stations (Table 4.1). Water temperature, salinity, and conductivity ranged from -(0.4) to -(1.77) °C, 33.47 to 34.12 PSU, and 26.45 – 28.11 S/m, respectively. In addition to the water temperature, salinity, and conductivity, each measured nutrient (nitrates, nitrites, ammonia, and phosphates) shared a negative relationship with latitude. Fluorescence, bacterial production, oxygen, and chlorophyll a all showed positive relationships with latitude moving towards the pole. Their measured quantities ranging from 0.15 to 2.42 mg m^{-3}, 0.61 to 9.3 µg C L^{-1} d^{-1}, 6.23 to 7.93 mL L^{-1}, 0.1 to 1.6 mg m^{-3}, respectively (Table 4.1, Table 4.2).

Table 4.1 Mean and standard deviation of the abiotic environmental parameters throughout the WAP region.

	Environmental Parameters	North	South	Offshore*
Water Column	Mixed Layer Depth (ZML, m)	17.08 ± 5.26	35.64 ± 5.75	19.8
	Depth of Photic Zone (Ze, m)	57.92 ± 8.35	43.55 ± 4.91	52.47
	Deep Chlorophyll Maxima Depth (ZCM, m)	21.73 ± 15.3	23.51 ± 16.25	32.68
	Bottom (m)	472.25 ± 318.56	427.25 ± 253.8	432
	Ice (%)	60 ± 39.3	2.5 ± 4.63	0
	Air T (°C)	-1.15 ± 0.42	-3.05 ± 3.12	-1.1
	Surface Photosythetically Active Radiation (sPAR)	468.4 ± 413.16	228.1 ± 148.1	710.3
Surface	Water T (°C)	-1.33 ± 0.47	-1.33 ± 0.11	-1.62
	Conductivity (mS cm^{-1})	27.01 ± 0.52	26.6 ± 0.11	27.1
	Salinity PSU	33.76 ± 0.19	33.5 ± 0.04	33.8
	BeamTrans (%)	98.48 ± 0.44	96.43 ± 0.98	96.5
	NH_4^+ (µM)	1.37 ± 0.08	1.29 ± 0.02	1.29
	NO_2^-/NO_3^- (µM)	30.46 ± 0.48	25.68 ± 0.15	27.83
	PO_4^{3-} (µM)	3.04 ± 0.09	2.90 ± 0.24	2.94
	Oxygen (mL L^{-1})	6.77 ± 0.33	7.78 ± 0.17	7.92
	Oxygen saturation (mL L^{-1})	8.36 ± 0.12	8.45 ± 0.03	8.36
	Fluorescence (mg m^{-3})	0.24 ± 0.12	1.43 ± 0.53	0.53
Deep Chlorophyll Maximum	Water T (°C)	-1.14 ± 0.50	-1.56 ± 0.14	-1.23
	Conductivity (mS cm^{-1})	27.28 ± 0.56	26.67 ± 0.15	27.23
	Salinity PSU	33.91 ± 0.22	33.54 ± 0.04	33.95
	BeamTrans (%)	98.78 ± 0.24	96.67 ± 0.86	97.63
	NH_4^+ (µM)	1.29 ± 0.06	1.29 ± 0.01	1.3
	NO_2^-/NO_3^- (µM)	30.87 ± 0.38	26.48 ± 0.89	28.54
	PO_4^{3-} (µM)	3.19 ± 0.01	2.96 ± 0.08	3.39
	Oxygen (mL L^{-1})	6.45 ± 0.22	7.63 ± 0.16	7.78
	Oxygen saturation (mL L^{-1})	8.32 ± 0.12	8.44 ± 0.03	8.34
	Fluorescence (mg m^{-3})	0.44 ± 0.23	1.92 ± 0.63	0.88

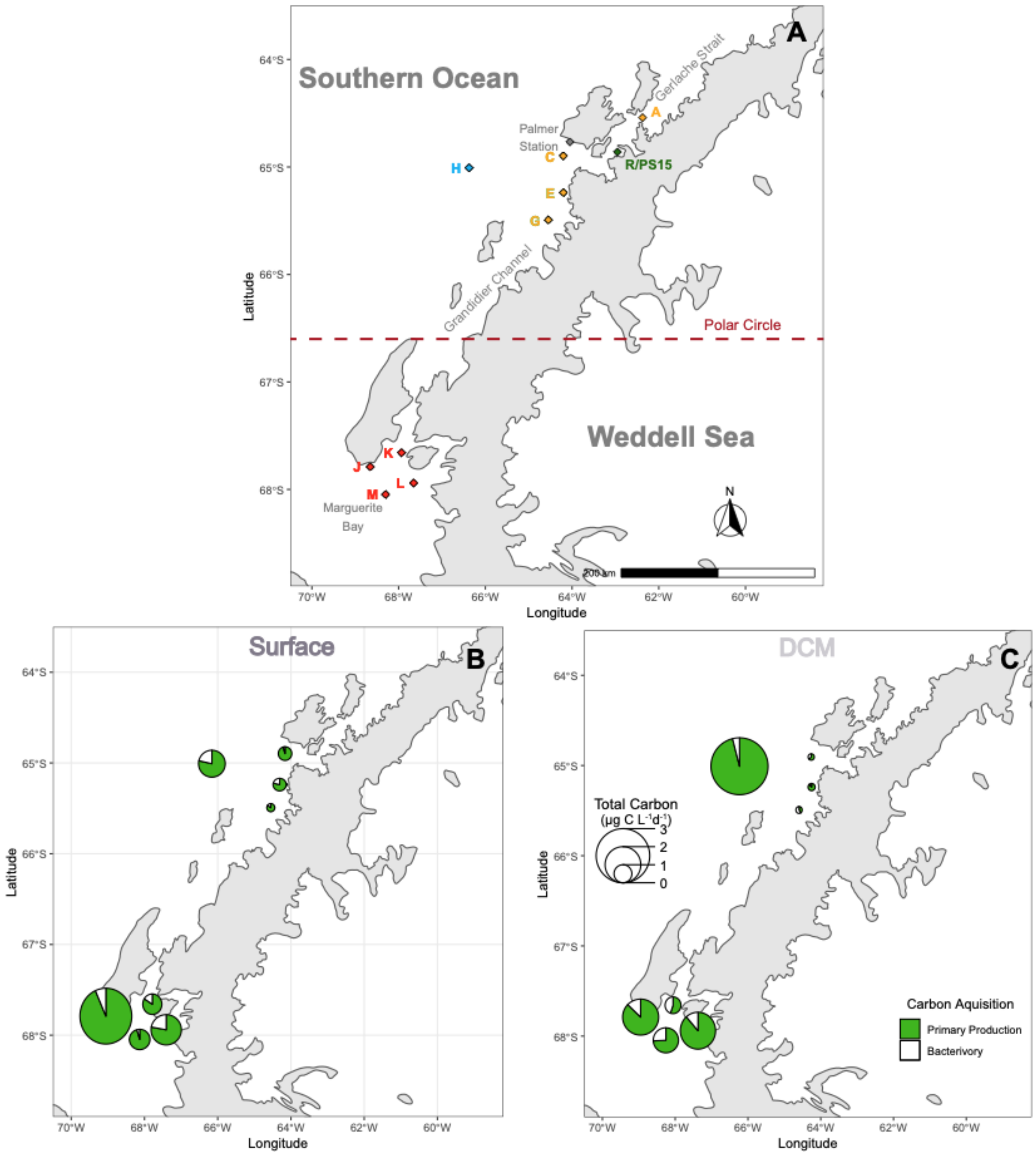

Figure 4.1 <u>The sampling locations (A) in the Western Antarctic Peninsula region.</u> Mixotrophic nanoflagellate carbon acquisition and percent contribution of bacterivory and primary production to Mixotrophic nanoflagellate carbon demand at the (B) surface and at the (C) DCM depths, showing a strong latitudinal gradient for MNAN total carbon acquisition. Pie radius represents total mixotrophic carbon presented as ug C L^{-1} d^{-1}.

4.4.1 Distribution of Nanoflagellate Functional Groups Throughout the WAP

Via epifluorescent microscopy methods, PNANs were the largest fraction of the functional community, consistently remaining almost an order of magnitude above MNAN and HNAN abundance. PNAN abundance ranged from 1 to 5 x 10^3 cells mL^{-1} and ranged from 0.8 to 0.95 proportion of total nanoflagellate population (Figure 4.2, Table 4.2). PNAN abundance doubled in the South and Offshore stations (from 1.3 to 3.0 and 2.7 x 10^3, respectively). The differences between depths were slight in comparison to the latitudinal gradient. The range of the surface was 1 to 3.2 x 10^3 cells mL^{-1}, with an average of 2.2 x 10 ^{3} cells mL^{-1}. The DCM was marginally elevated compared to the surface with a range of 1.1 to 4.9 x 10^3 cells mL^{-1} and an average of 2.4 x 10^3 cells mL^{-1} (Table 4.2). Relative to PNANs, HNAN abundance was an order of magnitude lower ranging from 80 to 400 cells mL^{-1}, corresponding to approximately 0.05 – 0.1 proportion of total nanoflagellate abundance (Figure 4.2, Table 4.2). The average HNAN abundance in the north is 163 ± 60 cells mL^{-1} and 219 ± 59 cells mL^{-1} in the southern stations. MNAN abundance was the lowest of the functional groups, peaking at 225 cells mL^{-1} and dropping to 13 cells mL^{-1}, representing <0.01 to 0.1 proportional fraction of total nanoflagellate population. The north station averaged 45 ± 34 cells mL^{-1} and 91 ± 39 cells mL^{-1} for MNAN abundance in the south (Table 4.2). All three functional groups exhibited a latitudinal gradient, however, the PNANs ($p < 0.05$, r = -0.6 (Figure 4.2) exhibited a stronger correlation compared to the MNANs and HNANs (r = -0.346 and -0.401, respectively; $p < 0.05$; Figure 4.2).

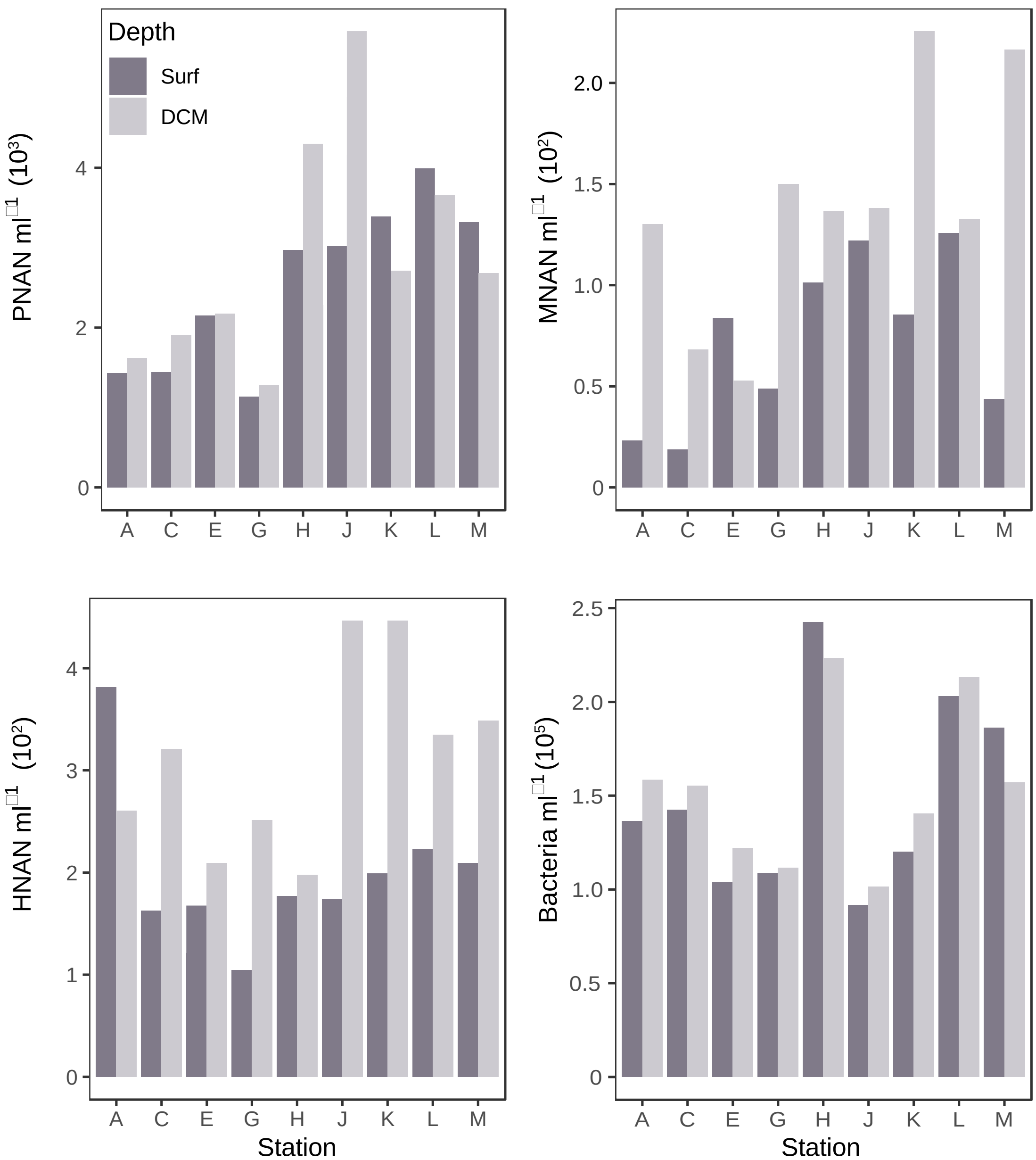

Figure 4.2 Abundance for each of the functional groups throughout the WAP region at the surface and deep chlorophyll maximum (DCM) depths. Samples are ordered from North to South locations and show the latitudinal gradient.

4.4.2 Distribution of Nanoflagellate Functional Group rRNA Reads Throughout the WAP

For relative proportional amounts of functional group rRNA reads, MNANs consistently represented the largest portion of the active community. Throughout the WAP region, MNANs averaged 0.67 ± 0.1 of the community rRNA reads. By latitudinal group, MNAN percent rRNA reads averaged 0.72 ± 0.04, 0.84 ± 0.01, and 0.59 ± 0.06 for the North, Offshore, and South stations, respectively (Figure 4.3, Table 4.2). For the Surface layer, MNANs averaged 0.69 ± 0.08, while they averaged 0.67 ± 0.11 (Figure 4.3, Table 4.2). PNANs were the next largest group by contributing 0.23 ± 0.09 throughout the study. For the North, Offshore, and South stations, PNANs made up 0.23 ± 0.05, 0.06 ± 0.05, and 0.27 ± 0.08, respectively. At the surface depth, PNANs averaged 0.2 ± 0.08, and 0.25 ± 0.09 at the DCM depth (Figure 4.3, Table 4.2). The smallest functional group was the HNANs. On average, they contributed only 0.1 ± 0.06 of the total WAP community rRNA read counts. Going from North to South, HNANs averaged 0.06 ± 0.05, 0.1 ± 0.05, and 0.15 ± 0.04, with their largest contribution to community occurring at the Southern stations (Figure 4.3, Table 4.2). There were negligible differences between the depths for HNANs, where they averaged 0.11 ± 0.07 at the surface and 0.1 ± 0.05 at the DCM depths (Figure 4.3, Table 4.2).

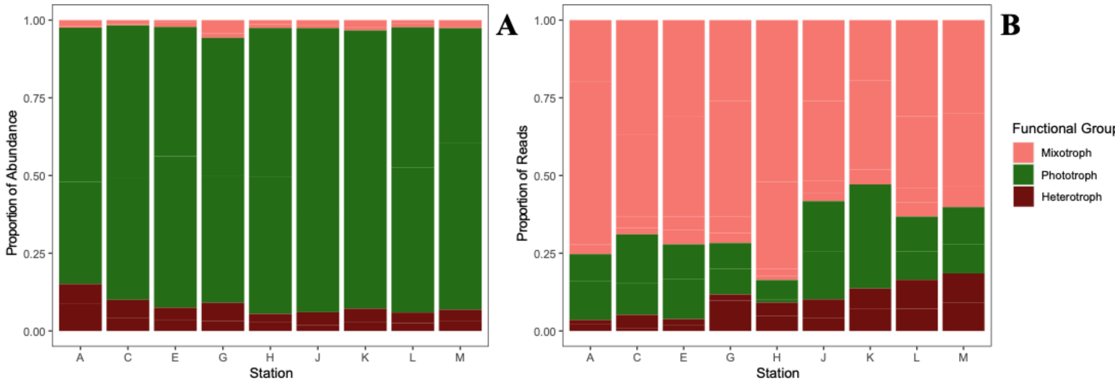

Figure 4.3 Distribution of functional groups based on (A) nanoflagellate estimates from epifluorescent microscopy and (B) classification based on the number of RNA reads. The large discrepancy between the relative amounts of MNANs estimated using the indirect and direct methods within the plastidic portion of the community are presented as the difference of the percentage estimated. We see a latitudinal gradient and decrease in the MNAN discrepancy as we move further south.

All functional groups (MNAN, HNAN and PNAN) resulted in a significant relationship with latitude ($r = 0.78, -0.74, -0.39$; $p < 0.05$, respectively). However, both HNAN and PNAN resulted in negative correlation coefficient corresponding to a positive relationship with latitude due to the latitude being negative in the Southern Hemisphere. The MNANs the opposite relationship resulting in a negative relationship with latitude. Comparable to the population metrics, all functional groups showed no significant relationship with depth ($p > 0.05$).

There were some significant differences in the fraction estimated from the molecular and epifluorescent microscopy estimation of the functional groups. The differences between the groups were not consistent for all the regions. For MNANs, the calculated proportional composition in the rRNA read data was always larger than the proportional estimated via epifluorescent microscopy with an average increase of around 0.64 ± 0.1. The Northern stations saw the second largest difference in percent functional composition with an average difference of 0.69 ± 0.05. The Offshore station saw the largest difference in percent functional composition with an average difference of 0.81 ± 0.02. However, the smallest difference between the two measurements occurred at the southernmost stations, with an average of 0.56 ± 0.07 (Figure 4.3). This difference is also reflected in the estimate proportions of the PNAN and HNAN functional groups, which saw an average difference of -0.7 ± 0.1 and 0.02 ± 8.6. In strong contrast to the MNAN group, PNANs had higher proportions of the community in the epifluorescent microscopy technique compared to the rRNA reads. In the North, Offshore, and South stations, PNAN proportions were reduced by -0.68 ± 0.06, -0.89 ± 0.03, and -0.67 ± 0.09, respectively. HNANs proportions were only smaller in the rRNA estimates in the North stations by an average of -0.05 ± 0.08. In the Offshore and South stations, the HNAN fractional composition increased by 0.04 ± 0.04 and 0.08 ± 0.04 (Figure 4.3), respectively. For both MNANs and HNANs there was significant correlation of latitude, however, opposing relationships. MNANs proportional difference between the rRNA and cell abundance measures decreased consistently as we move further south, except for station H, which is the Offshore station ($r = 0.75$, $p < 0.05$). HNAN initially decreased in estimated proportional difference followed by increasing proportions as we move further south ($r = -0.69$, $p < 0.05$). There was so significant correlation with latitude for the PNAN functional group ($p > 0.05$).

4.4.3 *Distribution of Nanoflagellate Activity Throughout the WAP*

Overall, MNANs had the larger bacterivorous impact through the WAP region. For the bacterivorous portion of the community activity, both HNAN and MNAN had similar minimum values of bacterial standing stock (1-2% of bacterial standing stock removed day^{-1}, Figure 4.4, Appendix G), but they had very different peak values. Max HNAN feeding was 8.1% bacterial SS removed d^{-1} (Appendix G), which equates to 0.16 ug C L^{-1} d^{-1} (Appendix E). Max MNAN ingestion nearly quadrupled HNAN feeding with 30% bacterial SS removed d^{-1}, for an estimated removal of 0.42 ug C L^{-1} d^{-1}. Overall HNAN consumption averaged 5 ± 2.1% bacterial SS removed d^{-1} (0.07 ± 0.04 ug C L^{-1} d^{-1}) and MNAN consumption averaged 12.8 ± 8.8% bacterial SS removed d^{-1} (0.18 ± 0.12 ug C L^{-1} d^{-1}) throughout the duration of the study (Appendix G, Table 4.2). Like abundance, there is a latitudinal gradient to both sources of bacterivorous activity. As we move from north to south, we see an increase in both HNAN and MNAN bacterivory. HNAN and MNAN bacterial consumption averaged 3.5 ± 1.25 % and 8 ± 6.47% bacterial SS removed d^{-1} (0.05 ± 0.02, 0.1 ± 0.07 µg C L^{-1} d^{-1}, respectively; Table 4.2) in the northern stations and increased to 7% and 18% bacterial SS removed d^{-1} (0.1 ± 0.03, 0.26 ± 0.12 µg C L^{-1} d^{-1}, respectively; Table 2.2) in the south, respectively (Figure 4.4, Appendix G, Table 4.2).

As an additional measure, we calculated the percent of bacterial production consumed by each functional group. HNAN and MNAN bacterial consumption ranged from 15 % to 65% and 11 % to 198 %, respectively (Appendix F). Unlike all other metrics, however, there was no significant latitudinal gradient signal. The lack of a latitudinal gradient is caused by the collinear and proportional increase in both the bacterial production and subsequent nanoflagellate bacterivorous activity (Figure 4.5, Table 4.2).

Table 4.2 Mean and standard deviation of measured nanoflagellate biotic measures and mixotrophic nanoflagellate carbon budget estimations throughout the WAP region.

Response Variables	**North**	**South**	**Offshore***
MNAN (cell mL^{-1})	45 ± 34	91 ± 39	76.06
PNAN (cell mL^{-1})	1297 ± 290	2980 ± 812	2661.82
HNAN (cell mL^{-1})	162 ± 60	219 ± 59	164.84
Chlorophyll a (mg m^{-3})	0.33 ± 0.15	1.11 ± 0.23	0.59
Primary Production (µg C L^{-1} d^{-1})	0.99 ± 0.72	5.07 ± 1.31	3.66
<20 µm Primary Production (µg C L^{-1} d^{-1})	0.51 ± 0.3	2.05 ± 1.11	2.29
Bacteria (10^8 L^{-1})	1.3 ± 0.21	1.52 ± 0.46	2.33
Bacterial Production (µg C L^{-1} d^{-1})	0.11 ± 0.08	0.27 ± 0.06	0.19
Bacterial Sized Ingestions (BSP) per MNAN	8.33 ± 2.36	11.96 ± 3	12.3
Bacterial Sized Ingestions (BSP) per HNAN	1.23 ± 0.39	2.04 ± 0.69	1.78
MNAN % bacterial SS removed	8 ± 6.47	18.5 ± 8.7	9.43
HNAN % bacterial SS removed	3.5 ± 1.25	6.91 ± 1.08	3.02
Apportioned Carbon Budget (µg C L^{-1} d^{-1})			
MNAN Carbon consumed	0.1 ± 0.07	0.26 ± 0.12	0.22
HNAN Carbon consumed	0.05 ± 0.02	0.1 ± 0.03	0.07
MNAN Primary Production	0.35 ± 0.21	1.23 ± 0.73	2.01
PNAN Primary Production	0.12 ± 0.08	0.64 ± 0.42	0.19
Percent difference of MNAN estimate	71. 8 ± 0.13	51.4 ± 0.13	61.7

Note. Estimates are reported as combine averages across depths as there are no significant differences between depths.

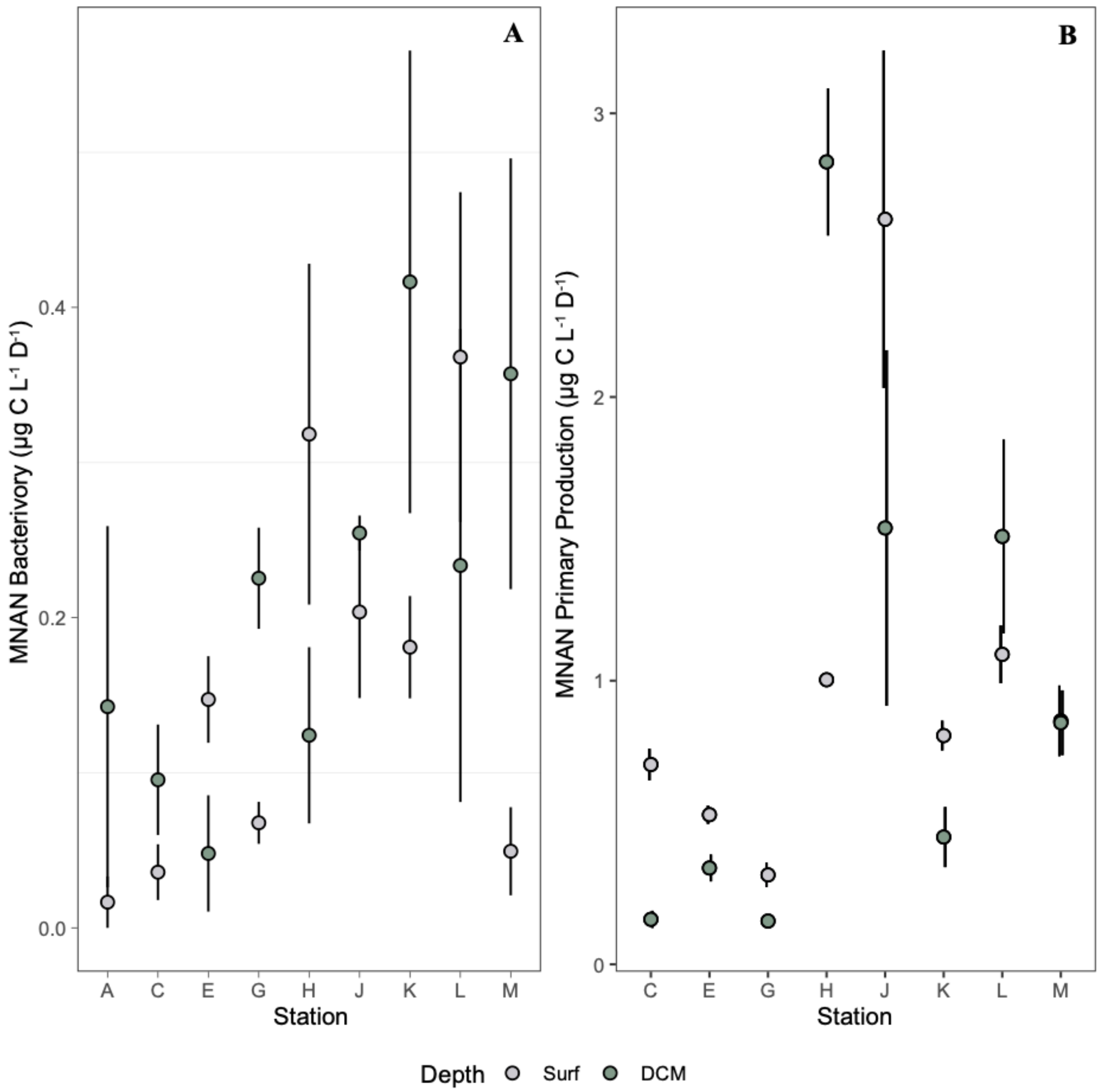

Figure 4.4 <u>Activity measures for mixotrophic nanoflagellates throughout the WAP region at the surface and deep chlorophyll maximum (DCM) depths</u>. Presented as (A) bacterivory (µg C $L^{-1}d^{-1}$) estimated from ingestion experiments and (B) primary production (µg C $L^{-1}d^{-1}$) both estimated from total nanoflagellate bacterivory and primary production using the percentage of RNA reads (Grattepanche et al., 2022).

Using the percent RNA read approach to partition <20 µm fraction of primary production, PNAN primary production is estimated to range from 0.04 to ~ 1.55 µg C L^{-1}

d^{-1}. Average PNAN production at the northern stations was 0.12 ± 0.08 μg C L^{-1} d^{-1}, while the average production in the south was 0.64 ± 0.42 μg C L^{-1} d^{-1} (Appendix E, Table 4.2). Average production among the surface samples was 0.41 ± 0.48 μg C L^{-1} d^{-1}, and the average production among the DCM samples was 0.37 ± 0.31 μg C L^{-1} d^{-1}. MNAN primary production has a similar minimum at 0.13 μg C L^{-1} d^{-1} but double the PNAN maximum with a peak of 2.9 μg C L^{-1} d^{-1} (Figure 4.4, Table 2.2). Resembling PNAN production, the MNAN production average of the southern stations, 1.23 ± 0.73 μg C L^{-1} d^{-1}, was higher than the northern stations, 0.35 ± 0.21 μg C L^{-1} d^{-1}. When comparing the different depths, we see the average surface (1.13 ± 0.77 μg C L^{-1} d^{-1}) and average DCM production (1.1 ± 1.01 μg C L^{-1} d^{-1}) are not significantly different. In the North and Offshore stations, 33% and 38% of primary production was attributed to nanoflagellate community. South station primary production saw a reduced role of primary production with an average of 28% of system primary production attributed to the nanoflagellate community (Figure 4.4, Appendix H, Table 2.2).

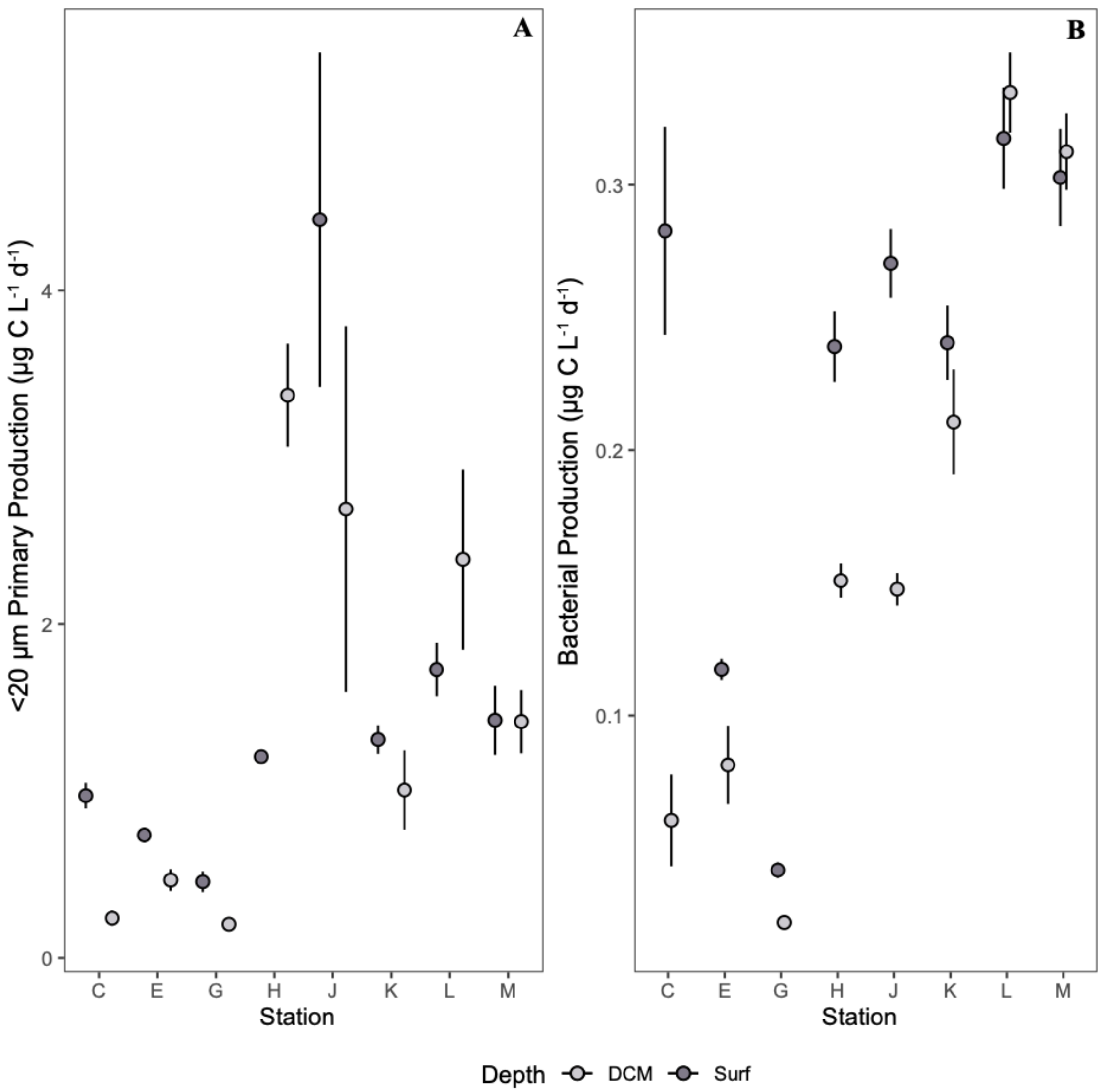

Figure 4.5 Estimates of (A) nanoplanktonic (<20 µm) primary production (µg C $L^{-1}d^{-1}$) and (B) bacterial production (µg C $L^{-1}d^{-1}$) at the surface and deep chlorophyll maximum (DCM) depths throughout the Western Antarctic Peninsula region. Both show a latitudinal gradient increasing the further south the station is located.

4.4.4 Percent of Carbon MNANs Attained via Phototrophy Compared to Heterotrophy

Total MNAN contribution to carbon acquisition varied largely throughout the study. The northern stations saw much smaller total carbon capture, typically <1 µg C L^{-1}

d^{-1}. However, moving offshore and south total MNAN contribution markedly increases to 3.56 μg C $L^{-1}d^{-1}$. Primary production was the dominant source of carbon for MNANs, ranging from 37 to 96% of the MNAN carbon budget. Average primary production percentage of the MNAN carbon budget in the north was 73 ± 22% and the average percentage in the south was 85 ± 14% and the offshore station averaged 78% ± 15% (Figure 4.1, Table 4.2). When comparing surface waters to the DCM, the percent primary production to MNAN carbon budget is 83% ± 9% compared to 70% ± 21%. However, there were three occurrences where the amount of carbon was near a 50/50 or above split in favor of bacterivory, with all occurrences at the DCM depth but within different station groups (North/Palmer, stn C; North/Grandidier, stn G; South/Marguerite Bay, stn K). Bacterivorous contribution towards the MNAN carbon budget ranged from 4 to 62%. When looking along the latitudinal gradient from north to south, the average bacterivorous input towards the MNAN carbon budget is 28% ± 21%, 15% ± 14%, and 22% ± 15%, respectively. The surface had lower average bacterivorous contribution with a 17% ± 9$ input, while the DCM had a larger, but still minority, carbon contribution of 30% ± 21% (Figure 4.1, Table 4.2).

4.5 Discussion

There is a growing body of literature that examines the distribution, diversity, and activity of protists, including the environmental conditions that impact them throughout the Antarctic. However, relatively few studies include phagotrophic phytoflagellates. Those studies were restricted to the Ross Sea and assessed their bacterivorous impacts and/or diversity. In this study, we examined MNAN distribution of abundance and their role as both a primary producer and consumer throughout the WAP region (from the

Palmer Deep region to Marguerite Bay), for both surface and deep chlorophyll maximum depths. During the austral late spring and early summer, the MNANs were found to be active throughout the duration of the study. While significant contributors to bacterivory, the WAP MNAN community gained much of its carbon from primary production. Throughout the region, the most important environmental variables influencing the MNAN and the greater eukaryotic functional nanoflagellate community, were related to the North-South latitudinal gradient, with some weaker influences along the (Sub)Surface to DCM comparison.

4.5.1 The Western Antarctic Peninsula Late Spring Oceanographic Trends

The majority of studies investigating the role of microorganisms within the WAP region have been confined to later in the season, typically between January and April (summer to autumn) (Arrigo et al., 2008; Z. Li et al., 2016; Schofield et al., 2018b; Vives et al., 2022). This reduced some of the sampling constraints caused by more expansive ice coverage during the late spring/early summer. However, climate change is rapidly influencing the area's sea ice extent and coverage and despite the temporary reversal from 2008 to 2015, overall sea ice extent and number of ice days has been declining for decades (Arrigo et al., 2008; Henley et al., 2019; Schofield et al., 2017). Changes in sea ice days may allow for earlier seasonal sampling, but recent work indicates major implications on the both the abundance and the community composition of microorganisms following a season of early sea ice melt and wind advection (Nardelli et al., 2023). Lower local ice melt due to rapid advection out of the WAP region resulted in a low chlorophyll year, characterized by the larger proportions of chrysophytes and mixed flagellates; whereas, the following year saw slower wind-driven advection, net positive ice melt compared to local ice formation, and higher chlorophyll a dominated by larger diatoms (Nardelli et al., 2023). The current study did not examine total regional coverage, but local ice floe concentrations. The local ice floe coverage showed a strong latitudinal gradient. The north stations, which were sampled first, had greater ice floe coverage. The southern stations and the offshore location (Station H) saw little to no ice floe coverage at the time of sampling.

The structure of the water column also showed strong differences along the North to South latitudinal gradient. The mixed layer was several meters deeper in the south compared to the north, which was consistent with previous observations within the region (Grattepanche et al., 2022; Schofield et al., 2018a). Generally, the mixed layer, calculated from salinity and temperature profiles, was deeper than the deep chlorophyll maximum depth, which may explain the lack of a strong difference between the subsurface and DCM samples for both the environmental variables and functional nanoflagellate community. Dissolve nutrients (NO_2^-/NO_3^-, NH^{4+}, PO^{3-}) showed an inverse trend along the latitudinal gradient by decreasing as we move poleward. Despite the observed gradient, all nutrients were within ranges considered to be non-limiting for phytoplankton growth in the region during the same season (Arrigo et al., 2017; Nardelli et al., 2023). Light intensity obviously affects planktonic primary production within the region during different periods of the growing season (Arrigo et al., 2017)**.** In our study water column irradiance at "mid-day" was greater at the northern stations despite primary production (and all other activity metrics) increasing at the southern stations. This incongruity between light and productivity may have been due to increasing day length as southern samples were collected later in the spring, but also suggests additional drivers influencing primary production in the WAP. The bacterial, phytoplanktonic, and nanophytoplanktonic (<20 µm) primary production all saw increased activity at the offshore and south stations, compared to the north stations. Chlorophyll a, fluorescence, and plankton abundance are all well within the ranges reported over the last few decades and increased along the poleward gradient (Arrigo et al., 2017; Ishikawa et al., 2002; Nardelli et al., 2023; Schofield et al., 2018a)**.**

4.5.2 Nanoflagellate Abundances During the WAP Late Spring

As expected, MNANs were detected at each station and depth surveyed but were surprisingly the smallest portion of the community by abundance, typically making up <10% of the nanoflagellate community. The range of MNAN abundance found (<250 cells mL^{-1}) is within the reported ranges of similar polar studies in both the Arctic and Antarctic region. During the Arctic autumn and Antarctic Ross Sea spring, MNANs were found to be < 200 mL^{-1}, while in the Antarctic Ross Sea summer ranged from 2 – 300 mL^{-1} (Gast et al., 2018; Moorthi et al., 2009; Sanders & Gast, 2012)**.** Abundances for all nanoflagellate groups were measured directly using epifluorescent microscopy, which is most effective in studies that measure HNANs (nucleus and no plastid) or PNANs (nucleus and plastid) when ignoring MNANs as part of the local population. Issues arise when we consider the possibility of MNANs existing as part of the community. MNANs can only be identified via epifluorescent microscopy when they ingest a prey (or a prey tracer such as fluorescent microspheres or fluorescently labelled bacteria). We know the entire MNAN population is not consuming at the same time, but rather a portion of a population is eating at any given time (Gast et al., 2018). Therefore, MNAN abundances reported are considered minimum estimates.

The nanoflagellate functional community was dominated by estimated phototrophs throughout the WAP region during the spring. PNAN (10^4) abundance was consistently estimated to be an order of magnitude above the MNAN and HNAN (10^3) portions of the community (0.8 – 0.95 fraction of total nanoflagellate abundance). From their strong contribution to community nanoplanktonic population, total nanoplanktonic abundance was heavily influenced by PNAN abundance. Even though the PNANs dominated the community, their abundances occur on the lower end of the previously reported ranges within the WAP region (Arrigo et al., 2017; Schofield et al., 2017, 2018a). These data in conjunction with consistently low overall planktonic abundance, fluorescence, and chl a values of our study compared to previous investigations suggest 2019 was likely a low chlorophyll year in the WAP, as defined by Nardelli et al (2023).

Contrary to what we expected, the second largest functional group of the WAP community was the HNANs. Compared to PNANs, they still made up a minor fraction of the community, peaking at 20% of community composition. A previous study looking at bacterivorous nanoflagellates during the Ross Sea found similar abundances on the same order of magnitude (10^3) with maximums of 1200 cells mL^{-1} in the sea brine channels (Moorthi et al., 2009). Additionally, an investigation in the Indian sector of the Southern Ocean during the summer of 2018 found similar abundances on the order of 10^3 cells mL^{-1} (Christaki et al., 2020). Similar to the PNANs, reported abundances are within the reported ranges in the Polar Oceans, but unlike PNANs, are not near the lower portion of the range (Duarte et al., 2005a; Maranger et al., 2015; Moreau et al., 2010; Vaque et al., 2004).

Because PNAN abundance is an order of magnitude larger than HNAN abundance, MNANs comprise a larger fraction of the bacterivorous community compared to the primary producing portion of the community throughout the WAP. A trend that has been continuously reported from Spring to Autumn throughout the Polar Oceans, with generally the percentage of heterotrophic protists double that of the percentage of phototrophic protists (Gast et al., 2018; Moorthi et al., 2009; Sanders & Gast, 2012). From this, one could conclude MNANs would have a greater influence over the bacterivorous portion of the community activity compared to the primary producing portion of the community. However, we address this by attempting to quantify both bacterivory and primary production in our study.

4.5.3 Caveats and Differences Between Abundance and Molecular Reads

To quantify both primary production and bacterivory, we employed a new method utilizing the rRNA sequencing dataset from Grattepanche et al (2022). We used this method in several ways. First, this indirect approach allows for estimation of the MNANs contribution to the primary production in the *in situ* system. Second, we could compare the proportional functional composition with that of estimated abundance proportions. Additionally, it yields a range of potential MNANs missed or unobserved using microscopy data for reasons mentioned above. And in turn, gives an idea of the overestimation of PNANs within a given system when MNANs are not accounted for in a study. However, the differences were not consistent throughout the study. Additionally, as previously outlined in the methods, there are a few assumptions/caveats that need to be considered when drawing conclusions with any new method.

The further South the station, the less the proportional difference is between the two proportional estimates. One potential reason for the difference may be due to the species-specific differences in rRNA read number. As we did not identify specific nanoflagellate species using epifluorescent microscopy this comparison would be difficult to determine quantitatively. A second reason may be due to latitudinal differences in plastidic protistan abundances between stations. An increase in the number of plastidic organisms would also increase the encounter rate with bacterivory proxies (microspheres), which would allow for more accurate/consistent assessment of the Antarctic bacterivorous community, especially among the MNAN functional group. Third, due to inherently low estimates of feeding from the WAP region, even within heterotrophs (Duarte et al., 2005b; Vaque et al., 2004), grazing events would be greatly harder to see visually using epifluorescent microscopy. However, because HNANs had an overall negligible difference in estimates over the course of the study, the second and third scenarios seem less likely. Last and most likely, is the discrepancy in the amount of feeding MNANs. In the molecular estimation we are considering all "active" mixotrophic nanoflagellates, but this includes those which are not currently feeding. This discrepancy could be the difference between the actively feeding MNAN community and the presently active community (only primary production) at each station.

4.5.4 Nanoflagellate Primary Production in the Late Spring WAP

Using the rRNA proportions to quantify nanoflagellate, primary production related to the mixotrophs using the activity estimates from RNA seq data. The percentage of reads from RNA seq data and abundances estimated via the classical microscopy approach are vastly different. A difference of scale is to be expected as there is a near 10-

fold difference between the proportion of MNANs and PNANs using epifluorescent microscopy and molecular methods, which is expected as we know there is an underestimation of MNAN abundance using direct measures. This thereby, caused a dramatic changed in estimated PNANs as this redistributes the plastidic faction more towards MNANs and away from PNANs, which would also be reflected in the estimated carbon produced by MNANs and PNANs.

During the WAP austral spring, a large fraction of the nanoplankton primary production was contributed by mixotrophs. As a primary producer, MNANs supplied at least 50% of nanoflagellate community primary production throughout the study, which were consistent with the RNA seq data identifying above half of the total nanoflagellate RNA reads classified as MNANs (Grattepanche et al., 2022). However, there were a few exceptions in the Marguerite Bay, where the activity was similar for both MNANs and PNANs. Additionally, MNAN contribution peaked at the offshore station H (avg 90% between DCM and subsurface depths). This may be due to the theoretical and empirical success of smaller plankton in more offshore bodies of water, which favors chrysophytes and mixed flagellates, clades that have a higher propensity to be mixotrophic. A one-to-one ratio was used regarding the importance of mixotrophs over autotrophs for the primary production. Similar PSII activity was reported for mixotrophic and autotrophic growth of *Ochromonas danica* (Wilken et al., 2014), suggesting that our approach using activity based on percent RNA is appropriate for deciphering the proportion of primary production related to mixotrophic nanoflagellates. However, other studies have also reported a lower primary production, related to lower chlorophyll content of *Poterioochromonas malhamensis* when grew with bacteria (PP/5 for mixotroph, Holen

2001; O2/3 [most likely PP too] in Wilken et al. 2014). So, the contribution of mixotroph might be overestimated by this approach but has the advantage of the first estimation of primary production associated to mixotrophs from *in situ* measurements and assert this as the upper limit of MNAN potential influence.

Even though PNANs were the largest group, they were mostly secondary when compared to the MNAN contribution to nanoflagellate primary production. Typically, the PNAN primary production consisted of less than half of the community primary production. Activity measures of PNANs (total primary production, and nanoplanktonic (<20 µm) primary production) were within reported ranges from previous studies during both spring and summer seasons, but were on the low end of the range (Arrigo et al., 2017; Lin et al., 2021; Nardelli et al., 2023; Schofield et al., 2018a). In addition to low overall primary production during a seemingly low chlorophyll Late Spring, our study accounts for MNAN contribution towards total primary production, which results in a reduction in estimated PNAN relative contributions to the whole nanoflagellate community production.

4.5.5 Nanoflagellate Bacterivory in the WAP Late Spring

Despite being a smaller fraction by abundance, MNANs contributed markedly to the total nanoflagellate community bacterivory during the late austral spring. As a consumer, MNANs generally estimated to contribute over half of the bacterivorous carbon consumed and peaked at over three fourths of nanoflagellate community carbon consumption. The bacterial standing stock removed was on the higher portion of the reported ranges for polar regions but still low compared to some freshwater and marine temperate studies (Havskum & Hansen, 1997; Havskum & Riemann, 1996; Unrein et al., 2007, 2014). Previous estimations of MNAN activity during the summer Ross Sea had much lower bacterial grazing, with a maximum of 14% and 9% of bacterial standing stock removed from the surface and DCM depths, respectively (Gast et al., 2018). In contrast, a second study during the Ross Sea spring saw a up to a maximum of 100% bacterial standing stock removed, with an average of 54% (Moorthi et al., 2009). Due to low bacterial production estimates throughout our study, MNANs consistently consumed around one hundred percent of the bacterial production throughout the WAP. Some stations saw consumption rates of bacterial production above one hundred percent with examples occurring across the latitudinal gradient and at both surveyed depths (i.e., DCM Station C, Surface Station K). Regardless of consumption metric or estimation method, MNANs were the largest fraction of bacterivory in the WAP during the Austral Spring.

While larger in abundance, HNANs exhibited a smaller portion of the bacterivorous activity regardless of method used for estimation by consuming at most 13% of bacterial standing stock, or a max of 68% of community nanoflagellate bacterivorous activity. Indirect feeding estimation via percentage of RNA reads (ribosomal activity estimates) suggested an even lower influence of HNANs within the community. However, due to the low amount of estimated bacterial production, HNANs still consumed a large portion (65%) of the bacterial production. The consumption reported here has been shown throughout the Southern Ocean, with rates of up to 100% of bacterial production (Becquevort, 1997; Becquevort et al., 2000; Duarte et al., 2005a; Pearce et al., 2010; Vaque et al., 2004). Even though HNANs proportion of the community bacterivory is smaller, they can still play an important secondary role within the carbon cycle by consuming non-negligible amounts of the bacterial production.

4.5.6 *MNAN Carbon Acquisition and Demand*

In addition to analyzing the abundance and activity of the MNAN community, we assessed how much of their carbon budget originates from their role as either a producer or consumer. Given the trends from abundance and activity, it's unsurprising the carbon derived from the MNAN portion of the community increased as we move towards higher latitudes, regardless of depth. This is not to be confused with the percent of total MNAN carbon contributed to the nanoflagellate community, which we do not directly assess here. The increase in total carbon contribution is driven primarily by the increase in primary production, while noting that both increases. In general, the MNANs gained most of their carbon from primary production, typically >75% of total MNAN carbon intake. However, there were 3 occurrences where the amount of carbon was near a 50/50 split, all occurrences were at DCM depth but within different station groups (Palmer, stn C; Grandidier, stn G; Marguerite Bay, stn K). While the exact cause of differences between these samples are unknown, there could be a generally difference in the types of mixotrophs within these samples that could be causing the difference in percent carbon estimation.

Along the mixotrophy spectrum, the WAP MNAN community is generally more phototrophic than heterotrophic during the spring/early summer growing period by carbon integration measures. Yet, they maintain a significant role as consumers due to overall low nanoflagellate bacterivorous activity, especially HNANs (which is reflected in the low amount of proportional RNA reads), in the WAP region during this time of year. Their feeding may be for additional carbon to supplement or aid their growth during the late spring. However, they may be feeding to gain nutrients (N, P) or micronutrients (Fe, Si). It is unlikely they would be feeding for additional nitrogen or phosphorous as they were at replete levels throughout the study. However, Si and Fe were not measured and have been shown to limit growth for primary producing protists (Nodwell & Price, 2001; Stukel et al., 2011). Specifically, Phytoplankton production in the Southern Ocean is mostly limited by iron (Martin et al., 1990); which can be acquired via bacterivory (e.g., *Ochromonas*; Maranger et al. 1998). This can explain the relatively low proportion of Carbon obtained through bacterivory compared to primary production. However, the contribution of bacterivory to PP is mostly in the range of a mesocosm study, where the relation bacterivory-primary production was related to temperature with increasing bacterivory with increasing temperature (5-10%; Wilken et al. 2020). In our case, the bacterivory can be low related to the low temperature observed in the Southern Ocean.

The overall high percentage of primary production derived carbon suggests a MNAN community largely composed of primary production leaning MNANs, with a community composition of species with an average carbon budget similar to percentages found in a 2016 study from a temperate species *Dinobryon sociale* , compared to those of *Ochromonas sp.*which has a larger portion of its carbon budget come from bacterivory (Princiotta et al., 2016; Sanders et al., 1990)**.** Few studies have attempted to allocate the amount of cellular carbon attributed to bacterivorous feeding. Havskum and Hansen reported a range of carbon budget acquisition for the nanoflagellate community of 11 to 77% in a Norwegian fjord and Crespo et al. found the nanoflagellate gained approximately 76% of their carbon from bacterivory in the Northwest Iberian upwelling zone during the spring season (Crespo et al., 2011; Havskum & Hansen, 1997)**.**

4.5.7 Latitudinal/Depth Gradients

All measures of abundance and activity showed significant signs of a strong latitudinal gradient, including MNANs. Their abundance and both forms of activity increased as we move from the northern to southern stations. Consistently, latitude was one of the most important variables identified regardless within the correlation matrix. Many studies investigating bacterial, phototrophic and heterotrophic eukaryotic activity and abundance have found similar results along the Western Antarctic Peninsula latitudinal gradient and ice (Arrigo et al., 2017; Ducklow et al., 2012; Henley et al., 2019; Z. Li et al., 2016; Luria et al., 2014; Nardelli et al., 2023; Schofield et al., 2018b). Even though latitude's strong collinearity precludes us from properly identifying the mechanisms behind the observed gradient, we provide some possibilities by removing latitude from the analysis attempting to identify ***potential*** driving parameters of this gradient. Our analysis suggests that while latitude is the main driver but there may be some ***potential*** for depth and local ice floe differences to play a secondary role where light levels are lower and bacterivory may be more preferred, however, additional sampling is required to provide certainty.

4.5.8 Conclusions

This study found MNANs not only persist throughout the WAP region, but they also play important roles as both a consumer and producer during austral late spring/early summer. While the community abundance is dominated by the functional group PNAN (including strict phototrophs and non-grazing mixotrophs), MNANs (grazing mixotrophs) contribute largely to the active portion of the community and provide similar or greater amounts of carbon fixation as a primary producer. Similarly, MNANs consume a larger portion of the bacterial community as a bacterivore. Activity measures were ascertained using a novel molecular approach leveraging percent RNA reads as a proxy for a functional group's activity. While there are several assumptions to consider during interpretation, I believe this method has merit in attaining the upper limit of potential primary production and provides and empirical data for the elusive MNAN contribution to system primary production during in situ studies. Using molecular estimation in conjunction with microscopy-based abundances allows for the most comprehensive assessment of phagotrophic phytoflagellate's primary production and bacterivory *in* situ. This study suggests a need for further research into mixotrophic primary production and bacterivory throughout the WAP during different times of the year (mid-late summer and winter) due to their potential for significant contributions to the carbon cycle and aids in the advancement of in silico modelling by providing additional empirical data for primary production measures estimated and their potential role in the greater system carbon flux.

CHAPTER 5

CONCLUSIONS

This dissertation improves our understanding of the distribution and interaction between mixotrophic phytoflagellates and microplastics in the marine aquatic environments, as evidenced via *in vitro* examinations of mixotrophic physiological responses to microplastic exposure and *in situ* observations of mixotrophs and microplastics in the Southern Ocean. I explored how mixotrophs interact and physiologically respond to increasing microplastic exposure. In addition, I reveal how latitudinal, seasonal, and bathymetric gradients can potentially impact the microbial community (MNAN, HNAN, PNAN) and microplastics microbial community in both distribution, primary production, and bacterivory throughout the WAP region. Additionally, This work pushes forward our understanding of anthropogenic driven changes, specifically microplastic pollution, in a relatively new field within environmental pollution (Thevenon & Carroll, 2015).

The use of plastic microspheres to estimate bacterivory within mixotrophic organisms within this dissertation and in literature forms the basis for chapter two (Princiotta & Sanders, 2017; Sanders et al., 1989; Urabe et al., 1999). In response to increasing direct microplastic exposure, maximal growth rate and bacterivory decreased, whereas primary production increased over the course of the week for *Ochromonas* sp. Conversely, indirect exposure resulted in a decrease in bacterivory, although no significant changes in abundance or primary production were observed. Overall, phagotrophic phytoflagellates were able to withstand increased high amounts of microplastic exposure with regards to abundance, but their foraging behavior changed significantly. The reduction in bacterivory could negatively alter their role in the ecosystem as a consumer and shift more towards a primary producer, ultimately altering their biotic relationships towards more directly competing with other primary producers and so their fitness.

My third chapter investigates the bathymetric and seasonal differences for microplastic distribution and their polymers throughout the water column. I accomplish this at two different years/seasons during the Late Spring (2019) and Early Winter (2022). The small-microplastic size range (0.22 – 20 μm) dominated total microplastic abundance, consisting of 99% of overall microplastic. While there was a low number of polymers identified in the study, the positively buoyant, PE, was the most detected polymer in the two smaller size classes (small- and medium-microplastics). However, the large-microplastics, the largest size class, consisted of mostly PET, which is negatively buoyant, throughout the water column. The importance and dynamics of inter and intra differences between microplastic particle size for both overall abundance and polymer community composition has recently emerged in literature (Bergmann et al., 2023; Leistenschneider et al., 2024). In addition, there were significant differences between seasons on the distribution of microplastic abundance and their polymer composition, with more abundance and polymers observed during the late Spring compared to early Winter. The greatest differences in microplastics seen between size class and season, yet several environmental variables were identified as potential influencers of microplastic distribution. Variables such as density, depth, fluorescence, and beam transmission exhibited different relationships with microplastics across size classes and polymers, varying in both directionality and significance. Additionally, there is evidence that the environmental parameters influence on microplastic distribution is dependent upon both the size of the plastic particle and the chemical composition (polymer), suggesting microplastic pollution should be assessed separately. The partitioning of microplastics into size fractions and polymer is crucial to investigate potential environmental indicators used to predict their distributions. Although specific drivers of seasonal variation remain unclear, this study represents an important step towards the accurately estimating and predicting microplastic movement microplastic and plastic pollution continues to rise.

Traditionally, the microbial community food webs were perceived through the traditional dichotomy of strictly heterotrophic or phototrophic (Flynn et al., 2013). Today, mixotrophs are considered as an integral part of the food web as evidenced through the literature (Mitra et al., 2016; Stoecker et al., 2017; Worden et al., 2015). However, research of mixotrophy in the Southern Ocean is extremely limited, my fourth chapter addresses this gap by unveiling the distribution, primary production, and bacterivory of the nanoflagellate community (heterotrophic, phototrophic, and mixotrophic). I showed that MNANs are not only important consumers of bacterial production, but also a significant source of primary production within the WAP nanoflagellate community. As a consumer, MNANs consistently made up a larger portion of the bacterivory across the WAP. Despite this, the community of MNANs within the region were more phototrophic (attained more carbon from phototrophy compared to heterotrophy). Using the novel method developed here, the carbon fixation estimates of MNANs were often similar to or greater than those for strict phototrophs, despite a 4-fold difference in their estimated abundance. Similarly, mixotrophs consistently consumed a greater portion of the bacterial community in their role as a bacterivore. As a result, MNANs within the WAP region were significant contributors to the potential carbon flux as both a consumer and primary producer. Despite prominent roles as a primary producer and consumer, mixotrophs acquired most of their carbon from primary production in the WAP region. While there are several assumptions to consider during interpretation, I believe this method has merit in attaining the upper limit of potential primary production and provides an empirical dataset for mixotrophic contribution to community primary production *in situ*.

Based on the findings of this dissertation, microplastic concentrations in Paradise Bay are sufficiently high to potentially have negative impacts on the local phagotrophic phytoflagellates of the WAP, though the extent of this impact remains unknown. The current microplastic concentrations in Paradise Bay are comparable to those observed in the low treatment tested here, which induced significant changes in mixotrophic behavior during the microplastic exposure. However, conclusions should be drawn with caution, as the microspheres used in the experiments differ in chemical composition, microplastic type (primary vs secondary microplastic), and shape from those identified in chapter 3. Additionally, the estimated abundance of mixotrophs in the Southern Ocean, as presented in chapter 4, was consistently two orders of magnitude lower than the levels used in the laboratory experiments from chapter 2. Further research is needed to evaluate the susceptibility of the Southern Ocean community to microplastic pollution. Nevertheless, if microplastic concentrations continue to rise as predicted, the potential for alterations in the role of mixotrophic protists as key contributors to bacterivory in the Southern Ocean increases. Such changes could disrupt the carbon flux within the Southern Ocean's food web, potentially leading to widespread cascading effects across the region.

BIBLIOGRAPHY

Alimi, O. S., Farner Budarz, J., Hernandez, L. M., & Tufenkji, N. (2018). Microplastics and Nanoplastics in Aquatic Environments: Aggregation, Deposition, and Enhanced Contaminant Transport. In *Environmental Science and Technology* (Vol. 52, Issue 4, pp. 1704–1724). American Chemical Society. https://doi.org/10.1021/acs.est.7b05559

Amaral-Zettler, L. A., Zettler, E. R., & Mincer, T. J. (2020). Ecology of the plastisphere. *Nature Reviews Microbiology*, *18*(3), 139–151. https://doi.org/10.1038/S41579-019-0308-0

Amaral-Zettler, L. A., Zettler, E. R., Slikas, B., Boyd, G. D., Melvin, D. W., Morrall, C. E., Proskurowski, G., & Mincer, T. J. (2015). The biogeography of the Plastisphere: Implications for policy. *Frontiers in Ecology and the Environment*, *13*(10), 541–546. https://doi.org/10.1890/150017

Anderson, M. R., & Rivkin, R. B. (2001). Seasonal patterns in grazing mortality of bacterioplankton in polar oceans: A bipolar comparison. *Aquatic Microbial Ecology*, *25*(2), 195–206. https://doi.org/10.3354/AME025195

Anderson, R., Charvet, S., & Hansen, P. J. (2018). Mixotrophy in Chlorophytes and Haptophytes—Effect of Irradiance, Macronutrient, Micronutrient and Vitamin Limitation. *Frontiers in Microbiology*, *9*. https://doi.org/10.3389/fmicb.2018.01704

Andersson, A., Falk, S., Samuelsson, G., & Hagstr6m, I. (1989). MICROBIAL ECOLOGY Nutritional Characteristics of a Mixotrophic Nanoflagellate, Ochromonas sp. In *Microb Ecol* (Vol. 17).

Andrady, A. L. (2011). Microplastics in the marine environment. *Marine Pollution Bulletin*, *62*(8), 1596–1605. https://doi.org/10.1016/j.marpolbul.2011.05.030

Andrady, A. L. (2017). The plastic in microplastics: A review. *Marine Pollution Bulletin*, *119*(1), 12–22. https://doi.org/10.1016/j.marpolbul.2017.01.082

Andrady, A. L. (2022). Plastics in the Anthropocene. *Plastics and the Ocean: Origin, Characterization, Fate, and Impacts*, 1–42.

Arrigo, K. R., Van Dijken, G. L., Alderkamp, A.-C., Erickson, Z. K., Lewis, K. M., Lowry, K. E., Joy-Warren, H. L., Middag, R., Nash-Arrigo, J. E., Selz, V., & Van De Poll, W. (2017). Early Spring Phytoplankton Dynamics in the Western Antarctic Peninsula. *Journal of Geophysical Research: Oceans*, *122*, 9350–9369. https://doi.org/10.1002/2017JC013281

Arrigo, K. R., van Dijken, G. L., & Bushinsky, S. (2008). Primary production in the Southern Ocean, 1997-2006. *Journal of Geophysical Research: Oceans*, *113*(8). https://doi.org/10.1029/2007JC004551

Atkinson, A., Siegel, V., Pakhomov, E., & Rothery, P. (2004). Long-term decline in krill stock and increase in salps within the Southern Ocean. *Nature*, *432*(7013), 97–100. https://doi.org/10.1038/nature02950

Auta, H. S., Emenike, C. U., & Fauziah, S. H. (2017a). Distribution and importance of microplastics in the marine environmentA review of the sources, fate, effects, and potential solutions. *Environment International*, *102*, 165–176. https://doi.org/10.1016/j.envint.2017.02.013

Auta, H. S., Emenike, C. U., & Fauziah, S. H. (2017b). Distribution and importance of microplastics in the marine environmentA review of the sources, fate, effects, and potential solutions. *Environment International*, *102*, 165–176. https://doi.org/10.1016/j.envint.2017.02.013

Azam, F., Fenchel, T., Field, J. G., Gray, J. S., Meyerreil, L. A., & Thingstad, F. (1983). The Ecological Role of Water-Column Microbes in the Sea. *Marine Ecology Progress Series*, *10*(3), 257–263. https://doi.org/Doi 10.3354/Meps010257

Azzarello, M. Y., & Van Vleet, E. S. (1987). Marine birds and plastic pollution. *Marine Ecology Progress Series*, *37*(2/3), 295–303.

B.G. Crespo, O. Espinoza-González, I.G. Teixeira, C.G. Castro, & F.G. Figueiras. (2011). Crespo et al. *Estuarine, Coastal and Shelf Science*, *94*(2), 172–181. https://doi.org/https://doi.org/10.1016/j.ecss.2011.06.008

Becquevort, S. (1997). Nanoprotozooplankton in the Atlantic sector of the Southern Ocean during early spring: Biomass and feeding activities. *Deep-Sea Research Part II: Topical Studies in Oceanography*, *44*(1–2), 355–373. https://doi.org/10.1016/S0967-0645(96)00076-8

Becquevort, S., Menon, P., & Lancelot, C. (2000). Differences of the protozoan biomass and grazing during spring and summer in the Indian sector of the Southern Ocean. *Polar Biology*, *23*(5), 309–320. https://doi.org/10.1007/S003000050450

Beleites, C., & Sergo, V. (n.d.). *hyperSpec: a package to handle hyperspectral data sets in R*. https://github.com/r-hyperspec/hyperSpec

Bergmann, M., Allen, S., Krumpen, T., & Allen, D. (2022). High Levels of Microplastics in the Arctic Sea Ice Alga Melosira arctica, a Vector to Ice-Associated and Benthic Food Webs. *Environmental Science and Technology*. https://doi.org/10.1021/acs.est.2c08010

Bergmann, M., Allen, S., Krumpen, T., & Allen, D. (2023). High Levels of Microplastics in the Arctic Sea Ice Alga Melosira arctica, a Vector to Ice-Associated and Benthic Food Webs. *Environmental Science and Technology*, *57*(17), 6799–6807. https://doi.org/10.1021/acs.est.2c08010

Blazewicz, S. J., Barnard, R. L., Daly, R. A., & Firestone, M. K. (2013). Evaluating rRNA as an indicator of microbial activity in environmental communities: Limitations and uses. In *ISME Journal* (Vol. 7, Issue 11, pp. 2061–2068). https://doi.org/10.1038/ismej.2013.102

Boenigk, J., Pfandl, K., Stadler, P., & Chatzinotas, A. (2005). High diversity of the "Spumella-like" flagellates: An investigation based on the SSU rRNA gene sequences of isolates from habitats located in six different geographic regions. *Environmental Microbiology*, *7*(5), 685–697. https://doi.org/10.1111/j.1462-2920.2005.00743.x

Boerger, C. M., Lattin, G. L., Moore, S. L., & Moore, C. J. (2010). Plastic ingestion by planktivorous fishes in the North Pacific Central Gyre. *Marine Pollution Bulletin*, *60*(12), 2275–2278. https://doi.org/10.1016/j.marpolbul.2010.08.007

Booth, B. C., & Horner, R. A. (1997). Microalgae on the arctic ocean section, 1994: species abundance and biomass. *Deep Sea Research Part II: Topical Studies in Oceanography*, *44*(8), 1607–1622. https://doi.org/10.1016/S0967-0645(97)00057-X

Brown, M. S., Munro, D. R., Feehan, C. J., Sweeney, C., Ducklow, H. W., & Schofield, O. M. (2019). Enhanced oceanic CO2 uptake along the rapidly changing West Antarctic Peninsula. In *Nature Climate Change* (Vol. 9, Issue 9, pp. 678–683). Nature Publishing Group. https://doi.org/10.1038/s41558-019-0552-3

Caron, D. A. (2016). Mixotrophy stirs up our understanding of marine food webs. *Proceedings of the National Academy of Sciences*, *113*(11), 2806–2808. https://doi.org/10.1073/pnas.1600718113

Caron, D. A., Sanders, R. W., Lim, E. L., Marrasé, C., Amaral, L. A., Whitney, S., Aoki, R. B., & Porters, K. G. (1993). Light-dependent phagotrophy in the freshwater mixotrophic chrysophyte Dinobryon cylindricum. *Microbial Ecology*, *25*(1), 93–111. https://doi.org/10.1007/BF00182132

Carpenter, E. J., & Smith Jr, K. L. (1972). Plastics on the Sargasso Sea surface. *Science*, *175*(4027), 1240–1241.

Chae, Y., Kim, D., & An, Y. J. (2019). Effects of micro-sized polyethylene spheres on the marine microalga Dunaliella salina: Focusing on the algal cell to plastic particle size ratio. *Aquatic Toxicology, 216*. https://doi.org/10.1016/J.AQUATOX.2019.105296

Cheng, W., Zhou, Y., Xie, Y., Li, Y., Zhou, R., Wang, H., Feng, Y., & Wang, Y. (2023). Combined effect of polystyrene microplastics and bisphenol A on the human embryonic stem cells-derived liver organoids: The hepatotoxicity and lipid accumulation. *Science of the Total Environment*, *854*. https://doi.org/10.1016/j.scitotenv.2022.158585

Choy, C. A., & Drazen, J. C. (2013). Plastic for dinner? Observations of frequent debris ingestion by pelagic predatory fishes from the central North Pacific. *Marine Ecology Progress Series*, *485*, 155–163.

Choy, C. A., Robison, B. H., Gagne, T. O., Erwin, B., Firl, E., Halden, R. U., Hamilton, J. A., Katija, K., Lisin, S. E., Rolsky, C., & S. Van Houtan, K. (2019). The vertical distribution and biological transport of marine microplastics across the epipelagic and mesopelagic water column. *Scientific Reports*, *9*(1). https://doi.org/10.1038/s41598-019-44117-2

Christaki, U., Gueneugues, A., Liu, Y., Blain, S., Catala, P., Colombet, J., Debeljak, P., Jardillier, L., Irion, S., Planchon, F., Sassenhagen, I., Sime-Ngando, T., & Obernosterer, I. (2020). Seasonal microbial food web dynamics in contrasting Southern Ocean productivity regimes. *Limnology and Oceanography*, 1–15. https://doi.org/10.1002/lno.11591

Cimmino, I., Fiory, F., Perruolo, G., Miele, C., Beguinot, F., Formisano, P., & Oriente, F. (2020). Potential mechanisms of bisphenol a (BPA) contributing to human disease. In *International Journal of Molecular Sciences* (Vol. 21, Issue 16, pp. 1–22). MDPI AG. https://doi.org/10.3390/ijms21165761

Coble, P. G., Gagosian, R. B., Codlspotl, L. A., Friederich, G. E., & Christensenii, J. P. (1991). *Vertical distribution of dissolved and particulate fluorescence in the Black Sea* (Vol. 38).

Cole, M., Lindeque, P., Fileman, E., Halsband, C., & Galloway, T. S. (2015). The Impact of Polystyrene Microplastics on Feeding, Function and Fecundity in the Marine Copepod Calanus helgolandicus. *Environmental Science & Technology*, *49*(2), 1130–1137. https://doi.org/10.1021/es504525u

Cole, M., Lindeque, P., Fileman, E., Halsband, C., Goodhead, R., Moger, J., & Galloway, T. S. (2013). Microplastic ingestion by zooplankton. *Environmental Science and Technology*, *47*(12), 6646–6655. https://doi.org/10.1021/es400663f

Costa, D. P., & Crocker, D. E. (1996). Marine Mammals of the Southern Ocean. In R. M. Ross, E. E. Hofmann, & L. B. Quetin (Eds.), *Foundations for Ecological Research West of the Antarctic Peninsula* (Vol. 70, pp. 287–301). Antarctic Research Series.

Cowger, W., Gray, A., Christiansen, S. H., DeFrond, H., Deshpande, A. D., Hemabessiere, L., Lee, E., Mill, L., Munno, K., Ossmann, B. E., Pittroff, M., Rochman, C., Sarau, G., Tarby, S., & Primpke, S. (2020). Critical Review of Processing and Classification Techniques for Images and Spectra in Microplastic Research. *Applied Spectroscopy*, *74*(9), 989–1010. https://doi.org/10.1177/0003702820929064

Cowger, W., Steinmetz, Z., Gray, A., Munno, K., Lynch, J., Hapich, H., Primpke, S., De Frond, H., Rochman, C., & Herodotou, O. (2021). Microplastic Spectral Classification Needs an Open Source Community: Open Specy to the Rescue!

Analytical Chemistry, *93*(21), 7543–7548. https://doi.org/10.1021/acs.analchem.1c00123

Cozar, A., Echevarria, F., Gonzalez-Gordillo, J. I., Irigoien, X., Ubeda, B., Hernandez-Leon, S., Palma, A. T., Navarro, S., Garcia-de-Lomas, J., Ruiz, A., Fernandez-de-Puelles, M. L., & Duarte, C. M. (2014). Plastic debris in the open ocean. *Proceedings of the National Academy of Sciences*, *111*(28), 10239–10244. https://doi.org/10.1073/pnas.1314705111

De Stephanis, R., Giménez, J., Carpinelli, E., Gutierrez-Exposito, C., & Cañadas, A. (2013). As main meal for sperm whales: plastics debris. *Marine Pollution Bulletin*, *69*(1–2), 206–214.

Dong, S., Sprintall, J., Gille, S. T., & Talley, L. (2008). Southern ocean mixed-layer depth from Argo float profiles. *Journal of Geophysical Research: Oceans*, *113*(6). https://doi.org/10.1029/2006JC004051

Duarte, C. M., Agustí, S., Vaqué, D., Agawin, N. S. R., Felipe, J., Casamayor, E. O., & Gasol, J. M. (2005a). Experimental test of bacteria-phytoplankton coupling in the Southern Ocean. *Limnology and Oceanography*, *50*(6), 1844–1854. https://doi.org/10.4319/LO.2005.50.6.1844

Duarte, C. M., Agustí, S., Vaqué, D., Agawin, N. S. R., Felipe, J., Casamayor, E. O., & Gasol, J. M. (2005b). Experimental test of bacteria-phytoplankton coupling in the Southern Ocean. *Limnology and Oceanography*, *50*(6), 1844–1854. https://doi.org/10.4319/lo.2005.50.6.1844

Ducklow, H. W., Baker, K., Martinson, D. G., Quetin, L. B., Ross, R. M., Smith, R. C., Stammerjohn, S. E., Vernet, M., & Fraser, W. (2007). Marine pelagic ecosystems: The West Antarctic Peninsula. In *Philosophical Transactions of the Royal Society B: Biological Sciences* (Vol. 362, Issue 1477, pp. 67–94). Royal Society. https://doi.org/10.1098/rstb.2006.1955

Ducklow, H. W., Schofield, O., Vernet, M., Stammerjohn, S., & Erickson, M. (2012). Multiscale control of bacterial production by phytoplankton dynamics and sea ice along the western Antarctic Peninsula: A regional and decadal investigation. *Journal of Marine Systems*, *98–99*, 26–39. https://doi.org/10.1016/J.JMARSYS.2012.03.003

Edwards, K. F. (2019). Mixotrophy in nanoflagellates across environmental gradients in the ocean. *Proceedings of the National Academy of Sciences of the United States of America*, *116*(13), 6211–6220. https://doi.org/10.1073/PNAS.1814860116/-/DCSUPPLEMENTAL

Elloumi, J., Carrias, J.-F., Ayadi, H., Sime-Ngando, T., & Bouaïn, A. (2009). Communities structure of the planktonic halophiles in the solar saltern of Sfax, Tunisia. *Estuarine, Coastal and Shelf Science*, *81*(1), 19–26.

Enders, K., Lenz, R., Stedmon, C. A., & Nielsen, T. G. (2015). Abundance, size and polymer composition of marine microplastics ≥10 µm in the Atlantic Ocean and their modelled vertical distribution. *Marine Pollution Bulletin*, *100*(1), 70–81. https://doi.org/10.1016/j.marpolbul.2015.09.027

Eriksen, M., Lebreton, L. C. M., Carson, H. S., Thiel, M., Moore, C. J., Borerro, J. C., Galgani, F., Ryan, P. G., & Reisser, J. (2014). Plastic Pollution in the World's Oceans: More than 5 Trillion Plastic Pieces Weighing over 250,000 Tons Afloat at Sea. *PLoS ONE*, *9*(12), e111913. https://doi.org/10.1371/journal.pone.0111913

Eriksen, M., Mason, S., Wilson, S., Box, C., Zellers, A., Edwards, W., Farley, H., & Amato, S. (2013). Microplastic pollution in the surface waters of the Laurentian Great Lakes. *Marine Pollution Bulletin*, *77*(1–2), 177–182. https://doi.org/10.1016/j.marpolbul.2013.10.007

Erni-Cassola, G., Zadjelovic, V., Gibson, M. I., & Christie-Oleza, J. A. (2019). Distribution of plastic polymer types in the marine environment; A meta-analysis. *Journal of Hazardous Materials*, *369*, 691–698. https://doi.org/10.1016/j.jhazmat.2019.02.067

Everaert, G., Van Cauwenberghe, L., De Rijcke, M., Koelmans, A. A., Mees, J., Vandegehuchte, M., & Janssen, C. R. (2018). Risk assessment of microplastics in the ocean: Modelling approach and first conclusions. *Environmental Pollution*, *242*, 1930–1938. https://doi.org/10.1016/j.envpol.2018.07.069

Fendall, L. S., & Sewell, M. A. (2009). Contributing to marine pollution by washing your face: Microplastics in facial cleansers. *Marine Pollution Bulletin*, *58*(8), 1225–1228. https://doi.org/https://doi.org/10.1016/j.marpolbul.2009.04.025

Flegontova, O., Flegontov, P., Jachníková, N., Lukeš, J., & Horák, A. (2023). Water masses shape pico-nano eukaryotic communities of the Weddell Sea. *Communications Biology 2023 6:1*, *6*(1), 1–10. https://doi.org/10.1038/s42003-023-04452-7

Flynn, K. J., Stoecker, D. K., Mitra, A., Raven, J. A., Glibert, P. M., Hansen, P. J., Granéli, E., & Burkholder, J. M. (2013). Misuse of the phytoplankton-zooplankton dichotomy: The need to assign organisms as mixotrophs within plankton functional types. *Journal of Plankton Research*, *35*(1), 3–11. https://doi.org/10.1093/plankt/fbs062

Free, C. M., Jensen, O. P., Mason, S. A., Eriksen, M., & Williamson, N. J. (2014). High-levels of microplastic pollution in a large , remote , mountain lake. *Marine Pollution Bulletin*, *85*(1), 156–163. https://doi.org/10.1016/j.marpolbul.2014.06.001

Freudenthal, J., Ju, F., Bürgmann, H., & Dumack, K. (2022). Microeukaryotic gut parasites in wastewater treatment plants: diversity, activity, and removal. *Microbiome*, *10*(1). https://doi.org/10.1186/s40168-022-01225-y

Friedlaender, A. S., Halpin, P. N., Qian, S. S., Lawson, G. L., Wiebe, P. H., Thiele, D., & Read, A. J. (2006). Whale distribution in relation to prey abundance and oceanographic processes in shelf waters of the Western Antarctic Peninsula. *Marine Ecology Progress Series*, *317*, 297–310.

Fulfer, V. M., & Menden-Deuer, S. (2021). Heterotrophic Dinoflagellate Growth and Grazing Rates Reduced by Microplastic Ingestion. *Frontiers in Marine Science*, *8*. https://doi.org/10.3389/fmars.2021.716349

Galloway, T. S., Cole, M., & Lewis, C. (2017). Interactions of microplastic debris throughout the marine ecosystem. *Nature Ecology and Evolution*, *1*(5), 1–8. https://doi.org/10.1038/s41559-017-0116

Garzio, L. M., Steinberg, D. K., Erickson, M., & Ducklow, H. W. (2013). Microzooplankton grazing along the Western Antarctic Peninsula. *Aquatic Microbial Ecology*, *70*(3), 215–232. https://doi.org/10.3354/AME01655

Gast, R. J., Fay, S. A., & Sanders, R. W. (2018). Mixotrophic activity and diversity of Antarctic marine protists in austral summer. *Frontiers in Marine Science*, *5*(FEB), 13. https://doi.org/10.3389/FMARS.2018.00013/BIBTEX

Gast, R. J., McKie-Krisberg, Z. M., Fay, S. A., Rose, J. M., & Sanders, R. W. (2014a). Antarctic mixotrophic protist abundances by microscopy and molecular methods. *FEMS Microbiology Ecology*, *89*(2), 388–401. https://doi.org/10.1111/1574-6941.12334

Gast, R. J., McKie-Krisberg, Z. M., Fay, S. A., Rose, J. M., & Sanders, R. W. (2014b). Antarctic mixotrophic protist abundances by microscopy and molecular methods. *FEMS Microbiology Ecology*, *89*(2), 388–401. https://doi.org/10.1111/1574-6941.12334

Geisen, S., Tveit, A. T., Clark, I. M., Richter, A., Svenning, M. M., Bonkowski, M., & Urich, T. (2015). Metatranscriptomic census of active protists in soils. *ISME Journal*, *9*(10), 2178–2190. https://doi.org/10.1038/ismej.2015.30

Geng, X., Wang, J., Zhang, Y., & Jiang, Y. (2021). How do microplastics affect the marine microbial loop? Predation of microplastics by microzooplankton. *Science of The Total Environment*, *758*, 144030. https://doi.org/10.1016/J.SCITOTENV.2020.144030

Gewert, B., Plassmann, M. M., & MacLeod, M. (2015). Pathways for degradation of plastic polymers floating in the marine environment. *Environmental Science: Processes & Impacts*, *17*(9), 1513–1521.

Geyer, R., Jambeck, J. R., & Law, K. L. (2017). *Production, use, and fate of all plastics ever made*. https://www.science.org

Ghosal, S., Chen, M., Wagner, J., Wang, Z. M., & Wall, S. (2018). Molecular identification of polymers and anthropogenic particles extracted from oceanic water and fish stomach – A Raman micro-spectroscopy study. *Environmental Pollution*, *233*, 1113–1124. https://doi.org/10.1016/j.envpol.2017.10.014

Goldstein, M. C., Rosenberg, M., & Cheng, L. (2012). Increased oceanic microplastic debris enhances oviposition in an endemic pelagic insect. *Biology Letters*, *8*(5), 817–820.

Gordon, M. (2006). Eliminating land-based discharges of marine debris in California: A plan of action from the Plastic Debris Project. *California State Water Resources Control Board, Sacramento, CA*.

Grattepanche, J. D., Jeffrey, W. H., Gast, R. J., & Sanders, R. W. (2022). Diversity of Microbial Eukaryotes Along the West Antarctic Peninsula in Austral Spring. *Frontiers in Microbiology*, *13*. https://doi.org/10.3389/FMICB.2022.844856

Guilhermino, L., Martins, A., Cunha, S., & Fernandes, J. O. (2021). Long-term adverse effects of microplastics on Daphnia magna reproduction and population growth rate at increased water temperature and light intensity: Combined effects of stressors and interactions. *Science of The Total Environment*, *784*, 147082. https://doi.org/https://doi.org/10.1016/j.scitotenv.2021.147082

Gulizia, A. M., Patel, K., Philippa, B., Motti, C. A., van Herwerden, L., & Vamvounis, G. (2023). Understanding plasticiser leaching from polystyrene microplastics. *Science of the Total Environment*, *857*. https://doi.org/10.1016/j.scitotenv.2022.159099

Gurumoorthi, K., & Luis, A. J. (2023). Recent trends on microplastics abundance and risk assessment in coastal Antarctica: Regional meta-analysis. In *Environmental Pollution* (Vol. 324). Elsevier Ltd. https://doi.org/10.1016/j.envpol.2023.121385

Haram, L. E., Carlton, J. T., Ruiz, G. M., & Maximenko, N. A. (2020). A plasticene lexicon. *Marine Pollution Bulletin*, *150*, 110714.

Harshvardhan, K., & Jha, B. (2013). Biodegradation of low-density polyethylene by marine bacteria from pelagic waters, Arabian Sea, India. *Marine Pollution Bulletin*, *77*(1–2), 100–106.

Hartmann, M., Grob, C., Tarran, G. a., Martin, a. P., Burkill, P. H., Scanlan, D. J., & Zubkov, M. V. (2012). Mixotrophic basis of Atlantic oligotrophic ecosystems. *Proceedings of the National Academy of Sciences of the United States of America*, *109*(15), 5756–5760. https://doi.org/10.1073/pnas.1118179109

Havskum, H., & Hansen, A. S. (1997). *Nano-Sized Protists As Grazers on Nanoplankton and in Enclosures*. *12*(1996), 139–151.

Havskum, H., & Riemann, B. (1996). Ecological importance of bacterivorous, pigmented flagellates (mixotrophs) in the Bay of Aarhus, Denmark. *Marine Ecology*

Progress Series, *137*(1–3), 251–263. https://doi.org/10.3354/meps137251

Henley, S. F., Schofield, O. M., Hendry, K. R., Schloss, I. R., Steinberg, D. K., Moffat, C., Peck, L. S., Costa, D. P., Bakker, D. C. E., Hughes, C., Rozema, P. D., Ducklow, H. W., Abele, D., Stefels, J., Van Leeuwe, M. A., Brussaard, C. P. D., Buma, A. G. J., Kohut, J., Sahade, R., … Meredith, M. P. (2019). Variability and change in the west Antarctic Peninsula marine system: Research priorities and opportunities. *Progress in Oceanography*, *173*, 208–237. https://doi.org/10.1016/j.pocean.2019.03.003

Hitchcock, J. N. (2022). Microplastics can alter phytoplankton community composition. *Science of The Total Environment*, *819*, 153074. https://doi.org/10.1016/J.SCITOTENV.2022.153074

Hobbie, J. E., Daley, R. J., & Jasper, S. (1977). Use of nuclepore filters for counting bacteria by fluorescence microscopy. *Applied and Environmental Microbiology*, *33*(5), 1225–1228.

Hofmann, E. E., Klinck, J. M., Lascara, C. M., & Smith, D. A. (1996). Water mass distribution and circulation west of the Antarctic Peninsula and including Bransfield Strait. In *Foundations for Ecological Research West of the Antarctic Peninsula* (pp. 61–80). https://doi.org/10.1029/ar070p0061

Holen, D. A. (2001). The effects of heterotrophy on chlorophyll a and photosynthesis in a mixotrophic chrysophyte. *Nova Hedwigia Beifeft*, *122*, 107–118. https://www.researchgate.net/publication/263766542

Holmes, R. M., Aminot, A., Kérouel, R., Hooker, B. A., & Peterson, B. J. (1999). A simple and precise method for measuring ammonium in marine and freshwater ecosystems. *Canadian Journal of Fisheries and Aquatic Sciences*, *56*(10), 1801–1808. https://doi.org/10.1139/f99-128

Hulot, F. D., Morin, P. J., & Loreau, M. (2001). Interactions between algae and the microbial loop in experimental microcosms. *Oikos*, *95*(2), 231–238.

Ijaz, U., Baki, A. B. M., Wu, W., & Zhang, W. (2024). Settling velocity of microplastics in turbulent open-channel flow. *Science of the Total Environment*, *946*(March), 174179. https://doi.org/10.1016/j.scitotenv.2024.174179

Ilechukwu, I., Das, R. R., & Reimer, J. D. (2023). Review of microplastics in museum specimens: An under-utilized tool to better understand the Plasticene. *Marine Pollution Bulletin*, *191*, 114922.

Inkinen, J., Jayaprakash, B., Siponen, S., Hokajärvi, A. M., Pursiainen, A., Ikonen, J., Ryzhikov, I., Täubel, M., Kauppinen, A., Paananen, J., Miettinen, I. T., Torvinen, E., Kolehmainen, M., & Pitkänen, T. (2019). Active eukaryotes in drinking water distribution systems of ground and surface waterworks. *Microbiome*, *7*(1). https://doi.org/10.1186/s40168-019-0715-5

Ishikawa, A., Wright, S. W., van den Enden, R., Davidson, A. T., & Marchant, H. J. (2002). Abundance, size structure and community composition of phytoplankton in the Southern Ocean in the austral summer 1999/2000. In *Polar Biosci* (Vol. 15).

Isobe, A., Uchiyama-Matsumoto, K., Uchida, K., & Tokai, T. (2017). Microplastics in the Southern Ocean. *Marine Pollution Bulletin*, *114*(1), 623–626. https://doi.org/10.1016/j.marpolbul.2016.09.037

Jambeck, J. R., Geyer, R., Wilcox, C., Siegler, T. R., Perryman, M., Andrady, A., Narayan, R., & Law, K. L. (2015). Plastic waste inputs from land into the ocean. *Science*, *347*(6223), 768–771. https://doi.org/10.1126/SCIENCE.1260352

Jeong, C.-B., Won, E.-J., Kang, H.-M., Lee, M.-C., Hwang, D.-S., Hwang, U.-K., Zhou, B., Souissi, S., Lee, S.-J., & Lee, J.-S. (2016). Microplastic size-dependent toxicity, oxidative stress induction, and p-JNK and p-p38 activation in the monogonont rotifer (Brachionus koreanus). *Environmental Science & Technology*, *50*(16), 8849–8857.

Kara, A. B., Rochford, P. A., & Hurlburt, H. E. (2003). Mixed layer depth variability over the global ocean. *Journal of Geophysical Research: Oceans*, *108*(3). https://doi.org/10.1029/2000jc000736

Kelly, A., Lannuzel, D., Rodemann, T., Meiners, K. M., & Auman, H. J. (2020). Microplastic contamination in east Antarctic sea ice. *Marine Pollution Bulletin*, *154*. https://doi.org/10.1016/j.marpolbul.2020.111130

King, J. C., Turner, J., Marshall, G. J., Connolley, W. M., & Lachlan-Cope, T. A. (2003). ANTARCTIC PENINSULA CLIMATE VARIABILITY AND ITS CAUSES AS REVEALED BY ANALYSIS OF INSTRUMENTAL RECORDS. *ANTARCTIC PENINSULA CLIMATE VARIABILITY ANTARCTIC RESEARCH SERIES*, *79*, 17–30. https://doi.org/10.1029/079ARS02

Klinck, J. M. (1998). Heat and salt changes on the continental shelf west of the Antarctic Peninsula between January 1993 and January 1994. *Journal of Geophysical Research: Oceans*, *103*(3334), 7617–7636. https://doi.org/10.1029/98jc00369

Koid, A. E., Liu, Z., Terrado, R., Jones, A. C., Caron, D. A., & Heidelberg, K. B. (2014). Comparative transcriptome analysis of four prymnesiophyte algae. *PLoS ONE*, *9*(6). https://doi.org/10.1371/journal.pone.0097801

Kong, Q., Li, Y., Xu, X., Cheng, J., Sun, Y., Zhang, L., Huang, Y., & Yang, Z. (2021). Microplastics interfere with mixotrophic Ochromonas eliminating toxic Microcystis. *Chemosphere*, *265*, 129030. https://doi.org/10.1016/J.CHEMOSPHERE.2020.129030

Koppelle, S., Ivanković, M., Bengtsson, M. M., Preiler, C., Huisman, J., Brussaard, C. P. D., Engelmann, J. C., Ptáčník, R., & Wilken, S. (2024). Contrasting responses of different mixotrophic protists to light and nutrient availability. *Limnology and Oceanography*, *69*(5), 1233–1246. https://doi.org/10.1002/lno.12565

Korb, R. E., & Whitehouse, M. (2004). Contrasting primary production regimes around South Georgia, Southern Ocean: large blooms versus high nutrient, low chlorophyll waters. *Deep Sea Research Part I: Oceanographic Research Papers*, *51*(5), 721–738. https://doi.org/https://doi.org/10.1016/j.dsr.2004.02.006

Kuklinski, P., Wicikowski, L., Koper, M., Grala, T., Leniec-Koper, H., Barasiński, M., Talar, M., Kamiński, I., Kibart, R., & Małecki, W. (2019). Offshore surface waters of Antarctica are free of microplastics, as revealed by a circum-Antarctic study. *Marine Pollution Bulletin*, *149*. https://doi.org/10.1016/j.marpolbul.2019.110573

Law, K. L., Morét-Ferguson, S., Maximenko, N. A., Proskurowski, G., Peacock, E. E., Hafner, J., & Reddy, C. M. (2010). Plastic accumulation in the North Atlantic subtropical gyre. *Science*, *329*(5996), 1185–1188.

Le Guen, C., Suaria, G., Sherley, R. B., Ryan, P. G., Aliani, S., Boehme, L., & Brierley, A. S. (2020). Microplastic study reveals the presence of natural and synthetic fibres in the diet of King Penguins (Aptenodytes patagonicus) foraging from South Georgia. *Environment International*, *134*. https://doi.org/10.1016/j.envint.2019.105303

Lebreton, L.-M., Greer, S. D., & Borrero, J. C. (2012). Numerical modelling of floating debris in the world’s oceans. *Marine Pollution Bulletin*, *64*(3), 653–661.

Lee, S., & Fuhrman, J. A. (1987). Relationships between Biovolume and Biomass of Naturally DerivedMarine Bacterioplankton. *Applie and Environmental Microbiology*, *53*(6), 1298–1303.

Lehtiniemi, M., Hartikainen, S., Näkki, P., Engström-Öst, J., Koistinen, A., & Setälä, O. (2018). Size matters more than shape: Ingestion of primary and secondary microplastics by small predators. *Food Webs*, *17*. https://doi.org/10.1016/j.fooweb.2018.e00097

Leistenschneider, C., Wu, F., Primpke, S., Gerdts, G., & Burkhardt-Holm, P. (2024). Unveiling high concentrations of small microplastics (11–500 µm) in surface water samples from the southern Weddell Sea off Antarctica. *Science of the Total Environment*, *927*. https://doi.org/10.1016/j.scitotenv.2024.172124

Lewis, C., Lenton, T. M., Clark, J. R., Galloway, T. S., Blackford, J., Cole, M., Fileman, E., & Lindeque, P. K. (2016). Marine microplastic debris: a targeted plan for understanding and quantifying interactions with marine life. *Frontiers in Ecology and the Environment*, *14*(6), 317–324. https://doi.org/10.1002/fee.1297

Li, W. K. W., McLaughlin, F. A., Lovejoy, C., & Carmack, E. C. (2009). Smallest Algae Thrive As the Arctic Ocean Freshens. *Science*, *326*(5952), 539–539.

https://doi.org/10.1126/science.1179798

Li, Z., Cassar, N., Huang, K., Ducklow, H., & Schofield, O. (2016). Interannual variability in net community production at the Western Antarctic Peninsula region (1997–2014). *Journal of Geophysical Research: Oceans*, *121*(7), 4748–4762. https://doi.org/10.1002/2015JC011378

Lin, Y., Moreno, C., Marchetti, A., Ducklow, H., Schofield, O., Delage, E., Meredith, M., Li, Z., Eveillard, D., Chaffron, S., & Cassar, N. (2021). Decline in plankton diversity and carbon flux with reduced sea ice extent along the Western Antarctic Peninsula. *Nature Communications*, *12*(1). https://doi.org/10.1038/s41467-021-25235-w

Long, M., Moriceau, B., Gallinari, M., Lambert, C., Huvet, A., Raffray, J., & Soudant, P. (2015). Interactions between microplastics and phytoplankton aggregates: Impact on their respective fates. *Marine Chemistry*, *175*, 39–46. https://doi.org/10.1016/j.marchem.2015.04.003

Long, M., Paul-Pont, I., Hégaret, H., Moriceau, B., Lambert, C., Huvet, A., & Soudant, P. (2017). Interactions between polystyrene microplastics and marine phytoplankton lead to species-specific hetero-aggregation. *Environmental Pollution*, *228*, 454–463. https://doi.org/10.1016/j.envpol.2017.05.047

Lovejoy, C., Legendre, L., Martineau, M. J., Bâcle, J., & Von Quillfeldt, C. H. (2002). Distribution of phytoplankton and other protists in the North Water. *Deep Sea Research Part II: Topical Studies in Oceanography*, *49*(22–23), 5027–5047. https://doi.org/10.1016/S0967-0645(02)00176-5

Lozoya, J. P., Rodríguez, M., Azcune, G., Lacerot, G., Pérez-Parada, A., Lenzi, J., Rossi, F., & de Mello, F. T. (2022). Stranded pellets in Fildes Peninsula (King George Island, Antarctica): New evidence of Southern Ocean connectivity. *Science of the Total Environment*, *838*. https://doi.org/10.1016/j.scitotenv.2022.155830

Luria, C. M., Ducklow, H. W., & Amaral-Zettler, L. A. (2014). Marine bacterial, archaeal and eukaryotic diversity and community structure on the continental shelf of the western Antarctic Peninsula. *Aquatic Microbial Ecology*, *73*(2), 107–121. https://doi.org/10.3354/ame01703

M'Rabet, C., Pringault, O., Zmerli-Triki, H., Ben Gharbia, H., Couet, D., & Kéfi-Daly Yahia, O. (2018). Impact of two plastic-derived chemicals, the Bisphenol A and the di-2-ethylhexyl phthalate, exposure on the marine toxic dinoflagellate Alexandrium pacificum. *Marine Pollution Bulletin*, *126*(October 2017), 241–249. https://doi.org/10.1016/j.marpolbul.2017.10.090

MacIntyre, H. L., Geider, R. J., & McKay, R. M. (1996). PHOTOSYNTHESIS AND REGULATION OF RUBISCO ACTIVITY IN NET PHYTOPLANKTON FROM DELAWARE BAY1. *Journal of Phycology*, *32*(5), 718–731. https://doi.org/10.1111/j.0022-3646.1996.00718.x

Magalhães, K. M., Rosa Filho, J. S., Teixeira, C. E. P., Coelho-Jr, C., Lima, M. C. S., Costa Souza, A. M., & Soares, M. O. (2022). Oil and plastic spill: 2021 as another challenging year for marine conservation in the South Atlantic Ocean. *Marine Policy*, *140*, 105076. https://doi.org/https://doi.org/10.1016/j.marpol.2022.105076

Manríquez-Guzmán, D., & Ramírez-García, P. (2023). *Effect of ABS secondary microplastics on survival, mortality rate, life expectancy and fecundity of the freshwater cladocerans Moina macrocopa*. https://doi.org/10.21203/rs.3.rs-3657139/v1

Maranger, R., Bird, D. F., & Price, N. M. (1998). Iron acquisition by photosynthetic marine phytoplankton from ingested bacteria. *Nature*, *396*(6708), 248–251.

Maranger, R., Vaqué, D., Nguyen, D., Hébert, M. P., & Lara, E. (2015). Pan-Arctic patterns of planktonic heterotrophic microbial abundance and processes: Controlling factors and potential impacts of warming. *Progress in Oceanography*, *139*(November), 221–232. https://doi.org/10.1016/j.pocean.2015.07.006

Martin, J. H., Fitzwater, S. E., & Gordon, R. M. (1990). Iron deficiency limits phytoplankton growth in Antarctic waters. *Global Biogeochemical Cycles*, *4*(1), 5–12.

Martinson, D. G., Stammerjohn, S. E., Iannuzzi, R. A., Smith, R. C., & Vernet, M. (2008). Western Antarctic Peninsula physical oceanography and spatio–temporal variability. *Deep Sea Research Part II: Topical Studies in Oceanography*, *55*(18), 1964–1987. https://doi.org/https://doi.org/10.1016/j.dsr2.2008.04.038

Marturano, V., Cerruti, P., & Ambrogi, V. (2019). Polymer additives. *Physical Sciences Reviews*, *2*(6). https://doi.org/10.1515/psr-2016-0130

Mateos-Cárdenas, A., Scott, D. T., Seitmaganbetova, G., van, van P., John, O. H., & Marcel A.K., J. (2019). Polyethylene microplastics adhere to Lemna minor (L.), yet have no effects on plant growth or feeding by Gammarus duebeni (Lillj.). *Science of the Total Environment*, *689*, 413–421. https://doi.org/10.1016/j.scitotenv.2019.06.359

Matrai, P. A., Vernet, M., Hood, R., Jennings, A., Brody, E., & Saemundsd6ttir, S. (1995). Light-dependence of carbon and sulfur production by polar clones of the genus Phaeocystis. In *Marine Biology* (Vol. 124). Springer-Verlag.

Maximenko, N., Hafner, J., & Niiler, P. (2012). Pathways of marine debris derived from trajectories of Lagrangian drifters. *Marine Pollution Bulletin*, *65*(1–3), 51–62.

McKie-Krisberg, Z. M., Gast, R. J., & Sanders, R. W. (2015). Physiological Responses of Three Species of Antarctic Mixotrophic Phytoflagellates to Changes in Light and Dissolved Nutrients. *Microbial Ecology*, *70*(1), 21–29. https://doi.org/10.1007/s00248-014-0543-x

McKie-Krisberg, Z. M., & Sanders, R. W. (2014). Phagotrophy by the picoeukaryotic green alga Micromonas: implications for Arctic Oceans. *The ISME Journal*, *8*(10), 1953–1961. https://doi.org/10.1038/ismej.2014.16

Menden-Deuer, S., & Lessard, E. J. (2000). Carbon to Volume Relationships for Dinoflagellates, Diatoms, and Other Protist Plankton. *Limnology and Oceanography*, *45*(3), 569–579.

Meredith, M. P., & King, J. C. (2005). Rapid climate change in the ocean west of the Antarctic Peninsula during the second half of the 20th century. *Geophysical Research Letters*, *32*(19), 1–5. https://doi.org/10.1029/2005GL024042

Metzl, N. (2019). A canary in the Southern Ocean. In *Nature Climate Change* (Vol. 9, Issue 9, pp. 651–652). Nature Publishing Group. https://doi.org/10.1038/s41558-019-0562-1

Miller, R. Z., Watts, A. J. R., Winslow, B. O., Galloway, T. S., & Barrows, A. P. W. (2017). Mountains to the sea: River study of plastic and non-plastic microfiber pollution in the northeast USA. *Marine Pollution Bulletin*. https://doi.org/10.1016/j.marpolbul.2017.07.028

Millette, N. C., Gast, R. J., Luo, J. Y., Moeller, H. V, Stamieszkin, K., Andersen, K. H., Brownlee, E. F., Cohen, N. R., Duhamel, S., & Dutkiewicz, S. (2023). Mixoplankton and mixotrophy: future research priorities. *Journal of Plankton Research*, *45*(4), 576–596.

Mitra, A., Flynn, K. J., Tillmann, U., Raven, J. A., Caron, D., Stoecker, D. K., Not, F., Hansen, P. J., Hallegraeff, G., Sanders, R., Wilken, S., McManus, G., Johnson, M., Pitta, P., Våge, S., Berge, T., Calbet, A., Thingstad, F., Jeong, H. J., … Lundgren, V. (2016). Defining Planktonic Protist Functional Groups on Mechanisms for Energy and Nutrient Acquisition: Incorporation of Diverse Mixotrophic Strategies. *Protist*, *167*(2), 106–120. https://doi.org/10.1016/J.PROTIS.2016.01.003

Montes-Hugo, M., Doney, S. C., Ducklow, H. W., Fraser, W., Martinson, D., Stammerjohn, S. E., & Schofield, O. (2009). Recent Changes in PhytoplanktonCommunities Associated with RapidRegional Climate Change Along theWestern Antarctic Peninsula. *Science*, *323*, 1470–1473. https://doi.org/10.1126/science.1128834

Moorthi, S., Caron, D. A., Gast, R. J., & Sanders, R. W. (2009). Mixotrophy: A widespread and important ecological strategy for planktonic and sea-ice nanoflagellates in the Ross Sea, Antarctica. *Aquatic Microbial Ecology*, *54*(3), 269–277. https://doi.org/10.3354/AME01276

Moreau, S., Ferreyra, G. A., Mercier, B., Lemarchand, K., Lionard, M., Roy, S., Mostajir, B., Roy, S., van Hardenberg, B., & Demers, S. (2010). Variability of the microbial community in the western Antarctic Peninsula from late fall to spring during a low ice cover year. *Polar Biology*, *33*(12), 1599–1614. https://doi.org/10.1007/s00300-010-0806-z

Näkki, P., Setälä, O., & Lehtiniemi, M. (2019). Seafloor sediments as microplastic sinks in the northern Baltic Sea–negligible upward transport of buried microplastics by bioturbation. *Environmental Pollution*, *249*, 74–81.

Nardelli, S. C., Gray, P. C., Stammerjohn, S. E., & Schofield, O. (2023). Characterizing coastal phytoplankton seasonal succession patterns on the West Antarctic Peninsula. *Limnology and Oceanography*. https://doi.org/10.1002/lno.12314

Nava, V., & Leoni, B. (2021). A critical review of interactions between microplastics, microalgae and aquatic ecosystem function. *Water Research*, *188*, 116476. https://doi.org/10.1016/J.WATRES.2020.116476

Nerland, I. L., Halsband, C., Allan, I., & Thomas, K. V. (2014). *Microplastics in marine environments: Occurrence, distribution and effects*. http://www.miljodirektoratet.no/Documents/publikasjoner/M319/M319.pdf

Ng, P. H. R., Walker, S., Tahtouh, M., & Reedy, B. J. (2009). Detection of illicit substances in fingerprints by infrared spectral imaging. *Analytical and Bioanalytical Chemistry*, *394*, 2039–2048. https://api.semanticscholar.org/CorpusID:20955679

Nodwell, L. M., & Price, N. M. (2001). Direct use of inorganic colloidal iron by marine mixotrophic phytoplankton. *Limnology and Oceanography*, *46*(4), 765–777. https://doi.org/10.4319/lo.2001.46.4.0765

Obbard, R. W., Sadri, S., Wong, Y. Q., Khitun, A. A., Baker, I., & Thompson, R. C. (2014). Global warming releases microplastic legacy frozen in Arctic Sea ice. *Earth's Future*, *2*(6), 315–320. https://doi.org/10.1002/2014ef000240

Ogonowski, M., Schür, C., Jarsén, Å., & Gorokhova, E. (2016). The effects of natural and anthropogenic microparticles on individual fitness in daphnia magna. *PLoS ONE*, *11*(5). https://doi.org/10.1371/journal.pone.0155063

Orsi, A. H., Whitworth Iii, T., & Nowlin, W. D. (1995). *On the meridional extent and fronts of the Antarctic Circumpolar Current* (Vol. 42, Issue 5).

Parsons, T. R., Maita, Y., & Lalli, C. M. (1984). A manual of chemical and biological methods for seawater analysis / by Timothy R. Parsons, Yoshiaki Maita and Carol M. Lalli. In *A manual of chemical and biological methods for seawater analysis* (1st ed.). Pergamon Press.

Paul-Pont, I., Lacroix, C., González Fernández, C., Hégaret, H., Lambert, C., Le Goïc, N., Frère, L., Cassone, A. L., Sussarellu, R., Fabioux, C., Guyomarch, J., Albentosa, M., Huvet, A., & Soudant, P. (2016). Exposure of marine mussels Mytilus spp. to polystyrene microplastics: Toxicity and influence on fluoranthene bioaccumulation. *Environmental Pollution*, *216*, 724–737. https://doi.org/10.1016/j.envpol.2016.06.039

Paul Bissett, W., Meyers, M. B., Walsh, J. J., & Muller-Karger, F. E. (1994). The Effects of Temporal Variability of Mixed Layer Depth on Primary Productivity Around Bermuda. *Journal of Geophysical Research*, *99*, 7539–7553. https://scholarcommons.usf.edu/msc_facpub

Pearce, I., Davidson, A. T., Thomson, P. G., Wright, S., & van den Enden, R. (2010). Marine microbial ecology off East Antarctica (30 - 80°E): Rates of bacterial and phytoplankton growth and grazing by heterotrophic protists. *Deep-Sea Research Part II: Topical Studies in Oceanography*, *57*(9–10), 849–862. https://doi.org/10.1016/j.dsr2.2008.04.039

Peng, X., Chen, M., Chen, S., Dasgupta, S., Xu, H., Ta, K., Du, M., Li, J., Guo, Z., & Bai, S. (2018). Microplastics contaminate the deepest part of the world's ocean. *Geochemical Perspectives Letters*, *9*, 1–5. https://doi.org/http://dx.doi.org/10.7185/geochemlet.1829

Pennati, R., Castelletti, C., Parolini, M., Scarì, G., & Mercurio, S. (2022). Mixotrophic flagellate ingestion boosts microplastic accumulation in ascidians. *Journal of Experimental Zoology Part A: Ecological and Integrative Physiology*, *337*(6), 639–644. https://doi.org/10.1002/jez.2596

Piccardo, M., Provenza, F., Grazioli, E., Cavallo, A., Terlizzi, A., & Renzi, M. (2020). PET microplastics toxicity on marine key species is influenced by pH, particle size and food variations. *Science of the Total Environment*, *715*, 136947. https://doi.org/10.1016/j.scitotenv.2020.136947

Pinkerton, M. H., Boyd, P. W., Deppeler, S., Hayward, A., Höfer, J., & Moreau, S. (2021). Evidence for the Impact of Climate Change on Primary Producers in the Southern Ocean. *Frontiers in Ecology and Evolution*, *9*. https://doi.org/10.3389/fevo.2021.592027

PlasticsEurope. (2015). Plastics market data. *Plastics - the Facts 2014/2015: An Analysis of European Plastics Production, Demand and Waste Data*, 1–34. https://doi.org/10.1016/j.marpolbul.2013.01.015

Porter, K. G. (1988). Phagotrophic phytoflagellates in microbial food webs. *Hydrobiologia*, *159*(1), 89–97. https://doi.org/10.1007/BF00007370

Posch, T., Simek, K., Vrba, J., Pernthaler, J., Sattlerl, B., Sonntagl, B., & Psennerl, R. (1999). Predator-induced chancres of bacterial size-structure and productivity studied on an experimental microbial community. In *AQUATIC MICROBIAL ECOLOGY* (Vol. 18). http://www.lim.cz

Prend, C. J., Keerthi, M. G., Lévy, M., Aumont, O., Gille, S. T., & Talley, L. D. (2022). Sub-Seasonal Forcing Drives Year-To-Year Variations of Southern Ocean

Primary Productivity. *Global Biogeochemical Cycles*, *36*(7). https://doi.org/10.1029/2022GB007329

Price, J. F., Terray, E. A., & Weller, R. A. (1987). Upper ocean dynamics. *Reviews of Geophysics*, *25*(2), 193–203.

Primpke, S., Meyer, B., Falcou-Préfol, M., Schütte, W., & Gerdts, G. (2024). At second glance: The importance of strict quality control – A case study on microplastic in the Southern Ocean key species Antarctic krill, Euphausia superba. *Science of the Total Environment, 918*. https://doi.org/10.1016/j.scitotenv.2024.170618

Princiotta, S. D. V., & Sanders, R. W. (2017). Heterotrophic and mixotrophic nanoflagellates in a mesotrophic lake: Abundance and grazing impacts across season and depth. *Limnology and Oceanography*, *62*(2), 632–644. https://doi.org/10.1002/lno.10450

Princiotta, S. D. V., Smith, B. T., & Sanders, R. W. (2016). Temperature-dependent phagotrophy and phototrophy in a mixotrophic chrysophyte. *Journal of Phycology*, *52*(3), 432–440. https://doi.org/10.1111/jpy.12405

Quetin, L. B., Ross, R. M., Frazer, T. K., & Haberman, K. L. (1996). Factors affecting distribution and abundance of zooplankton, with an emphasis on Antarctic krill, Euphausia superba. In *Foundations for Ecological Research West of the Antarctic Peninsula* (pp. 357–371). https://doi.org/10.1029/ar070p0357

R Core Team. (2020). *R: A Language and Environment for Statistical Computing*. https://www.r-project.org/

Rangel-Buitrago, N., Neal, W., & Williams, A. (2022). The Plasticene: time and rocks. *Marine Pollution Bulletin*, *185*, 114358.

Reed, C. (2015). Dawn of the Plasticene age. *New Scientist*, *225*(3006), 28–32.

Reed, S., Clark, M., Thompson, R., & Hughes, K. A. (2018). Microplastics in marine sediments near Rothera Research Station, Antarctica. *Marine Pollution Bulletin*, *133*, 460–463. https://doi.org/10.1016/j.marpolbul.2018.05.068

Reisser, J., Slat, B., Noble, K., Plessis, K., Epp, M., Proietti, M., Sonneville, J. De, & Becker, T. (2015). *The vertical distribution of buoyant plastics at sea : an observational study in the North Atlantic Gyre*. 1249–1256. https://doi.org/10.5194/bg-12-1249-2015

Rist, S., Baun, A., & Hartmann, N. B. (2017). Ingestion of micro- and nanoplastics in Daphnia magna – Quantification of body burdens and assessment of feeding rates and reproduction. *Environmental Pollution*, *228*, 398–407. https://doi.org/10.1016/j.envpol.2017.05.048

Rowlands, E., Galloway, T., Cole, M., Peck, V. L., Posacka, A., Thorpe, S., & Manno, C.

(2023). Vertical flux of microplastic, a case study in the Southern Ocean, South Georgia. *Marine Pollution Bulletin*, *193*. https://doi.org/10.1016/j.marpolbul.2023.115117

Rowlands, E., Galloway, T., & Manno, C. (2021). A Polar outlook: Potential interactions of micro- and nano-plastic with other anthropogenic stressors. In *Science of the Total Environment* (Vol. 754). Elsevier B.V. https://doi.org/10.1016/j.scitotenv.2020.142379

Saba, G. K., Fraser, W. R., Saba, V. S., Iannuzzi, R. A., Coleman, K. E., Doney, S. C., Ducklow, H. W., Martinson, D. G., Miles, T. N., Patterson-Fraser, D. L., Stammerjohn, S. E., Steinberg, D. K., & Schofield, O. M. (2014). Winter and spring controls on the summer food web of the coastal West Antarctic Peninsula. *Nature Communications*, *5*. https://doi.org/10.1038/ncomms5318

Sallée, J. B., Pellichero, V., Akhoudas, C., Pauthenet, E., Vignes, L., Schmidtko, S., Garabato, A. N., Sutherland, P., & Kuusela, M. (2021). Summertime increases in upper-ocean stratification and mixed-layer depth. *Nature*, *591*(7851), 592–598. https://doi.org/10.1038/s41586-021-03303-x

Sanders, R. W., Caron, D. A., & Berninger, U. G. (1992). Relationships between bacteria and heterotrophic nanoplankton in marine and fresh waters: an inter-ecosystem comparison. *Marine Ecology Progress Series*, *86*(1), 1–14. https://doi.org/10.3354/meps086001

Sanders, R. W., Caron, D. A., Davidson, J. M., Dennett, M. R., & Moran, D. M. (2001). Nutrient acquisition and population growth of a mixotrophic alga in axenic and bacterized cultures. *Microbial Ecology*, *42*(4), 513–523. https://doi.org/10.1007/s00248-001-1024-6

Sanders, R. W., & Gast, R. J. (2012a). Bacterivory by phototrophic picoplankton and nanoplankton in Arctic waters. *FEMS Microbiology Ecology*, *82*(2), 242–253. https://doi.org/10.1111/j.1574-6941.2011.01253.x

Sanders, R. W., & Gast, R. J. (2012b). Bacterivory by phototrophic picoplankton and nanoplankton in Arctic waters. *FEMS Microbiology Ecology*, *82*(2), 242–253. https://doi.org/10.1111/j.1574-6941.2011.01253.x

Sanders, R. W., & Porter, K. G. (1988). Phagotrophic Phytoflagellates. *Advances in Microbial Ecology*, *10*(September), 167–192. https://doi.org/10.1007/978-1-4684-5409-3_5

Sanders, R. W., Porter, K. G., Bennett, S. J., & Debiase, A. E. (1989). Seasonal patterns of bacterivory by flagellates, ciliates, rotifers, and cladocerans in a freshwater planktonic community. *Limnology and Oceanography*, *34*(4), 673–687. https://doi.org/10.4319/lo.1989.34.4.0673

Sanders, R. W., Porter, K. G., & Caron, D. A. (1990). Relationship Between Phototrophy and Phagotrophy in the Mixotrophic Chrysophyte Poterioochromonas malhamensis. In *Microb Ecol* (Vol. 19).

Sanders, R. W., & Wickham, S. A. (1993). Planktonic protozoa and metazoa: predation, food quality and population control. *Marine Microbial Food Webs*, *7*(2), 197–223.

Santana, M. F. M., Ascer, L. G., Custódio, M. R., Moreira, F. T., & Turra, A. (2016). Microplastic contamination in natural mussel beds from a Brazilian urbanized coastal region: Rapid evaluation through bioassessment. *Marine Pollution Bulletin*, *106*(1–2), 183–189. https://doi.org/10.1016/j.marpolbul.2016.02.074

Schlitzer, R. (2002). Carbon export fluxes in the Southern Ocean: results from inverse modeling and comparison with satellite-based estimates. *Deep Sea Research Part II: Topical Studies in Oceanography*, *49*(9–10), 1623–1644. https://doi.org/10.1016/S0967-0645(02)00004-8

Schmidtke, A., Bell, E. M., & Weithoff, G. (2006). Potential grazing impact of the mixotrophic flagellate Ochromonas sp.(Chrysophyceae) on bacteria in an extremely acidic lake. *Journal of Plankton Research*, *28*(11), 991–1001.

Schnetger, B., & Lehners, C. (2014). Determination of nitrate plus nitrite in small volume marine water samples using vanadium(III)chloride as a reduction agent. *Marine Chemistry*, *160*, 91–98. https://doi.org/https://doi.org/10.1016/j.marchem.2014.01.010

Schoener, D. M., & McManus, G. B. (2012). Plastid retention, use, and replacement in a kleptoplastidic ciliate. *Aquatic Microbial Ecology*, *67*(3), 177–187.

Schofield, O., Brown, M., Kohut, J., Nardelli, S., Saba, G., Waite, N., & Ducklow, H. (2018a). Changes in the upper ocean mixed layer and phytoplankton productivity along the West Antarctic Peninsula. *Philosophical Transactions of the Royal Society A: Mathematical, Physical and Engineering Sciences*, *376*(2122). https://doi.org/10.1098/RSTA.2017.0173

Schofield, O., Brown, M., Kohut, J., Nardelli, S., Saba, G., Waite, N., & Ducklow, H. (2018b). Changes in the upper ocean mixed layer and phytoplankton productivity along the West Antarctic Peninsula. *Philosophical Transactions of the Royal Society A: Mathematical, Physical and Engineering Sciences*, *376*(2122). https://doi.org/10.1098/RSTA.2017.0173

Schofield, O., Saba, G., Coleman, K., Carvalho, F., Couto, N., Ducklow, H., Finkel, Z., Irwin, A., Kahl, A., Miles, T., Montes-Hugo, M., Stammerjohn, S., & Waite, N. (2017). Decadal variability in coastal phytoplankton community composition in a changing West Antarctic Peninsula. *Deep-Sea Research Part I: Oceanographic Research Papers*, *124*, 42–54. https://doi.org/10.1016/J.DSR.2017.04.014

Segal, R. D., Waite, A. M., & Hamilton, D. P. (2006). Transition from planktonic to benthic algal dominance along a salinity gradient. *Hydrobiologia*, *556*(1), 119–135. https://doi.org/10.1007/s10750-005-0916-8

Sellers, C. G., Gast, R. J., & Sanders, R. W. (2014). Selective feeding and foreign plastid retention in an Antarctic dinoflagellate. *Journal of Phycology*, *50*(6), 1081–1088. https://doi.org/10.1111/jpy.12240

Setälä, O., Fleming-Lehtinen, V., & Lehtiniemi, M. (2014). Ingestion and transfer of microplastics in the planktonic food web. *Environmental Pollution*, *185*, 77–83. https://doi.org/10.1016/j.envpol.2013.10.013

Setälä, O., Norkko, J., & Lehtiniemi, M. (2016). Feeding type affects microplastic ingestion in a coastal invertebrate community. *Marine Pollution Bulletin*, *102*(1), 95–101. https://doi.org/10.1016/j.marpolbul.2015.11.053

Sfriso, A. A., Tomio, Y., Rosso, B., Gambaro, A., Sfriso, A., Corami, F., Rastelli, E., Corinaldesi, C., Mistri, M., & Munari, C. (2020). Microplastic accumulation in benthic invertebrates in Terra Nova Bay (Ross Sea, Antarctica). *Environment International*, *137*, 105587. https://doi.org/10.1016/j.envint.2020.105587

Shamskhany, A., Li, Z., Patel, P., & Karimpour, S. (2021). Evidence of Microplastic Size Impact on Mobility and Transport in the Marine Environment: A Review and Synthesis of Recent Research. In *Frontiers in Marine Science* (Vol. 8). Frontiers Media S.A. https://doi.org/10.3389/fmars.2021.760649

Shannon, C. (2020). *Spatial & Temporal Patterns of Microplastic Pollution in Wellington, New Zealand, and the Southern Ocean*.

Sherr, B., & Sherr, E. (1993). Staining of heterotrohic protists for visualization via epifluorescence microscopy. *Handbook of Methods in Aquatic Microbial Ecology*, 231–237. https://cir.nii.ac.jp/crid/1571135649950713600.bib?lang=en

Sherr, E. B., & Sherr, B. F. (2002). Significance of predation by protists in aquatic microbial food webs. *Antonie Van Leeuwenhoek*, *81*, 293–308.

Sherr, E. B., & Sherr, B. F. (2018). Protistan Grazing Rates via Uptake of Fluorescently Labeied Prey. In *Handbook of methods in aquatic microbial ecology* (pp. 695–701). CRC Press.

Simon, M., & Azam, F. (1989). Protein content and protein synthesis rates of planktonic marine bacteria. In *Source: Marine Ecology Progress Series* (Vol. 51, Issue 3).

Sletten, A. (2023). *Microplastics in Spotted Seal Stomachs From the Bering and Chukchi Seas in 2012 and 2020*. University of Alaska Fairbanks.

Smith, D. C., & Azam, F. (1992). A simple, economical method for measuring bacterial protein synthesis rates in seawater using 3H-leucine 1. *Marine Microbial Food Webs*, *6*(2), 107–114.

http://www.gso.uri.edu/dcsmith/page3/page19/assets/smithazam92.PDF

Sonke, J. E., Koenig, A. M., Yakovenko, N., Hagelskjær, O., Margenat, H., Hansson, S. V., De Vleeschouwer, F., Magand, O., Le Roux, G., & Thomas, J. L. (2022). A mass budget and box model of global plastics cycling, degradation and dispersal in the land-ocean-atmosphere system. *Microplastics and Nanoplastics*, *2*(1). https://doi.org/10.1186/s43591-022-00048-w

Stammerjohn, S. E., Martinson, D. G., Smith, R. C., & Iannuzzi, R. A. (2008). Sea ice in the western Antarctic Peninsula region: Spatio-temporal variability from ecological and climate change perspectives. *Deep Sea Research Part II: Topical Studies in Oceanography*, *55*(18–19), 2041–2058. https://doi.org/10.1016/J.DSR2.2008.04.026

Stammerjohn, S., Massom, R., Rind, D., & Martinson, D. (2012). Regions of rapid sea ice change: An inter-hemispheric seasonal comparison. *Geophysical Research Letters*, *39*(6). https://doi.org/10.1029/2012GL050874

Stevens, A., & Ramirez-Lopez, L. (2022). *An introduction to the prospectr package*.

Stoecker, D. K. (1998). Conceptual models of mixotrophy in planktonic protists and some ecological and evolutionary implications. *European Journal of Protistology*, *34*(3), 281–290. https://doi.org/10.1016/S0932-4739(98)80055-2

Stoecker, D. K., Hansen, P. J., Caron, D. A., & Mitra, A. (2017). Mixotrophy in the Marine Plankton. *Annual Review of Marine Science*, *9*(1), 311–335. https://doi.org/10.1146/annurev-marine-010816-060617

Stoecker, D. K., Johnson, M. D., De Vargas, C., & Not, F. (2009). Acquired phototrophy in aquatic protists. *Aquatic Microbial Ecology*, *57*(3), 279–310. https://doi.org/10.3354/ame01340

Stukel, M. R., Landry, M. R., & Selph, K. E. (2011). Nanoplankton mixotrophy in the eastern equatorial Pacific. *Deep-Sea Research Part II: Topical Studies in Oceanography*, *58*(3–4), 378–386. https://doi.org/10.1016/j.dsr2.2010.08.016

Suaria, G., Perold, V., Lee, J. R., Lebouard, F., Aliani, S., & Ryan, P. G. (2020). Floating macro- and microplastics around the Southern Ocean: Results from the Antarctic Circumnavigation Expedition. *Environment International*, *136*. https://doi.org/10.1016/j.envint.2020.105494

Thevenon, F., & Carroll, C. (2015). *Plastic debris in the ocean: the characterization of marine plastics and their environmental impacts, situation analysis report. IUCN Librasy System. ISBN: 978-2-8317-1696-1*.

Thompson, R. (2017). *Future of the sea: plastic pollution - GOV.UK*. https://www.gov.uk/government/publications/future-of-the-sea-plastic-pollution

Thompson, R. C., Olsen, Y., Mitchell, R. P., Davis, A., Rowland, S. J., John, A. W. G., McGonigle, D., & Russell, A. E. (2004). Lost at Sea: Where Is All the Plastic? *Science*, *304*(5672), 838 LP – 838. https://doi.org/10.1126/science.1094559

Tommy. (2007). *Geb_287.Fm*. 1–16. https://doi.org/10.1111/j.1466-8238.2006.00287.x

Treguer, P., & Jacques, G. (1992). Dynamics of nutrients and phytoplankton, and fluxes of carbon, nitrogen and silicon in the Antarctic Ocean*. In *Polar Biology* (Vol. 12). Springer-Verlag.

Unrein, F., Gasol, J. M., Not, F., Forn, I., & Massana, R. (2014). Mixotrophic haptophytes are key bacterial grazers in oligotrophic coastal waters. *The ISME Journal*, *8*(1), 164–176. https://doi.org/10.1038/ismej.2013.132

Unrein, F., Massana, R., Alonso-Sáez, L., & Gasol, J. M. (2007). Significant year-round effect of small mixotrophic flagellates on bacterioplankton in an oligotrophic coastal system. *Limnology and Oceanography*, *52*(1), 456–469. https://doi.org/10.4319/lo.2007.52.1.0456

Urabe, J., Gurung, T. B., & Yoshida, T. (1999). Effects of phosphorus supply on phagotrophy by the mixotrophic alga Uroglena americana (Chrysophyceae). *Aquatic Microbial Ecology*, *18*(1), 77–83. https://doi.org/10.3354/ame018077

van Sebille, E., Wilcox, C., Lebreton, L., Maximenko, N., Hardesty, B. D., van Franeker, J. A., Eriksen, M., Siegel, D., Galgani, F., & Law, K. L. (2015). A global inventory of small floating plastic debris. *Environmental Research Letters*, *10*(12), 124006. https://doi.org/10.1088/1748-9326/10/12/124006

Vaque, D., Aqusti, S., & Duarte, C. M. (2004). Response of bacterial grazing rates to experimentalmanipulation of an Antarctic coastal nanoflagellatecommunity. *Aquatic Microbial Ecology*, *36*, 41–52.

Vaqué, D., Guadayol, Ò., Peters, F., Felipe, J., Angel-Ripoll, L., Terrado, R., Lovejoy, C., & Pedrós-Alió, C. (2008). Seasonal changes in planktonic bacterivory rates under the ice-covered coastal Arctic Ocean. *Limnology and Oceanography*, *53*(6), 2427–2438. https://doi.org/10.4319/lo.2008.53.6.2427

Vaughan, D. G., Marshall, G. J., Connolley, W. M., Parkinson, C., Mulvaney, R., Hodgson, D. A., King, J. C., Pudsey, C. J., & Turner, J. (2003). *RECENT RAPID REGIONAL CLIMATE WARMING ON THE ANTARCTIC PENINSULA*. http://www.giss.nasa.gov/

Verma, S. S. (2008). Roads from plastic waste. *The Indian Concrete Journal*, *3*(1), 43–44.

Vives, C. R., Schallenberg, C., Strutton, P. G., & Westwood, K. J. (2022). Iron and light limitation of phytoplankton growth off East Antarctica. *Journal of Marine Systems*, *234*. https://doi.org/10.1016/J.JMARSYS.2022.103774

Waller, C. L., Griffiths, H. J., Waluda, C. M., Thorpe, S. E., Loaiza, I., Moreno, B., Pacherres, C. O., & Hughes, K. A. (2017). Microplastics in the Antarctic marine system: An emerging area of research. *Science of the Total Environment*, *598*, 220–227. https://doi.org/10.1016/j.scitotenv.2017.03.283

Ward, B. A., & Follows, M. J. (2016). Marine mixotrophy increases trophic transfer efficiency, mean organism size, and vertical carbon flux. *Proceedings of the National Academy of Sciences of the United States of America*, *113*(11), 2958–2963. https://doi.org/10.1073/pnas.1517118113

Ward, J. E., & Kach, D. J. (2009). Marine aggregates facilitate ingestion of nanoparticles by suspension-feeding bivalves. *Marine Environmental Research*, *68*(3), 137–142. https://doi.org/10.1016/j.marenvres.2009.05.002

Wilken, S., Choi, C. J., & Worden, A. Z. (2020). Contrasting Mixotrophic Lifestyles Reveal Different Ecological Niches in Two Closely Related Marine Protists. *Journal of Phycology*, *56*(1), 52–67. https://doi.org/10.1111/jpy.12920

Wilken, S., Schuurmans, J. M., & Matthijs, H. C. P. (2014). Do mixotrophs grow as photoheterotrophs? Photophysiological acclimation of the chrysophyte ochromonas danica after feeding. *New Phytologist*, *204*(4), 882–889. https://doi.org/10.1111/nph.12975

Wollmann, K., Deneke, R., Nixdorf, B., & Packroff, G. (2000). Dynamics of planktonic food webs in three mining lakes across a pH gradient (pH 2–4). *Hydrobiologia*, *433*(1), 3–14.

Woodward, J., Li, J., Rothwell, J., & Hurley, R. (2021). Acute riverine microplastic contamination due to avoidable releases of untreated wastewater. *Nature Sustainability*, *4*(9), 793–802. https://doi.org/10.1038/s41893-021-00718-2

Worden, A. Z., Follows, M. J., Giovannoni, S. J., Wilken, S., Zimmerman, A. E., & Keeling, P. J. (2015). Rethinking the marine carbon cycle: Factoring in the multifarious lifestyles of microbes. *Science*, *347*(6223), 1257594. https://doi.org/10.1126/science.1257594 %J Science

Wu, H., Liu, Q., Yang, N., & Xu, S. (2023). Polystyrene-microplastics and DEHP co-exposure induced DNA damage, cell cycle arrest and necroptosis of ovarian granulosa cells in mice by promoting ROS production. *Science of the Total Environment*, *871*. https://doi.org/10.1016/j.scitotenv.2023.161962

Wu, Y., Guo, P., Zhang, X., Zhang, Y., Xie, S., & Deng, J. (2019). Effect of microplastics exposure on the photosynthesis system of freshwater algae. *Journal of Hazardous Materials*. https://doi.org/10.1016/J.JHAZMAT.2019.04.039

APPENDIX A

ABUNDANCE, PRIMARY PRODUCTION, AND BACTERIVORY PER CELL ASSESSED DURING DIRECT EXPOSURE EXPERIMENT

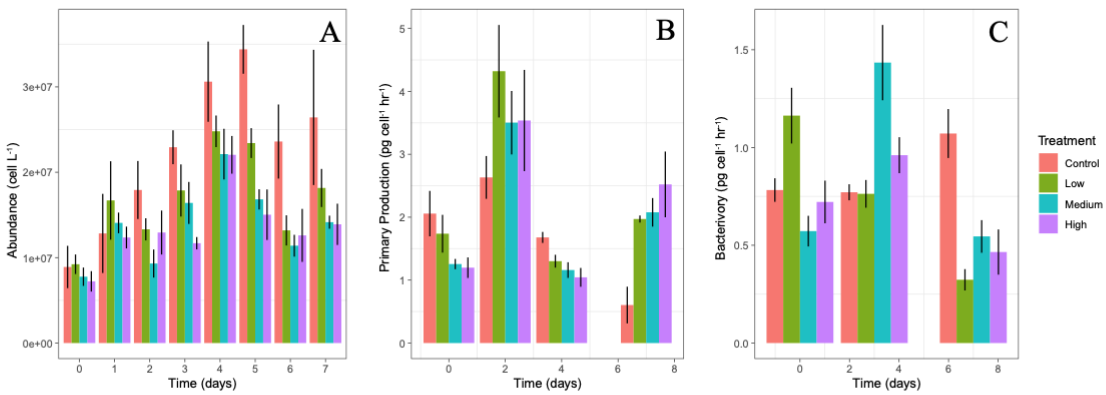

APPENDIX B

ABUNDANCE, PRIMARY PRODUCTION, AND BACTERIVORY PER CELL ASSESSED DURING INDIRECT EXPOSURE EXPERIMENT

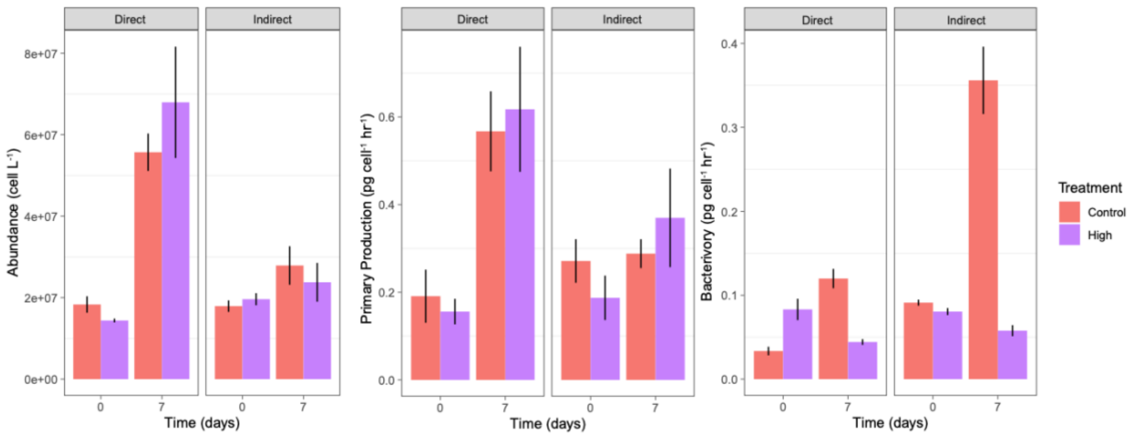

APPENDIX C

CORRELATION MATRICES OF POTENTIALLY INFLUENTIAL ENVIRONMENTAL VARIABLES AND MEASURES OF MICROPLASTIC POLLUTION

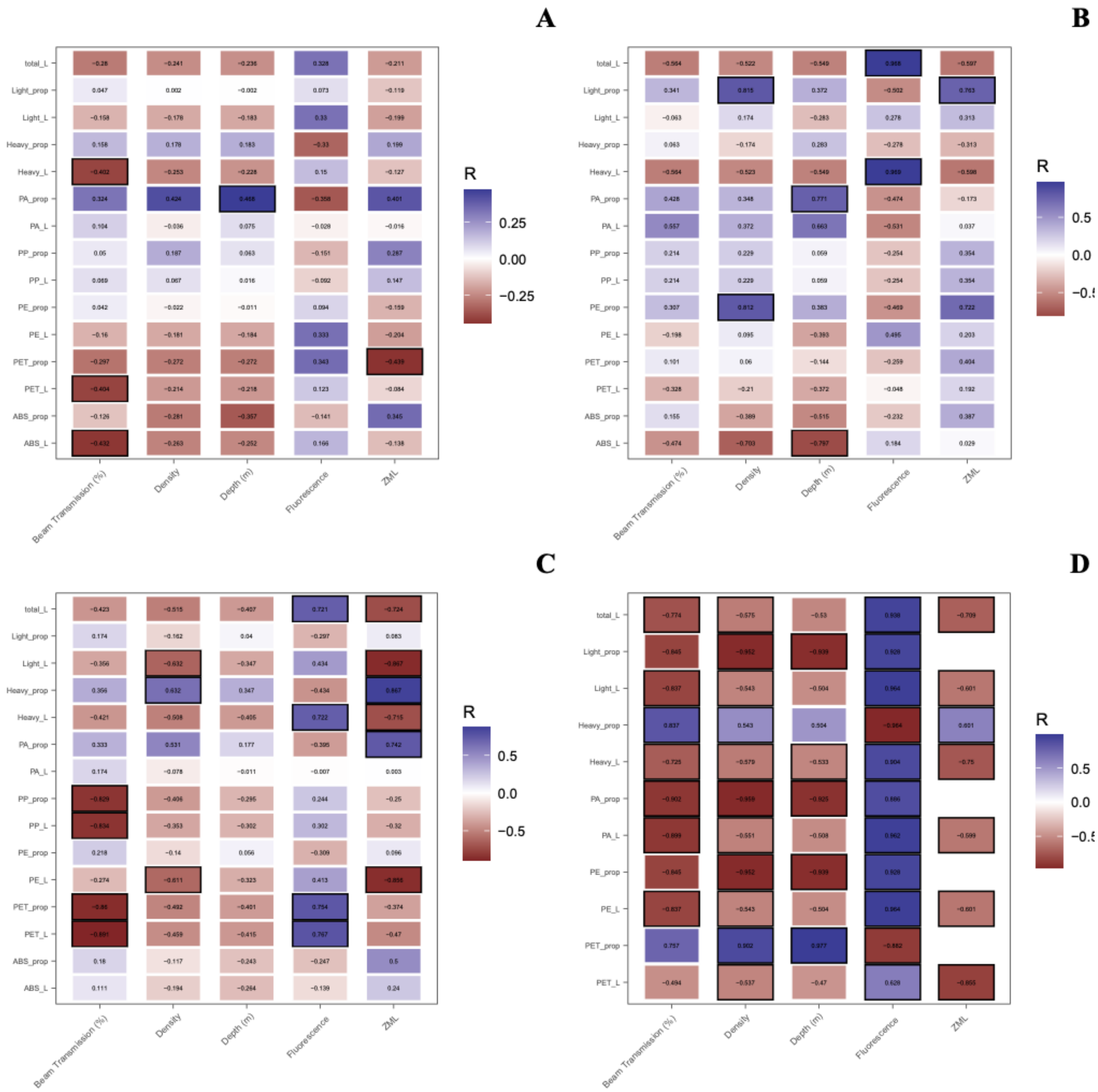

APPENDIX D

DEPTH VERSUS LOG TRANSFORMED ESTIMATED ABUNDANCE

SCATTERPLOTS

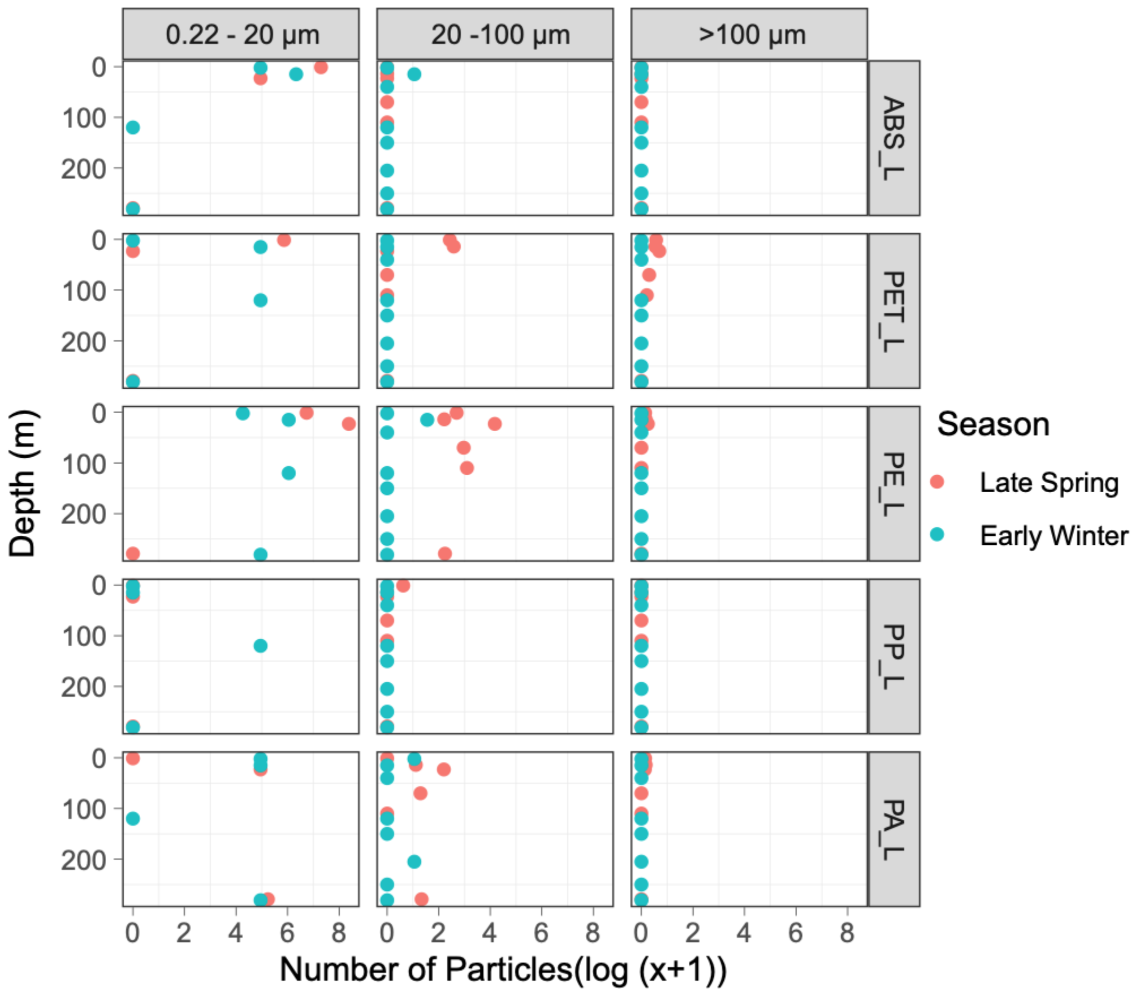

APPENDIX E

ACTIVITY MEASURES FOR NANOFLAGELLATES THROUGHOUT THE WAP REGION AT MULTIPLE DEPTHS

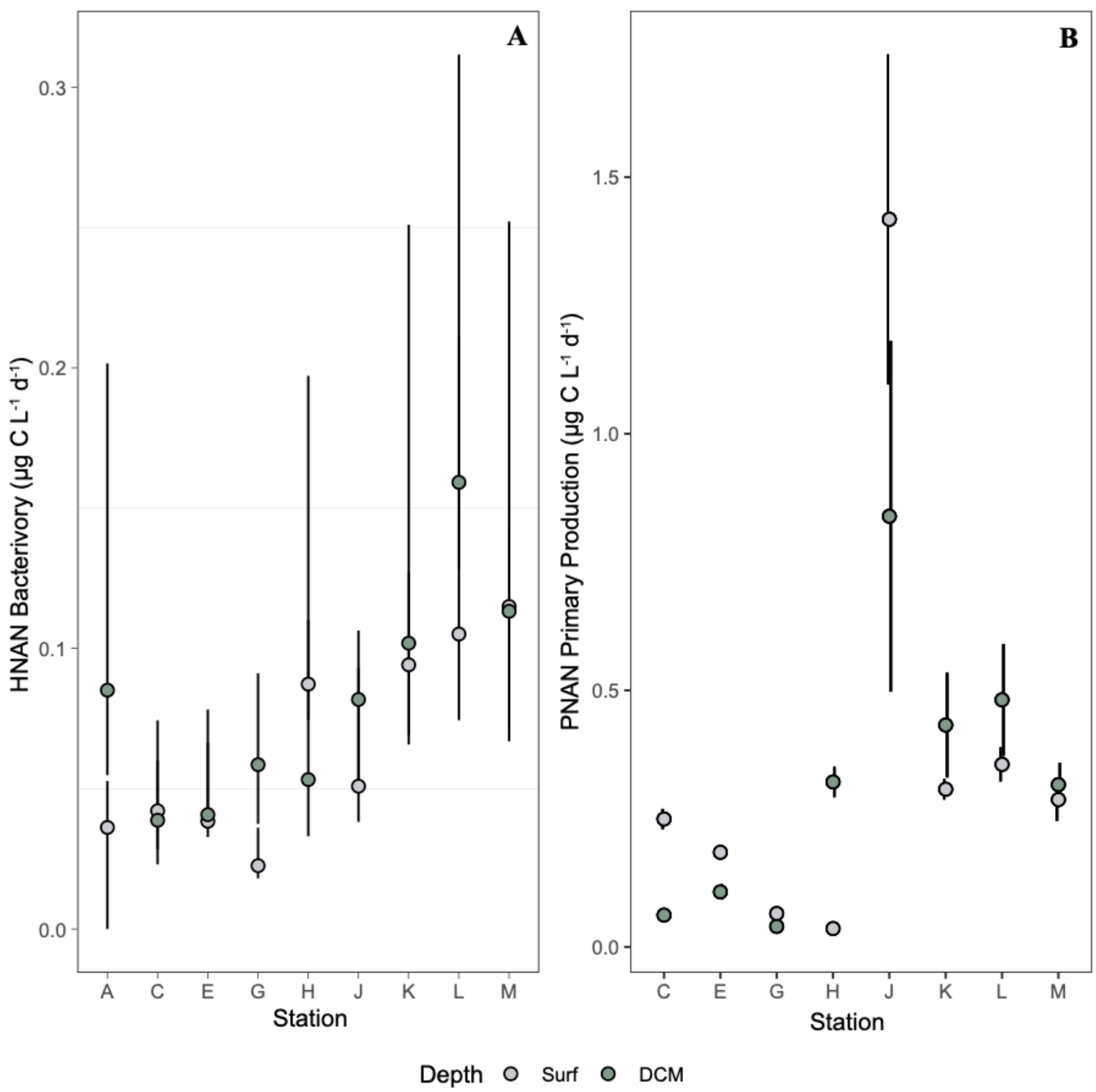

APPENDIX F

PERCENT OF BACTERIAL PRODUCTION REMOVED BY MNANS AND HNANS VIA EPIFLUORESCENT MICROSCOPY

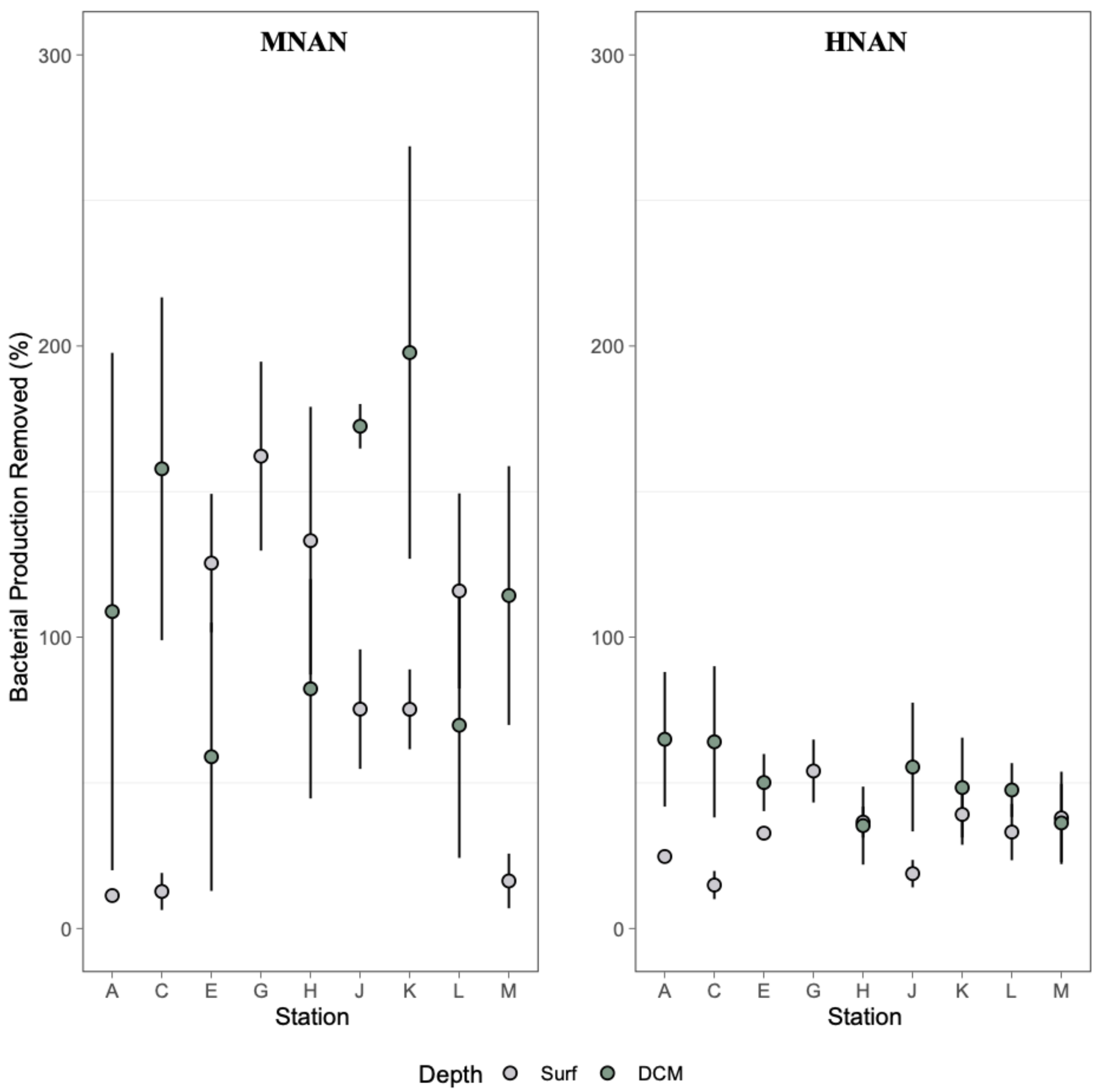

APPENDIX G

PERCENTAGE OF BACTERIAL STANDING STOCK REMOVED BY MNANS AND HNANS

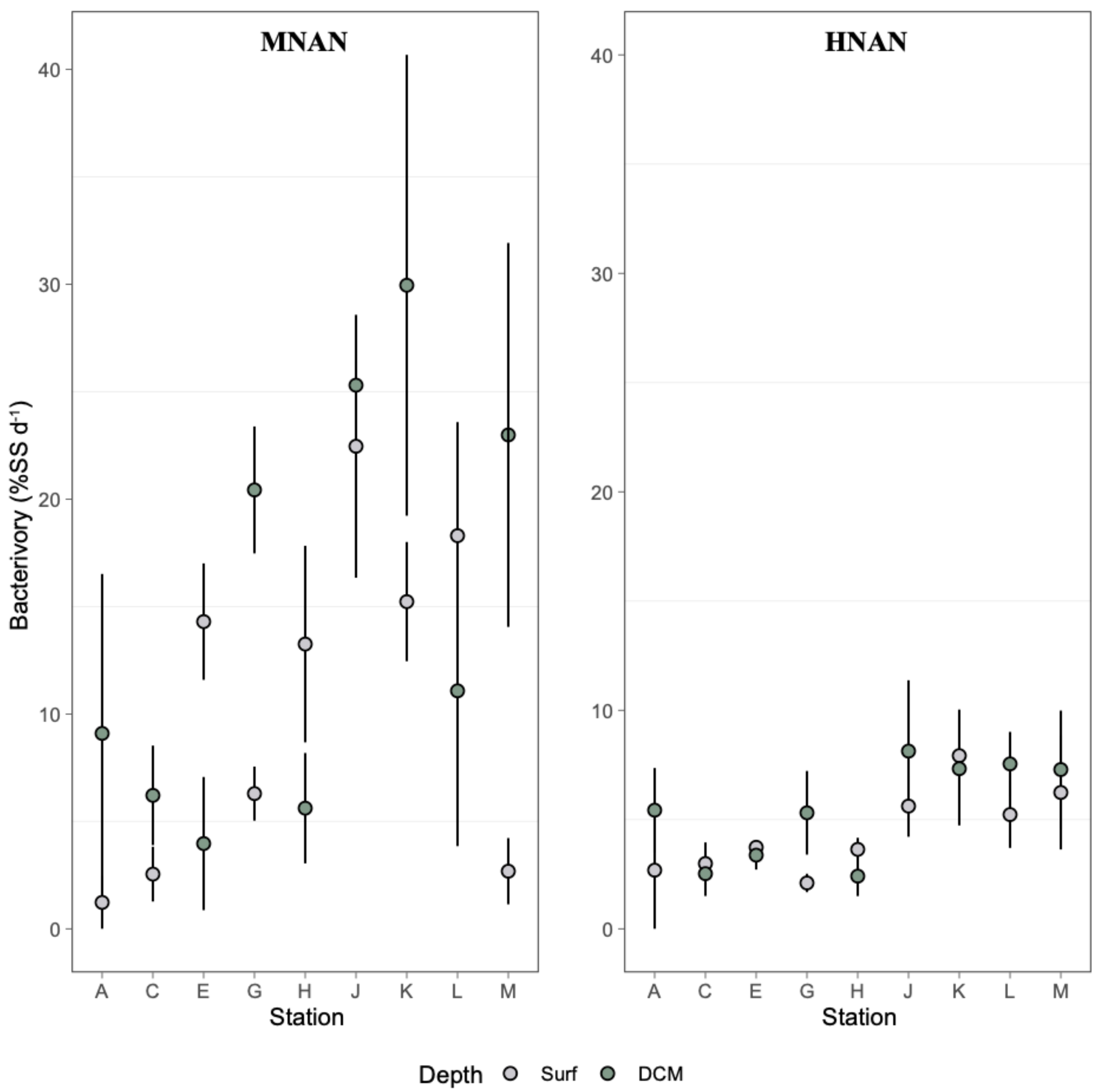

APPENDIX H

TOTAL PRIMARY PRODUCTION FOR WHOLE WATER FROM EACH STATION AND DEPTH SAMPLED